# BENTHIC MACROINVERTEBRATE MONITORING PLAN FOR LARGE TRANSBOUNDARY RIVERS IN THE ALBERTA-NWT REGION

## ASSESSMENT OF RESULTS FROM THE THIRD YEAR OF SAMPLING

2019

Alberta Government

Canadian Rivers Institute

UNB

Government of Northwest Territories / Gouvernement des Territoires du Nord-Ouest

Prepared by:

Jennifer Lento, MSc, PhD
Research Scientist
Canadian Rivers Institute and Department of Biology
University of New Brunswick
Fredericton, NB, Canada

Prepared for:

Alberta-Northwest Territories Bilateral Management Committee
Department of Environment and Parks, Government of Alberta
Department of Environment and Natural Resources, Government of the Northwest Territories

December, 2021

# Executive Summary


**Introduction**

The Government of the Northwest Territories (GNWT) and the Government of Alberta (GOA) are working to establish a monitoring program for the bioassessment of large transboundary rivers. The establishment of this program is in recognition of the potential for future impacts to transboundary waters as a result of activities in the upstream catchment and climate change. Establishment of long-term monitoring and assessment supports the future detection of impacts that may arise from human development, but also supports the detection of ecological changes in response to a warming climate. The initial focus of the transboundary monitoring program is on benthic macroinvertebrate (BMI) assemblages, which are an important ecosystem component to monitor in northern rivers as an integrated measure of water quality and habitat condition. Within the Northwest Territories-Alberta transboundary river regions, there is relatively little information about the current composition and natural variation of benthic communities. Therefore, it is vital that routine monitoring be established to secure information about current conditions in these assemblages and to provide sufficient information to allow for future detection of change.

One approach used in biological monitoring is estimation of the normal range of variability, which prescribes the collection of sufficient contemporary data from a region to allow estimation of the range of natural variability that is to be expected given current conditions in a system. In the case of the transboundary monitoring program, this approach provides an ideal method to characterize natural variability at the GNWT-GOA border in the absence of significant impacts and identify the magnitude of change in future conditions that would require additional monitoring/assessment and potentially management action. Quantifying the normal range for a system requires not only characterizing spatial variability but also assessing and controlling for short-term (inter-annual) temporal variability to allow for the detection of potentially subtle changes happening over a long time scale. The normal range also provides a measure of the level of change that would be deemed significant enough to be ecologically relevant, termed the critical effect size (CES). Initial establishment of CES to quantify within-year and temporal variability can be done with three or more years of monitoring data, but as more data are collected, it is important to refine the spatial CES to account for short-term temporal variability that is likely to be observed within systems. Assessment of temporal data allows for the development of location-specific CES that can be used in future years to detect deviations from normal range.

The objective of this report is to assess spatial variability within the Hay and Slave rivers from the third year of sampling in the GNWT and GOA large transboundary river BMI monitoring program, and to assess temporal variation within and among sites and reaches (from 2017-2019) as an initial estimate of normal range and critical effect size. The Hay River and the Slave River in northern Alberta-southern Northwest Territories were sampled in August and September 2019 (respectively). Water chemistry, sediment chemistry, physical habitat, and BMI kick samples were analyzed to characterize spatial and temporal variability within the rivers, including quantification of the normal range and CES for a number of biotic metrics. The emphasis of this report is on the quantification of temporal variability, which will build the foundation for future monitoring and detection of impacts in these systems.

**Methods**

During the third year of sampling, the Hay River and Slave River were sampled August 13-15 and September 12-15, respectively. Both rivers were accessed via boat launches on the Alberta side of the border. Kick-sampling reaches of approximately 500 m in length were chosen within each river. Sampling took place in each reach on the river bank where rocky habitat was located. Sample reach KS4 in the Slave River was the only location where sampling was feasible on both banks. In both rivers, five sites were selected within each reach, spaced evenly along the reach when habitat availability allowed. Sites were generally of similar substrate composition, dominated by pebble, gravel, and cobble size classes. Sample collection followed the Canadian Aquatic Biomonitoring Network (CABIN) sampling protocol modified for large rivers, as described in the monitoring plan (see Lento 2018). Water chemistry, physical habitat descriptions, and sediment chemistry samples were collected at kick sites as supporting variables.

Water chemistry, sediment chemistry, and biotic metrics were summarized by reach, and chemical parameter means were compared with CCME guidelines. Among-reach variation in water chemistry and BMI assemblage composition was assessed separately for Hay River and Slave River using a one-way analysis of variance (ANOVA) design, with an abiotic parameter or biotic metric as the response variable and the reach as the grouping factor. Regression analysis was used to assess the response of biotic metrics to site-specific measurements of flow velocity. Multivariate analysis (Principal Component Analysis or PCA) was used to fully characterize the biotic assemblage and abiotic environment of each river. The relationship between the BMI data from kick samples and abiotic data was tested with Redundancy Analysis (RDA), with a subset of abiotic parameters selected for inclusion based on their importance in the abiotic PCA.

Temporal patterns in biota were explored through the comparison of biotic metrics among years at the site and reach level. ANCOVA models were used to test for changes in biotic metrics across years (with year used as a categorical proxy for differing flow regimes in each year of sampling) while controlling for site-specific flow velocity.

The normal range of variability was assessed for within-year variability and temporal variability among sites and within reaches. Within-year variability was tested by developing single-year and multi-year CES limits and comparing 2019 data with those estimates of normal range. At the site scale, temporal variability was assessed by plotting 2017-2019 means ± standard error for each site and comparing with the grand mean (mean of means) ± 2 standard deviations (2SD) for the river. Within-reach variability was quantified by calculating the grand mean (mean of annual means) ± 2SD for each reach in each metric, as a measure of reach-specific normal range.

**Results and Discussion**

***Hay River***

*Spatial variation in the physical/chemical habitat*

Differences in water chemistry and BMI assemblages between 2017 and 2018 were partially attributed to differences in flow between years, so emphasis was placed on assessing hydrographs and the impact of flows in each river. The hydrograph for the Hay River from 2019 reflected a change in the timing and magnitude of peak flows, with a flatter hydrograph during the spring freshet and a more peaked and flashy hydrograph in the late summer/early fall. Antecedent hydrologic conditions in the 60 days and 30 days prior to sampling were compared among years by calculating two metrics of flow: the median discharge and the coefficient of variation of discharge. In the 30 days prior to sampling, median flow was more similar among years, but highest in 2019, and variability in flow was much higher in 2019 compared to previous years.

For many water chemistry parameters, the increased water levels in 2019 appeared to have the effect of reducing variability within and among reaches in the Hay River. Variability among sites in the Hay River was extremely low for some water chemistry parameters in 2019. Reaches were classified as eutrophic or hyper-eutrophic based on mean total phosphorus (TP) values, which ranged from 0.074 to 0.126 mg/L. However, total suspended solids (TSS) were elevated compared to previous years, and the high levels of TP may have been a reflection of the recent surge in water levels flushing more sediments through the system. Dissolved metals had generally low variability within reaches (between kick-sites) and among reaches. Many dissolved metals were below detection limit, or had low standard deviations within reaches. Total metals were somewhat more variable than dissolved metals, and there were high levels of some total metals that were due to higher TSS levels in the system. As these samples represented spot measurements, patterns in the data should not be taken to suggest long-term trends.

Velocity was high at Hay River sites in 2019, ranging from 0.25 to 0.49 m/s on average, in contrast with 2018, when velocity ranged from 0.14 to 0.21 m/s. This reflected the higher discharge at the time of sampling, which was more than six times the discharge at the time of sampling in 2017 and 2018. Wetted width was also much higher in 2019 than in 2018, with increases of 10 to 48 m wetted width in reaches in 2019.

The ordination of chemical and physical habitat variables indicated high similarity within reaches, with sites from the same reach generally plotting close together along the same gradient. Velocity and substrate size parameters had higher loadings on the PCA axes than many ions, nutrients, and physical water chemistry parameters, due in part to the low variability in water chemistry among sites.

Mean values of all PAHs were below detection limit in Hay River sediment samples, with the exception of chrysene, which was above the detection limit in one sample in Reach 3. Because most PAHs were below detection limit, the IACR (which is calculated as the sum of a number of PAHs) was also below detection limit, which indicated low risk to drinking water quality.

*Spatial variation in BMI assemblages*

In past years of sampling, the Hay River has shown a clear longitudinal gradient in abundance, with higher abundance of BMI in the three upstream reaches, and lower abundance in the three downstream reaches. However, there was no evidence of a pattern in total abundance moving from upstream to downstream reaches in 2019. There was higher relative abundance of EPT in the upstream reaches, though the difference was only statistically significant when Reach 2 and Reach 4 were compared. For most richness metrics, there was a high degree of similarity within and among reaches.

The PCA of assemblages in the Hay River had no strong outliers, which suggested that no sites were ecological outliers with respect to assemblage composition. The first axis of the PCA represented a gradient separating sites in Reach 1 and Reach 2 from the three downstream reaches. The second axis of the ordination largely separated the sites in Reach 4, Reach 5, and Reach 6 on the basis of assemblage composition.

Relationships of abundance metrics with velocity were variable, with few examples of a clear biotic response to differences in flow velocity among sites. Total abundance and relative abundance of Chironomidae appeared to increase with increasing flow, but the relationship was highly variable and only total abundance was found to vary significantly as a function of flow velocity. Richness metrics appeared to show a curvilinear (unimodal) response to flow velocity, with the highest richness found in the middle of the velocity range across all sites. The RDA ordination indicated that dissolved iron (which was variable only at a small number of sites, percent cobble, and velocity contributed were most strongly associated with assemblage structure. Few chemical parameters were significant in the model because water chemistry was so similar across sites.

*Temporal variation in BMI assemblages*

Shifts in the relative abundance of Chironomidae and EPT were evident in the Hay River over the three years of sampling. In 2017, these two groups together made up a large portion of the BMI assemblage. In 2018, when the relative abundance of Diptera decreased on average across all Hay River sites, there was a more clear upstream-downstream pattern in the relative abundance of EPT and Chironomidae, with EPT predominant in upstream reaches, and a greater dominance of Chironomidae in downstream reaches. In 2019, patterns in EPT and Chironomidae relative abundance once again resembled the patterns found in 2017, with similar peaks and troughs in the relative abundance patterns of each group among sites.

The relative abundance of EPT was lower in 2018 and 2019 than in 2017 in all reaches. The relative abundance of Chironomidae and of Diptera + Oligochaeta in 2018 was similar to or lower than that found in 2017 for most reaches, but there was a subsequent increase in relative abundance in most reaches in 2019. Together, these results indicate that a shift in relative proportions of EPT and Diptera/Oligochaeta has occurred in the Hay River since 2017. Richness metrics also indicated shifts over time that reflected a greater dominance of Chironomidae and other Diptera and Oligochaeta. Chironomidae richness and the richness of Diptera + Oligochaeta both increased in 2019 relative to earlier years, and these increases led to a net increase in total richness across all reaches.

Changes in the magnitude and timing of peak flows contributed to variation in water levels (ranging from extreme low flows to high flows) and different antecedent hydrologic conditions in each year of sampling. ANCOVA indicated that mean abundance in the Hay River (controlling for velocity) was significantly lower in 2019 than in 2017 or 2018, which suggested that the higher flows in 2019 contributed to lower abundance across sites. Significant differences in total richness among years (while controlling for velocity) indicated that higher flows in 2019 also contributed to greater taxonomic richness across sites.

*Normal range and CES*

Temporal variability in sites was compared with the normal range derived from the grand mean of all sites in each year. The normal range represents an early estimate based only on three years of data, and it will continue to be refined as more data are collected. Total abundance in the Hay River was extremely variable within sites (wide error bars, representing high temporal variability within a site). Abundance also varied among sites, but annual means were similar enough that the normal range based on the grand mean for this metric was narrow. Sites in the downstream reaches were below CES for EPT relative abundance, while upstream reaches were below CES for Chironomidae relative abundance, reflecting the longitudinal patterns that were particularly evident in these metrics in 2018. Deviations of sites outside the range of initial CES for abundance and relative abundance metrics (based on three years of data) indicate that additional years of data will be required to improve the accuracy of these descriptions of normal range. The normal range for richness metrics provided a much better fit to the data, and most sites fell within the CES boundaries for all richness metrics.

Temporal variability at the reach scale was quantified by estimating the reach-specific normal range and developing initial CES boundaries based on variability among years. The normal range for total abundance was wide in many reaches, particularly in Reach 3, where the CES boundaries covered a range of over 4000 individuals. Such a wide normal range would not be useful in identifying impaired samples, as it would be difficult for a sample to fall outside of the wide and all-encompassing CES boundaries. The normal range of variability for the relative abundance of EPT and the relative abundance of Chironomidae were generally more narrow and appeared to be more useful for future detection of impairment in reaches. CES limits were higher in the upstream reaches for EPT, reflecting the generally higher relative abundance of EPT taxa found in those reaches. This speaks to the importance of developing reach-specific normal ranges, as the high relative abundance of EPT that is within the range of natural variability in the upstream reaches may be above what can be expected in the downstream reaches, where Diptera and Oligochaeta are more prevalent.

***Slave River***

*Spatial variation in physical/chemical habitat*

Flows in the Slave River have been variable across the three years of sampling. In 2018, there was a late peak in water levels, occurring only 45 days prior to sampling, and this peak appeared to have influenced the biotic assemblages of the river, leading to strong shifts in abundance of Chironomidae (midges) in particular. The hydrograph in 2019 also differed from what was observed in 2017, this time showing a flatter profile during the typical spring freshet, with a more gradual increase in water levels across the summer, and a more gradual and flashy decline. When flow metrics were compared among years for the 30 days prior to sampling, 2018 was the most variable year, reflecting its flashier flows during that period, but 2019 had the highest median discharge.

Similar to patterns observed in the Hay River, higher flow in 2019 appeared to have the effect of reducing variability in water chemistry parameters in the Slave River, leading to low standard deviations within reaches and low interquartile ranges, particularly with respect to ions. Estimates of mean TP in the Slave River were all lower than 0.100 mg/L, and reaches were classified as eutrophic based on the Canadian Guidance Framework. Dissolved metal concentrations were generally low in Slave River reaches, with many metals at or below detection limits. Though total metals were more variable than dissolved metals, concentrations remained low or below detection limit for many metals.

Velocity ranged from 0.21 to 0.54 m/s on average across reaches, and was higher than observed in 2018 (range: 0.17 to 0.38 m/s on average), consistent with the higher discharge at the time of sampling (approximately 3970 $m^3$/s in 2019 compared with approximately 3600 $m^3$/s and 3080 $m^3$/s in 2017 and 2018, respectively). Substrate composition in reaches was predominantly a combination of gravel, pebble, and cobble size classes.

Because variability in water chemistry among sites was very low in the Slave River in 2019, gradients in physical habitat variables were important in the PCA ordination. Notably, a dominant gradient along both the first and second axes was a negative correlation of site KS4-1A with velocity. This site has been identified in previous years as an outlier due to its low velocity, and it was orthogonal to (uncorrelated with) the gradient along which the other Slave River sites varied in the ordination. The gradient along which the other sites varied was a gradient in substrate size, characterized by a contrast between sites positively correlated with gravel and sand, and those that were positively correlated with cobble and boulder, though a number of water chemistry parameters were also associated with the gradient.

Average values for several PAHs were above detection limits in sediment chemistry samples collected from Slave River reaches, though concentrations were low and all PAHs were below guideline levels. The B(a)P Total Potency Equivalent, which is a measure of cancer risk to humans, was below detection limit in all reaches. The IACR, which measures threat to drinking water, was above detection limit in Reach 2, but it was much lower than the guideline level of 1.0.

*Spatial variation in BMI assemblages*

Total abundance was low in Slave River samples in 2019, ranging from 125 to 888 individuals on average per reach, with four reaches having fewer than 300 individuals on average. EPT abundance followed similar patterns to total abundance because these three orders made up a large proportion of the total assemblage in several reaches. The abundance of Chironomidae, in contrast to EPT, was similar across all reaches, and mean abundance values were extremely low, ranging from only 9 to 36 individuals on average per reach. As a result, the average percent composition of Chironomidae in Slave River reaches ranged from 3.4% to 14.5%, indicating that they made up only a minor portion of the samples in 2019. Taxonomic richness ranged from 18 to 26 taxa on average per reach, and though there was some variability among reaches, there were no significant differences found when richness was tested in ANOVA. Variability among reaches was very low for EPT richness and Chironomidae richness, and similar numbers of taxa were found across reaches for each metric. Multivariate analysis indicated the presence of two strong outliers: KS2-1 and KS2-2. In the PCA ordination, these sites were positively correlated with a number of taxa that have a preference for low flows.

There was clear evidence of a relationship between total abundance of BMI and flow velocity among sites, with abundance increasing as a function of increasing velocity. The relative abundance of EPT was also found to increase significantly in response to increasing velocity, though the relationship was far more variable than that observed for total abundance. Total richness metrics appeared to show a curvilinear (unimodal) response to flow velocity, similar to the Hay River, with the highest richness found in the middle of the velocity range across all sites, but the relationship was not statistically significant. In the RDA ordination, sites KS2-1 and KS2-2 remained outliers, and the separation of these and other Reach 2 sites from the other reaches along the first axis was attributed to a positive correlation with sand, nitrate, and dissolved nitrogen (DN). DN had the strongest effect on the fit of the model, followed by percent sand and conductivity (the latter of which was correlated with velocity).

*Temporal variation in BMI assemblages*

At the site scale, large changes were evident when total abundance was compared between 2017 and 2018, but in 2019, abundance was more similar across sites. Changes in abundance over time in Slave River sites suggest that the flow regime in 2019, which included a gradual increase in flow (without a strong spring freshet) and higher water levels at the time of sampling and in the antecedent period, may have contributed to some homogenization of BMI assemblages with respect to abundance of individuals at a site.

There was strong evidence of changes to the relative abundance of taxonomic groups over the period 2017-2019, with the largest changes occurring between 2017 and 2018. The most obvious of these changes was the decline in relative abundance of Chironomidae. Changes in abundance of Chironomidae from 2017 to 2018 were extreme, as this taxonomic group went from being dominant to being found at very low abundances and relative abundances across all sites. Abundance and relative abundance of Chironomidae in Slave River reaches were similar 2018 and 2019. The continuation of high flows in 2019 supported the suggestion that high flows contributed to the strong decline in Chironomidae abundance and concurrent increase in the relative abundance of EPT. Changes in richness metrics over time primarily reflected the loss of Chironomidae taxa. EPT richness was highly invariable over time and was also similar among reaches.

Mean richness in the Slave River was statistically significantly lower in 2018 and 2019 than it was in 2017; however, there were no significant differences between 2018 and 2019. Similarly, Chironomidae relative abundance was significantly lower in 2018 and 2019 than in 2017, but there was no evidence of a significant difference between 2018 and 2019.

*Normal range and CES*

Annual means across all sites in the Slave River varied widely between 2017 and 2019, contributing to wide initial estimates of normal range for the river (based on three years of sampling data). For example, the estimated CES boundaries for Diptera + Oligochaeta relative abundance covered a range of approximately 0.70 (i.e., an acceptable percent Diptera + Oligochaeta ranging from 0% to 70% of the sample). These wide normal range boundaries reflected the sharp decline in abundance of Chironomidae that was observed after 2017, but they have low diagnostic power to detect impairment because they encompass so many possible values of the response variable. Variation within sites was also high for several metrics (particularly abundance-based metrics), as evidenced by wide error bars, representing high temporal variability within a site. The estimated initial normal range of variability in site-scale analyses was more narrow for richness metrics, but did suffer from wide inter-annual variability in site means across the entire river. The exception was EPT richness, which had an extremely narrow normal range based on the grand mean. Of the metrics tested for the Slave River, EPT richness appeared to have the greatest potential for developing monitoring and management triggers.

At the reach scale, initial estimates of the normal range of variability indicated wide CES boundaries for most abundance-based metrics, reflecting the large changes in abundance and relative abundance over the three sampling years in the Slave River. The width of CES boundaries was extreme for the relative abundance of EPT and relative abundance of Diptera + Oligochaeta in many reaches, and CES boundaries for these two metrics in Reach 5 covered nearly the entire range of possible values, indicating that these metrics would have no ability to detect potential impact in future sampling years. Similarly wide and all-encompassing ranges were evident in several other reaches, indicating low diagnostic power of abundance-based metrics in the Slave River reaches. The estimated initial normal range of variability was more narrow for richness-based metrics, reflecting weaker temporal variability in these metrics. In particular, EPT richness had extremely low variability within reaches and among years, contributing to narrow CES boundaries.

Though additional years of sample data would help to improve initial estimates of normal range for these metrics, an alternative option would be to develop two sets of normal range criteria for the river and the reaches: one based on data from 2017 and any additional sample years with similar flow levels (assuming that Chironomidae abundance returns to previous levels) and one based on samples collected in high flow years (including 2018 and 2019). Although such an approach would require more years of data to develop the two sets of normal ranges (at minimum three low flow and three high flow years), it would ensure narrower, more precise bounds for CES estimates that are a more accurate reflection of expected conditions in a given flow year.

**Recommendations and Conclusions**

This report summarizes spatial and temporal patterns in BMI assemblages and supporting variables in the Hay and Slave River, and it provides the first test of site- and reach-specific normal range and CES development using temporal variability. As the normal range is refined for different metrics, the diagnostic power of this approach will become evident, but in the initial years of sampling, the normal range is highly susceptible to inter-annual variation.

Variability in flow appeared to be the dominant driver of biotic change in the Hay and Slave Rivers, and the findings of this report indicate that stronger consideration of flow regimes is necessary as these sampling program proceeds. For example, choice of sampling dates must be made primarily based on current hydrographs, so sampling shortly following a peak in flow can be avoided if possible. The remote nature of this work does require significant pre-planning and scheduling, and re-scheduling due to highly variable flow can be difficult, but some flexibility will be required to ensure data are not affected by antecedent hydrological conditions.

Reach-specific CES calculations in this report provide an initial estimate of the normal range for each metric, and it will be important to use additional years of data to improve the precision of these boundaries. Though three years of sampling data allows for initial estimates of the normal range, generally a minimum of five years is required to achieve greater reliability in CES boundaries. Furthermore, the development of flow-specific normal ranges should be considered, particularly for the Slave River. The change in abundance of Chironomidae with increased flow in this river was so large that abundance-based metrics lacked diagnostic power because they covered too wide a range of possible values. If the data were split into those that were collected during high flow years (2018 and 2019) and those collected during lower flow years (2017), additional sample data could contribute to the development of CES boundaries that better reflect hydrologic influences. Such an approach would require a more in-depth assessment of hydrology within the Slave River system, to define low flow, moderate flow, and high flow conditions based on historical data. This can be accomplished using Indicators of Hydrologic Alteration (IHA) metrics, which quantify measures such as the frequency and duration of extreme hydrologic events and variability in timing and magnitude of flow events through the year (Gao et al. 2009). Scenario projections of future flows could also be utilized to examine how flows are predicted to change in the Slave and Hay River basins, and assess what such changes might mean for the normal range of variability in BMI metrics. In addition, flow-based metrics of BMI composition (e.g., CEFI; Monk et al. 2008, Monk et al. 2018) could be applied to aid in the characterization of BMI response to flow in these systems and the prediction of expected changes to composition with future flows. This strategy will allow for the classification of data in future years based on flow condition, and comparison of BMI monitoring data with appropriate normal range conditions. Samples collected in 2020 can be used in combination with the 2017-2019 samples and historical flow data for the rivers to begin to explore flow-based development of assessment criteria.

# Table of Contents

# 1. Introduction

The Government of the Northwest Territories (GNWT) and the Government of Alberta (GOA) are working to establish a monitoring program for the bioassessment of large transboundary rivers (MacDonald Environmental Sciences Ltd. 1995, Lento 2017). Transboundary rivers provide unique challenges to assessment, as monitoring designs must meet the objectives of multiple jurisdictions that may differ with respect to economic and social goals as well as environmental management strategies (MacDonald Environmental Sciences Ltd. 1995). However, the potential for upstream development within one jurisdiction to cause downstream impacts within another jurisdiction emphasizes the need for cooperation in the monitoring of transboundary waters to ensure the detection of changes to ecosystem health (Flotemersch et al. 2011). Establishment of long-term monitoring and assessment supports the future detection of impacts that may arise from human development, but also supports the detection of ecological changes in response to a warming climate.

## 1.1. General Approach of the Monitoring Program

Monitoring questions related to assessing ecosystem health may be focused on comparison of reference sites with test sites in the presence of a known stressor, or they may be focused on characterizing the contemporary status of biotic and abiotic ecosystem components and evaluating whether any temporal changes have occurred (e.g., see Environment Canada 2011, Culp et al. 2012b). One approach used in biological monitoring, particularly in the case of detecting future evidence of impairment, is to estimate the normal range of community composition based on natural variability in the system, and to detect any shifts in the diversity or abundance of organisms that occur over time (Munkittrick et al. 2009, Munkittrick and Arciszewski 2017). Where there is not a clear stressor in place, determining the range of "normal" variation in the data can be used to establish a baseline ecological condition, providing information that can be used in future years (with continued monitoring) to begin to address targeted questions as stressors increase (Munkittrick et al. 2009, Munkittrick and Arciszewski 2017). Quantification of variation that might be expected in the absence of impairment can support the development of "trigger" levels, or levels at which the magnitude of observed change is greater than expected, necessitating additional monitoring or management action (Arciszewski and Munkittrick 2015). Future assessments could focus on examining relationships of natural and anthropogenic drivers of change with ecosystem health, and detecting evidence of cumulative impacts (e.g., from a combination of climate change, development, resource exploration, or other stressors; Dubé 2003, Dubé et al. 2013, Somers et al. 2018). Establishing a strong baseline for comparison is a vital step in this process to allow for future detection of ecosystem responses to change (Culp et al. 2012b).

The initial focus of the GNWT and GOA transboundary monitoring program is on benthic macroinvertebrate (BMI) assemblages, which are an important ecosystem component to monitor in northern rivers as an integrated measure of water quality and habitat condition (Culp et al. 2012b, Buss et al. 2015, Lento et al. 2019). BMIs are commonly chosen for biomonitoring because they are widespread, easy to sample and identify, species-rich, have limited mobility, and have known tolerances and sensitivities to habitat conditions that can support the detection of anthropogenic impacts (Bonada et al. 2006, Resh 2008, Buss et al. 2015). Because they have generally low mobility, BMI respond to local-scale changes in water chemistry and habitat quality and are an excellent indicator of the physical and chemical impacts of disturbance. BMI provide a more time-integrated measure of change than spot

measurements of water chemistry, which only describe conditions at the time of sampling. Moreover, BMI diversity at northern latitudes is strongly linked with temperature as a result of taxon-specific thermal tolerances (Culp et al. 2018, Lento et al. 2019). With climate change, it is predicted that biodiversity in northern regions will begin to more closely resemble those of lower-latitude temperate systems through the northward movement of eurythermic and cold-intolerant species (Culp et al. 2012a, Lento et al. 2019). Thus, the long-term assessment of BMI assemblages has the potential to detect changes in response to a warming climate in addition to detecting future impacts from human development.

Within the Alberta-Northwest Territories transboundary river regions, there is relatively little information about the current state and composition of benthic assemblages. Assessments of BMI assemblages in the large transboundary rivers of the Alberta-Northwest Territories region have been limited (but see Paterson et al. 1991, Paterson et al. 1992 for baseline assessment of Slave River BMIs, and Golder Associates 2010 for an overview of existing assessments), and Dagg (2016) noted that this lack of background knowledge has made it difficult to identify water quality concerns and potential for impairment during local community discussions of potentially vulnerable ecosystem components. Therefore, it is vital that routine monitoring of large transboundary rivers be established to secure information about baseline conditions in these assemblages and to provide sufficient information to allow for future detection of trends.

## 1.2. Establishing Normal Ranges

In biomonitoring, the concept of the normal range is based on the idea that it is not always possible to access data from before any perturbation occurred in a region (Arciszewski and Munkittrick 2015), nor is it necessarily desirable to use such historical data if they do not accurately represent attainable water quality levels (Stoddard et al. 2006, Munkittrick and Arciszewski 2017). Instead, if sufficient contemporary data are collected to allow estimation of the range of variability that is acceptable given current conditions in a system, then this information can be used to detect any future deviations and pinpoint where targeted sampling should take place to identify causes of impacts (Kilgour et al. 2017, Munkittrick and Arciszewski 2017).

The normal range quantifies the range of variability in a community metric that is expected and acceptable for a system, given its current conditions. Values falling outside that range indicate that more monitoring is required or that management action must be taken. Quantifying the normal range for a system requires characterization of spatial variability within the system, but the ultimate goal is to describe temporal variability, to determine whether changes in metric values in subsequent monitoring years fall outside the range of acceptable variability. The use of the normal range allows us to estimate and control for short-term (inter-annual) temporal variability to allow for the detection of potentially subtle changes happening over a longer time scale (e.g., 10+ years; Arciszewski and Munkittrick 2015).

Baseline data must be collected for multiple reference sites over multiple years, with sampling taking place in a single season (e.g., fall), and subsequent monitoring activities must continue at multiple sites for many years to allow for effective detection of change (Arciszewski and Munkittrick 2015). In the first year of collecting baseline data, spatial variability among sites is described, and in subsequent years the natural temporal variability is quantified, and measures of temporal and spatial variability are refined. At least three years of baseline data must be collected before temporal variability can begin to be

estimated, including the characterization of the regional normal range. However, measurements based on three years of data are only initial estimates, and additional sampling beyond three years is recommended to achieve greater accuracy and precision in estimates of temporal variability and to detect any shifts in normal range due to climate change (Arciszewski and Munkittrick 2015). In their analysis of long-term fish monitoring data from the Moose River, Arciszewski and Munkittrick (2015) noted that the precision of their estimates of variability improved as additional years of data were added, and they recommended a minimum of 12 years of data to capture the variability in the system, though the number of years required will vary among systems and may differ among target organism groups. Jackson and Füreder (2006) suggested that five years of monitoring was the minimum number required to capture the range of ecological variability in BMI assemblages in response to short-term climatic cycles, but noted that at least 10 years of monitoring was required to capture the response to longer decadal cycles.

### 1.3. Quantifying Meaningful Change: Critical Effect Sizes

The concept of the normal range applies well to the situation where a monitoring program is being established in anticipation of potential future impacts, because it allows for quantification of the current status in the system as well as the level of change that would be deemed significant enough to warrant concern, termed the critical effect size (CES; Munkittrick et al. 2009, Arciszewski et al. 2017, Munkittrick and Arciszewski 2017). The CES is the magnitude of difference between sites or change across time (within a site) that is considered to be meaningful and to have ecological implications (Munkittrick et al. 2009). The CES forms the lower and upper boundaries of the normal range, indicating values below and above which there is meaningful change among sites or over time. It can act as a trigger point in adaptive monitoring plans to identify when additional sampling is necessary to investigate potential drivers of change (Somers et al. 2018).

In ongoing monitoring, the CES identifies the magnitude of change that is required before management action is taken, but in the development of monitoring programs, CES can also be used to ensure sampling designs are sufficient to detect impairment (Munkittrick et al. 2009). For example, as the normal range of variability across systems is quantified in pilot sampling years, the CES (values at the upper and lower limits or boundaries of the normal range) can be determined and used in power analysis to estimate the number of samples that would be required to detect a meaningful difference among sites. A number of different approaches have been used to determine CES for different groups of organisms (see review in Munkittrick et al. 2009); however, studies of BMI assemblages that assess natural variability within and among sites have generally relied on standard deviation units or similar approaches (e.g., confidence intervals or probability ellipses) to set CES. For example, the CES for invertebrate abundance might be set to 2 SDs above and below the mean abundance observed in baseline data. Exceedance of the CES by any site in future years would then act as a trigger to increase sampling efforts and determine if impairment has occurred. Initial establishment of variation among all sites in a river, as a measure of spatial variability, can be done with pilot-year monitoring data, but as more data are collected, it is important to refine the spatial CES to account for short-term temporal variability that is likely to be observed within systems (Arciszewski and Munkittrick 2015). Once at least three years of data have been collected (the minimum required to calculate CES), the CES can begin to be refined to capture site-specific temporal variability and quantify confidence intervals that can be used in future years to detect deviations from normal range. For example, river flow can be highly variable from one year to the next, and these changes in flow can have noticeable impacts on BMI

assemblage composition, with higher flow years favouring taxa that prefer fast velocities and low flow years resulting in a dominance of taxa that prefer slower velocities (Monk et al. 2008). Such shifts in assemblage composition might appear indicative of impacts if there is no quantification of the natural flow regime in a system.

### 1.4. Purpose and Objectives

The objective of this report is to assess spatial variability within the Hay and Slave rivers from the third year of sampling in the GNWT and GOA large transboundary river BMI monitoring program, and to assess temporal variation within and among sites and reaches (from 2017-2019) as an initial estimate of normal range and critical effect size. The Hay River and the Slave River in northern Alberta-southern Northwest Territories were sampled in August and September 2019 (respectively). Water chemistry, sediment chemistry, physical habitat, and BMI kick samples were collected using the methods described by Lento (2018), and data were analyzed to characterize spatial and temporal variability within the rivers, including quantification of CES for a number of biotic metrics. Though spatial variability within and among sampled reaches is assessed to characterize and describe the data collected in 2019, the emphasis of this report is on the initial quantification of temporal variability, which will build the foundation for future monitoring and detection of impacts in these systems. Analysis of the samples collected during this pilot project will be used to inform future sampling efforts in these rivers and will contribute to building a baseline database for continued monitoring.

## 2. Methods

### 2.1. Study area and sample timing

The pilot program of the GNWT and GOA large transboundary river monitoring program is focused on the Slave River and the Hay River. Both rivers originate in Alberta flowing north into the Northwest Territories and terminating in Great Slave Lake (Figure 1), but they differ with respect to size, flow, and upstream land use (see overview in Golder Associates 2010). The Slave River is a large, fast-flowing river, with a mean annual discharge rate of 3,400 $m^3/s$ (Sanderson et al. 2012) and a drainage basin of over 616,000 $km^2$ (Golder Associates 2010). The Hay River is narrower, more shallow, and slower-flowing, with a drainage basin of 48,100 $km^2$ (Golder Associates 2010). Details on the geology, climate, land cover, and land use history of both river catchments can be found in state of knowledge reports for the Hay River (Stantec Consulting Ltd. 2016) and Slave River (Pembina Institute 2016). Both rivers have the potential to be impacted by a variety of human activities in the upstream basin, including oil and gas development and pulp and paper mills. Though change may have already occurred in these systems due to upstream activities, lack of historical baseline data precludes the assessment of such changes. The current program is aimed at characterizing the current ecological condition of these rivers as a baseline for future assessments.

The differences between these rivers with respect to size, depth, and flow lead to unique challenges that must be considered when planning and conducting BMI sampling. For example, although sampling is designed to occur in the fall in part to take advantage of increased access to the shoreline that is gained when water levels recede, the exact timing required for sampling the Slave and Hay Rivers differs due to local conditions. The deep and fast-flowing Slave River has to be sampled late enough in the fall

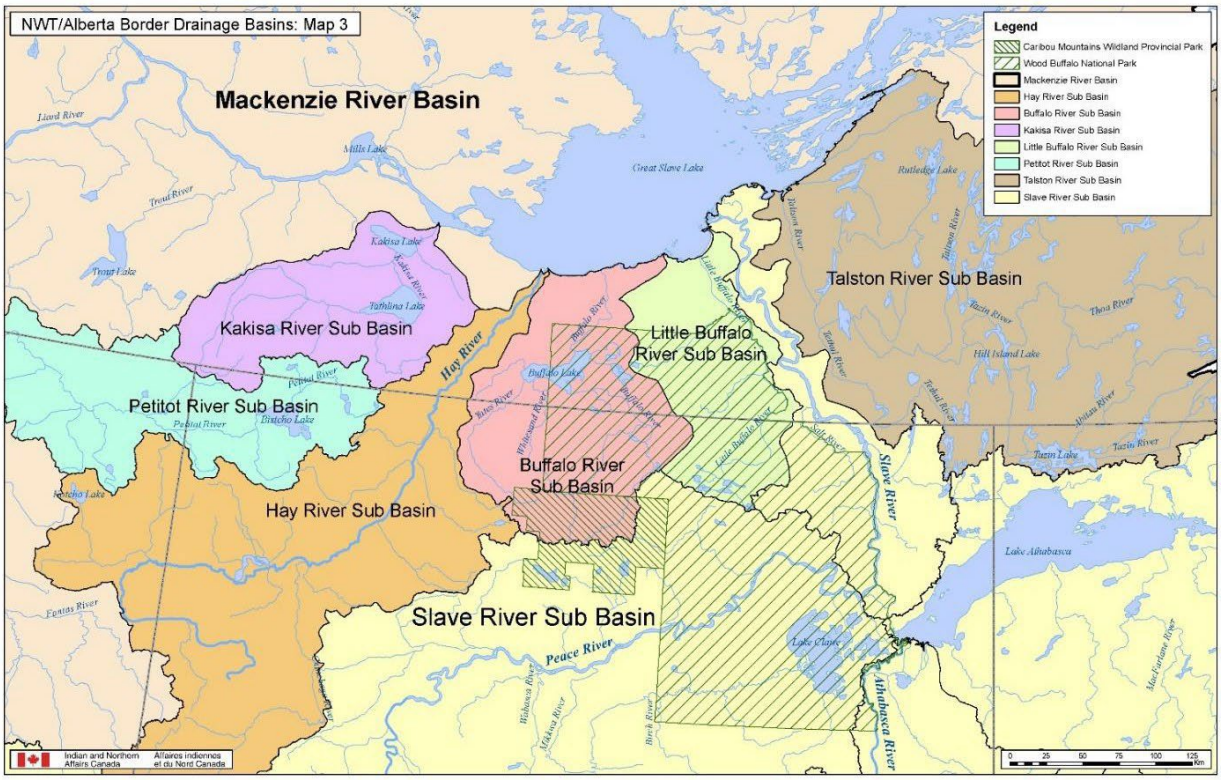


*Figure 1. Drainage basins at the NWT/Alberta border, including the Hay River Sub Basin and Slave River Sub Basin. Map created by Indian and Northern Affairs Canada.*

to allow safe access to shorelines for kick sampling, whereas the timing of sampling of the Hay River has to be early enough to ensure that the shallower river does not become inaccessible by boat. Furthermore, additional safety equipment is required to safely sample the deeper, faster-flowing Slave River, whereas the Hay River requires a lower-profile boat to maneuver through sand bars in low water level situations.

The exact timing of sampling for each river is dependent on flow conditions in the sampling year (see details for the Hay River in section 3.1.1 and for the Slave River in section 3.2.1.1). The Hay River is generally sampled before the Slave River, to ensure water levels are not too low to access the sampling locations. In 2019, the Hay River was sampled from August 13-15, and the Slave River was sampled from September 12-15.

## 2.1. Site selection

The BMI monitoring plan for large transboundary rivers (described briefly here, but see Lento 2018 for details) prescribes a sampling design with 5-10 approximately 500-m-long reaches sampled in a river. The number of reaches depends on how variable the reaches are, and how many would be required to characterize the river and achieve adequate power to detect biologically-meaningful differences among reaches, if they were to exist (with this number refined through the assessment of baseline monitoring data). Reaches are selected to have similar substrate composition throughout the reach. The goal is to select reaches with rocky substrate, as these will have the most diverse BMI assemblages, though soft


*Figure 2. Map of Hay River and Slave River, showing kick-sampling reaches (red points) sampled in 2019, and an overlay of the stream network. Stream network layer from National Hydro Network (NHN) GeoBase Series (open.canada.ca).*

sediments are deemed acceptable if comparable substrates can be sampled in additional reaches (see Lento 2017, 2018 for more details). Within each reach, five replicate kick-sites are sampled, approximately 50-125 m apart. If access to both banks of the river is possible, a total of 10 kick-sites are sampled within a reach (five on each river bank). This design allows for the application of multiple statistical analyses to characterize variability within a river. For example, sites can be compared directly along a longitudinal gradient, or sites can be treated as replicates in a statistical comparison of reaches. This design was applied during the first three years of sampling, though some adjustments were made to reflect local conditions.

Both rivers were accessed via boat launches on the Alberta side of the border (Figure 2). Five kick-sampling reaches were chosen within each river for the pilot year of sampling, and this number was increased to six in the Hay River in 2018 and to six in the Slave River in 2019 (Table 1; Figure 2). Sample reaches were selected to be approximately 500 m in length, though in some areas, the availability of suitable habitat limited the total length of reaches (e.g., in the Hay River, reaches were 250 m to 500 m in length, whereas in the Slave River, reaches were 250 m to 600 m in length). Sample reaches were numbered KS1 to KS5 or KS6 in each river, with KS1 representing the farthest upstream sampling

*Table 1. Approximate coordinates in decimal degrees (DD) for each kick-sampling reach sampled in the Hay River and Slave River in August-September 2019. Reach codes are explained in text.*

| River | Reach | Latitude (DD) | Longitude (DD) |
|---|---|---|---|
| Hay River | HR-KS1 | 59.9321 | -116.9524 |
| | HR-KS2 | 59.9465 | -116.9565 |
| | HR-KS3 | 59.9885 | -116.9304 |
| | HR-KS4 | 60.0026 | -116.9713 |
| | HR-KS5 | 60.0113 | -116.9218 |
| | HR-KS6 | 60.0279 | -116.9216 |
| Slave River | SR-KS1 | 59.4085 | -111.4620 |
| | SR-KS2 | 59.4276 | -111.4629 |
| | SR-KS3 | 59.5350 | -111.4577 |
| | SR-KS4A | 59.5912 | -111.4195 |
| | SR-KS4B | 59.5903 | -111.4225 |
| | SR-KS6 | 59.6766 | -111.4856 |
| | SR-KS5 | 59.7182 | -111.5058 |

location and KS5 or KS6 representing the farthest downstream sampling location (Figure 3). The exception is the Slave River: the name for reach KS6 was assigned because it was added two years after the other reaches were chosen (KS1 to KS5), but it is located upstream of KS5 (Figure 3B). Reach 4 of the Slave River was the only location where sampling took place on both banks of the river, resulting in two sets of sites (HR-KS4A and HR-KS4B) in the same reach (Table 1). In the Hay River, reaches were 2.5 to 6.7 km apart, whereas in the larger Slave River, reaches were 1.9 to 11.8 km apart.

The Hay River is sinuous with slow flow, and reaches with rocky habitat were generally found at the bends of the river, typically on the erosional banks (Figure 3A). The depositional bank was generally a thick silty/muddy substrate that would not have allowed for access or for sampling (unlike sandy habitats, in which kick sampling can be conducted). Because of the shallow nature of some extents of the river, site selection was limited in some areas to reaches that could be accessed from the boat launch in a timely manner using a canoe with outboard motor. Analysis of reaches sampled in 2017 indicated that there were some differences between reaches upstream (HR-KS1 to HR-KS3) and downstream (HR-KS4 and HR-KS5) of the boat launch and inflow from tributaries, and a recommendation was made to sample an additional reach downstream of the boat launch to ensure adequate replication in the downstream portion of the river. Reach HR-KS6 was added in 2018 in response to this recommendation (Table 1; Figure 3A), and it was found to resemble the two other downstream reaches (Lento 2020).

The Slave River is wider than the Hay River with a straighter channel and faster flow (Figure 3B). Rocky substrates were generally found in areas of rocky outcrops along the shoreline. In the analysis of data from 2017 and 2018, substrate and flow appeared to play a large role in determining the BMI assemblage that was characteristic of a particular reach, and a recommendation was made to add another reach with rocky habitat and fast flow. In 2019, Reach SR-KS6 was added upstream of reach SR-KS5 (Figure 3B). In this report, the suitability of this reach will be assessed through comparison with other reaches sampled in 2019.

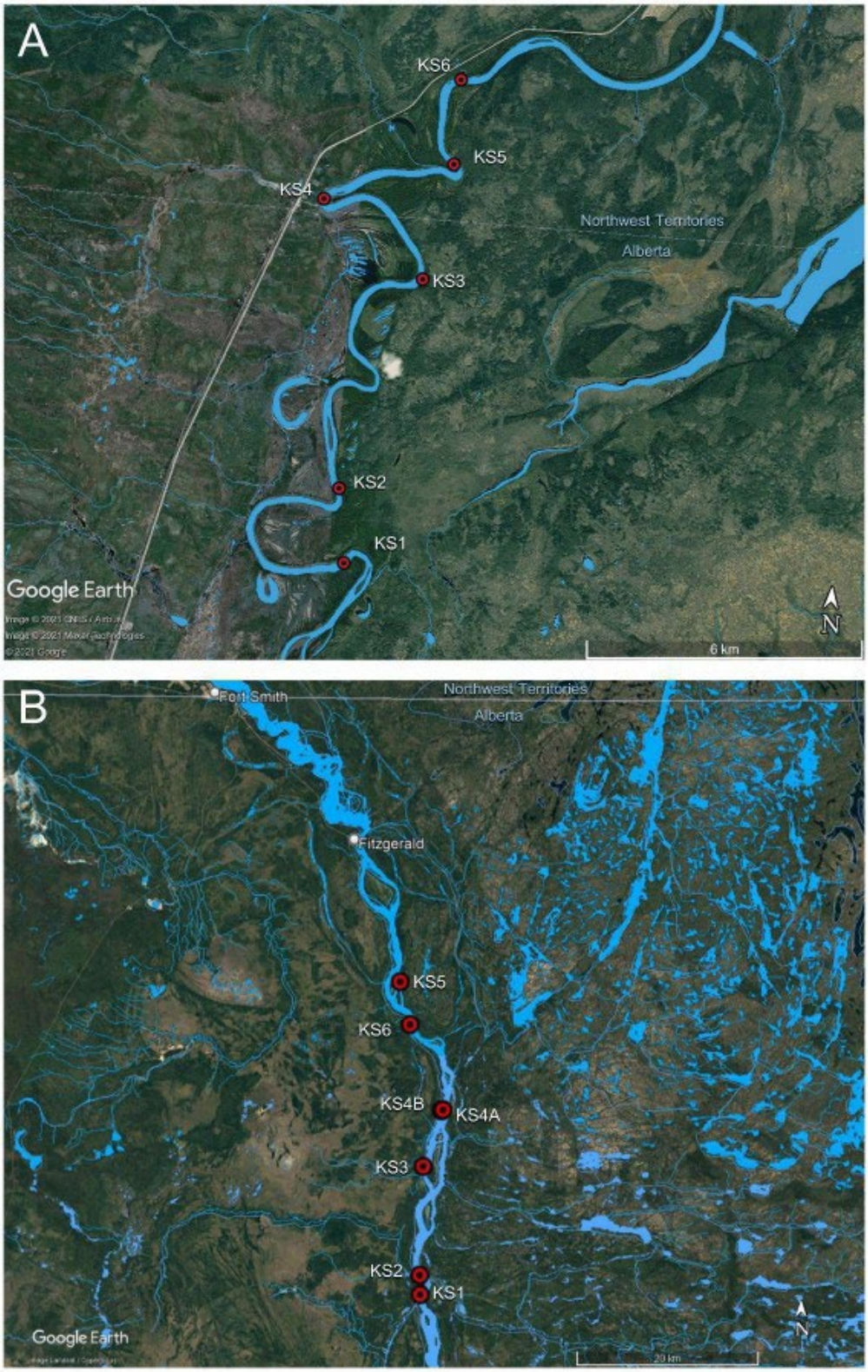


*Figure 3. Kick-sample reaches (red points) in the (A) Hay River and (B) Slave River in 2019. Reaches are labeled in white text. Water body and stream layers overlain on maps are from the National Hydro Network (NHN) GeoBase Series (open.canada.ca).*

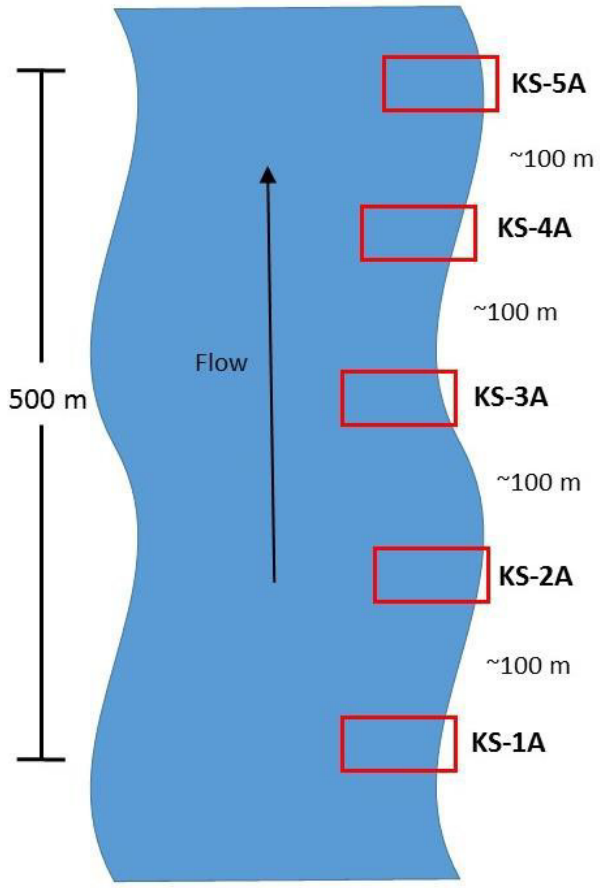


*Figure 4. Example sampling design used for a single reach within the Hay River and Slave River, indicating the location of 5 sites within the 500 m reach and numbering of sites with respect to flow direction. Sampling of sites began downstream, at site KS-5A and worked upstream towards site KS-1A. Sites located on the opposite bank (left bank, when facing downstream) were numbered KS-1B through KS-5B. Sites were located approximately 100 m apart (50 m to 125 m) and sampling extended out into the river to a depth of approximately 1 m (maximum safe depth for kick sampling).*

Sampling took place in each reach on the bank where rocky habitat was located (e.g., see Figure 4 for an example of single-bank sampling design). Kick-sites within a reach were numbered 1-5, with site 1 as the farthest upstream site and site 5 as the farthest downstream site (consistent with the numbering of reaches); however, sampling was done at kick-site 5 first to avoid downstream contamination of samples. The right-hand bank while facing downstream (river right) was called the A bank and the left-hand bank (river left) was the B bank, and each site code was appended with A or B to indicate which side of the river was sampled. Reach KS4 in the Slave River was the only location (for either river) where sampling was feasible on both banks, and samples were collected from both the A and B banks in this reach to compare habitat conditions and BMI composition. Kick-sites were evenly spaced within reaches, when habitat availability allowed. Distance between kick-sites was generally 50-125 m, as allowed by reach length. Kick-sites within each reach were generally of similar substrate composition, and were chosen to minimize differences in substrate composition. Based on data from 2017 and 2018, recommendations were made to shift some sites that appeared to be too silty (e.g., SR-KS2-1A, SR-KS4-1A, and SR-KS4-2A). These reaches were shifted to rockier habitat in 2019 to ensure data were more comparable with other reaches.

## 2.2. Sample Collection

Sample collection at kick-sampling locations followed the methods prescribed in the monitoring plan (Lento 2018), including collection of water chemistry samples, use of handheld meters for field chemistry, a habitat survey (modified from the Canadian Aquatic Biomonitoring Network - CABIN), a modified three-minute CABIN kick sample, and a modified rock walk (see details in Lento 2018).

At three of the kick-sites in each reach (odd-numbered kick-sites), water samples were collected for analysis of a standard suite of parameters, including nutrients, ions, and suspended solids. Additional water samples were collected for the analysis of metals (including mercury) at the same three kick-sites. These samples represented spot measurements of water chemistry, and were intended to characterize the chemical habitat at the time of sampling to provide supporting information that could help in understanding the distribution of BMI assemblages. Water chemistry samples were kept cool and sent to Taiga Environmental Laboratory for analysis. A handheld meter was used to record air and water temperature, pH, specific conductivity, dissolved oxygen, and turbidity on-site.

Sediment samples were collected to analyze metals and polycyclic aromatic hydrocarbons (PAHs) in soil. Because BMI live in contact with or burrow within the sediment, contaminant concentrations within the sediment may more accurately reflect their exposure levels. Sediment samples were taken from within the channel at two sites in each reach (sites 1 and 5) and placed into jars. Sediment samples were kept cool and sent to ALS Labs for analysis.

BMI kick samples were collected at each kick-site using a modified travelling kick method (Lento 2018). The operator held a 400-μm-mesh kicknet with an attached collection cup downstream while standing in the river near the shore at a wadeable depth (approximately 1 m). The operator then kicked and disturbed the substrate upstream of the net for a period of three minutes while moving upstream in a slight zig-zag fashion (maintaining the same approximate depth). Because of the size of each river, sampling remained in the nearshore habitat rather than attempting to cross the channel as in a standard kick sample method. Samples were retrieved from the net and collection cup and stored in 95% ethanol for transport to the lab for sorting and identification. Samples were sorted and identified following standard CABIN protocols (Environment Canada 2014) by Biologica Environmental Services Ltd. In brief, samples were sorted using a Marchant box to randomly sub-sample until at least 300 individuals were counted. BMI were identified to the lowest practical taxonomic level. In addition, a large/rare sort was completed following the sub-sampling procedure, with an abbreviated survey of the remaining cells in the Marchant box to pick out any large or particularly rare taxa that might have been missed as part of the sub-sampling process. Although a large/rare sort is not part of the standard CABIN laboratory procedures, the use of this approach recognizes that sub-sampling procedures may exclude large taxa that contribute a great deal to biomass and secondary production in the system, but that are fewer in number and thus less likely to be encountered than smaller, more common taxa. Inclusion of these organisms provides a more accurate measure of diversity. Individuals identified as part of a large/rare sort may include taxa from families of large-bodied dragonflies and stoneflies, as well as large molluscs.

CABIN field survey sheets (Environment Canada 2012) were completed at each site in order to characterize the in-stream and surrounding habitat. This survey included a description of riparian vegetation, surrounding land use, and % cover of macrophytes and % cover of periphyton in the river at each site. In addition, water velocity was measured and a modified rock walk was completed at each

site. Operators selected substrate particles at random and measured the intermediate axis (b-axis) of each particle to the nearest mm to characterize substrate composition. This was completed for 20 substrate particles at each site. Rock walk data were summarized as percent composition in each particle size class.

## 2.3. Data Analysis

2019 was the third year of data collection for the Hay and Slave Rivers, and as a result, the emphasis in this report is on estimating the range of variability within and among reaches from 2017-2019, to begin to describe the normal range for BMI assemblages in these systems. Spatial variation in 2019 data is initially considered to characterize abiotic conditions at the time of sampling and describe the most recently-collected BMI data. The focus is then placed on evaluating change over time and inter-annual variability in biotic metrics and assemblage structure. Normal range criteria developed in this report represent initial estimates based on only three years of data, which is the minimum number of years that can be used for this procedure. Because they are based on only three years of data, it is expected that these initial criteria will have low precision due to inter-annual variability in assemblage structure. In future years, estimates of normal range developed in this report will be revised and refined with the addition of new data, leading to better accuracy and precision in this measure.

### 2.3.1. Hydrology

Flow in the Hay and Slave Rivers was variable between 2017 and 2018, and it appeared to contribute to changes observed in the abundance and richness of BMI in the rivers, particularly the Slave River (Lento 2020). Because water levels differed again in 2019, the annual hydrographs for each river were examined, and simple flow metrics were compared between years. To reflect recent changes experienced by the BMI assemblage prior to sampling, antecedent conditions were summarized as the median flow in the 30 days preceding sampling and in the 60 days preceding sampling. The coefficient of variation (CV; calculated as the mean divided by the standard deviation, and converted to a percentage) was also calculated for each time period and for each year, in order to quantify variability in antecedent flow conditions.

### 2.3.2. Spatial characterization of reaches

#### *2.3.2.1. Chemical and physical habitat*

##### 2.3.2.1.1. Variation within and among reaches

Spatial variation in the chemical and physical habitat of the Hay and Slave Rivers were assessed to characterize the BMI habitat at the time of sampling. Variability in water chemistry, physical habitat (e.g., substrate size, velocity, etc.), and sediment chemistry was summarized for the Hay River and Slave River in a series of tables showing the mean ± standard deviation of chemical and physical habitat parameters for each reach. Water chemistry and sediment chemistry means were compared with CCME water and sediment quality guidelines, respectively (Canadian Council of Ministers of the Environment 2001b, a). However, it should be noted that as chemistry samples represented only spot measurements, any exceedances of guidelines should be interpreted with caution, as they may not reflect long-term trends.

Box plots were used to present summaries of variation in water chemistry within and among reaches, and among-reach variation in water chemistry was assessed separately for Hay River and Slave River

using a one-way analysis of variance (ANOVA) design, with a chemical parameter as the response variable and the reach as the grouping factor. Because sediment chemistry samples were only taken at two sites per reach, only summary statistics were provided. For water chemistry, the analysis focused on a selection of major ions, nutrients, physicals, and metals that displayed some variation among sites and where values were above detection limit for at least half of the sites (e.g., total suspended solids, total and dissolved nitrogen, total phosphorus, conductivity, alkalinity, aluminum, iron, manganese, and mercury). For the purpose of this analysis, values below the detection limit were changed to be half the detection limit. When the ANOVA indicated a significant difference among reaches, a Tukey HSD post-hoc test was used to determine which reaches differed. Chemical parameters were $\log_{10}$-transformed as needed to normalize residuals and stabilize residual variance. ANOVA is known to be robust to violations of the assumption of homoscedasticity in the residuals (Zar 1999), but when residuals were still heteroscedastic following transformation of the data, a non-parametric Kruskal-Wallis test was used to confirm the results of the ANOVA. If the results of the non-parametric test matched those of the parametric test, it was concluded that violations of the assumption of homoscedasticity were not severe enough to affect the outcome of the ANOVA. All ANOVAs were run in Systat12 (Version 12.02).

##### 2.3.2.1.2. Multivariate assessment of chemical/physical habitat

Multivariate analysis was used to fully characterize the abiotic environment of each river using measured water chemistry and physical habitat parameters. This analysis was intended to estimate variability within and among reaches, and to identify any potential ecological outliers (e.g., sites with extremely high axis scores) or gaps in sample sites. Water chemistry and physical habitat parameters measured at all sites were used to assess variation and identify major gradients in the abiotic environment through Principal Component Analysis (PCA) with standardization of variable scores. The analysis included major ions, nutrients, physicals, and metals (focusing on those that were above detection limit and that showed some variation among sites, i.e., were not the same across all sites), as well as water velocity and substrate composition. Water velocity was not recorded at one site (HR-KS4-1A), and that site was omitted from analysis as a result. It was not possible to conduct the rock walk at three sites in the Hay River (HR-KS1-5A, HR-KS3-5A, and HR-KS5-5A), but as water chemistry samples were only collected at odd-numbered sites, omission of these sites would have reduced three reaches to only two samples each for the analysis. Variation in substrate composition within reaches was fairly low in the Hay River, so substrate composition from site 4 in each of these reaches was substituted for the missing data. Prior to analysis, all abiotic parameters were $\log_{10}$- or logit-transformed as appropriate. Multivariate analyses were run in Canoco (version 4.05; ter Braak and Šmilauer 2002).

#### *2.3.2.2. Biotic assemblages*

##### 2.3.2.2.1. Variation within and among reaches

Variability in BMI assemblage composition was summarized for the Hay River and Slave River in tables showing the mean ± standard deviation of biotic metrics for each reach. Biotic metrics included many compositional metrics that are commonly used in biomonitoring (see background on metric development and diagnostic testing in Barbour et al. 1999 and references cited therein), including those that describe general patterns in diversity and abundance, and those that characterize diversity and abundance of dominant taxonomic groups (total abundance; total taxonomic richness; abundance, relative abundance, and richness of Ephemeroptera, Plecoptera, and Trichoptera (EPT; mayflies, stoneflies, and caddisflies), Chironomidae (midges), Diptera (true flies, including midges) + Oligochaeta

(segmented worms), and Mollusca. Calculations of richness (total taxonomic richness, EPT richness, Chironomidae richness, Diptera + Oligochaeta richness, and Mollusca richness) were based on the number of unique taxa identified at the lowest practical taxonomic level.

Box plots were used to present summaries of variation in BMI metrics within and among reaches, and among-reach variation in BMI assemblage composition was assessed separately for Hay River and Slave River using a one-way ANOVA design, with a biotic metric as the response variable and the reach as the grouping factor. This analysis was completed to identify any differences along the extent of the river, to characterize the degree of spatial variability among reaches. Due to a high number of zeroes, metrics based on Mollusca were omitted from this analysis. When the ANOVA for a metric indicated a significant difference among reaches, a Tukey HSD post-hoc test was used to determine which reaches differed. Biotic metrics were $\log_{10}$- or logit-transformed as needed to normalize residuals and stabilize residual variance. All ANOVAs were run in Systat12 (Version 12.02).

##### 2.3.2.2.2. Multivariate assessment of BMI assemblage composition

Multivariate analysis was used to fully characterize the biotic assemblage of each river using data for all identified taxa (not biotic metrics). This analysis was intended to assess correlations and variability within and among reaches, and to identify any potential ecological outliers (e.g., sites with extremely high axis scores) or gaps in sample sites. BMI relative abundance data were summarized for multivariate analysis at the family/subfamily level, with Chironomidae at subfamily and all other taxa at family or higher (as this level has been shown to be sufficient to characterize Arctic river BMI data while reducing noise from more detailed taxonomy; Lento et al. 2013, Culp et al. 2019). Taxa identified to genus level were combined at the family/subfamily level, and those identified to a coarser level (e.g., order or higher) were retained if they were unique (i.e., not identified at family/subfamily or genus level in any sample from the river). Spatial variation in assemblage structure among sites was assessed using PCA because there was low turnover among samples, which indicated that assemblage variance was best described by a linear model. PCA was run in Canoco (version 4.05; ter Braak and Šmilauer 2002).

Variability in assemblage structure within and among reaches was assessed statistically to determine whether there were significant differences in composition among reaches, and to evaluate whether compositional variability within reaches was similar along the sampled length of each river. PERMANOVA (Permutational Multivariate Analysis of Variance; McArdle and Anderson 2001, Anderson 2017), a rank-based multivariate approximate to ANOVA, was used to test whether there were significant differences in assemblage composition among reaches based on a dissimilarity measure (Sørenson dissimilarity index). Pairwise tests, analogous to post-hoc tests in univariate ANOVA, were used to identify differences among reaches when the PERMANOVA results indicated a significant effect of reach on composition. Variability within reaches was assessed using a test for homogeneity of multivariate dispersions (Anderson et al. 2006). This analysis used the site dissimilarity matrix to calculate the distance to centroid (in multivariate space) for each reach, as a measure of variability among reaches (the farther the distance to centroid, the greater the dissimilarity among sites in a reach). A permutational pairwise test was used to identify significant differences in the distance to centroid among reaches to compare the magnitude of within-reach variability. Distance to centroid was plotted with a box plot to visualize within-reach variability across reaches for each river. To control for an increased rate of Type I error, a false discovery rate (FDR) correction was applied to $\alpha\alpha$ for all pairwise comparisons (Benjamini and Hochberg 1995). PERMANOVA and homogeneity of multivariate

dispersions were run in R version 4.1.1 (R Development Core Team 2015) using the packages vegan (Oksanen et al. 2015) and pairwiseAdonis (Martinez Arbizu 2020).

##### 2.3.2.2.3. Biotic-abiotic relationships

Variation in biotic metrics within and among reaches in 2017 and 2018 was suggested to be driven in part by different flow velocity among sampling sites. To test whether this was the case in 2019, BMI metrics were plotted as a function of velocity, and a least-squares regression was run for each metric to determine whether it varied in response to velocity. Where regression residuals indicated that a curvilinear model would be a better fit to the data than a linear model (i.e., unimodal pattern in residuals), a polynomial regression was run using the model: BMI metric = velocity + velocity$^2$. All regressions were run in Systat12 (Version 12.02).

The relationship between the BMI assemblage data and abiotic data was tested with Redundancy Analysis (RDA), with a subset of abiotic parameters (water chemistry and physical habitat) selected for inclusion as constraining variables based on their importance in the abiotic PCA. Because there were BMI data for all 5 sites in each reach, but only water chemistry for odd-numbered sites, this analysis used average water chemistry values for site 2 and site 4 in each reach (e.g., site 2 used the average of sites 1 and 3, and site 4 used the average of sites 3 and 5 for each water chemistry parameter). This approach was found to be appropriate in the analysis of data from 2018 (Lento 2020). Prior to analysis, all abiotic parameters were $\log_{10}$- or logit-transformed as appropriate, and all BMI data were $\log_{10}(x+1)$ transformed. RDA was run in Canoco (version 4.05; ter Braak and Šmilauer 2002).

### 2.3.3. Temporal characterization of reaches

Analysis of temporal variation in monitoring data from 2017 to 2019 began with a general assessment of changes to composition, including taxonomic richness and abundance. Pie charts of the average relative abundance of major invertebrate groups (e.g., numerically abundant insect orders and orders or classes of non-insects) across all reaches were used to compare composition between years (2017, 2018, and 2019) for the Hay River and Slave River. These plots were used for a visual assessment of major changes that occurred between sampling years. Multi-year BMI metric box plots were created to assess reach-level changes over time, with separate boxes plotted for each year of sampling. In addition, line plots were created for each biotic metric, with all reaches overlain on the same plot to examine general patterns of change over time.

ANCOVA was used to assess the response of metrics to varying flow conditions between years, with site-scale velocity included as a covariate. The first step of the analysis was to test the full model: metric = velocity + year + velocity*year where year was a categorical variable that was used as a proxy for flow conditions, and the interaction term (velocity*year) tested whether the relationship between the biotic metric and velocity differed between flow years. If the interaction term was not significant, it was removed and a reduced model was run to test whether mean levels of metrics differed across years (while controlling for differences in velocity across sites). Tukey's HSD post hoc test was used in pairwise comparisons to identify significant differences in metrics between years.

### 2.3.4. Normal range and CES

The CES approach makes use of the variation among samples to determine if test samples are impaired (i.e., if they fall outside the normal range, or range of natural variability). The CES is based on variability

in the data, and changes in habitat conditions that result from natural variability (i.e., due to shifts in flow, timing of the spring freshet, water temperature, etc.) may lead to different normal ranges from one year to the next. The greater the number of years of data that can be used to develop normal range estimates and set CES, the closer the estimates will be to accurately and precisely capturing natural variability in the system. In this report, CES is used to assess within-year variability as well as variability across the three years of sampling.

#### *2.3.4.1. Within-year variability*

During the initial two years of monitoring, CES was developed spatially using all sites sampled in the river (Lento 2020). CES limits were determined for the Hay River and Slave River by calculating the mean and standard deviation of each BMI metric and setting bounds of CES equal to the mean ± 2 SD, following the approach of previous BMI monitoring programs (see Munkittrick et al. 2009). The CES was calculated based only on data from the current year of sampling, to assess within-year variability among sites (Arciszewski and Munkittrick 2015). With two years of data, BMI data from 2018 were also compared with CES limits calculated from the combined 2017 and 2018 data, to look at variation in the current year relative to all years of sampling (Lento 2020). The same approaches were followed here, to first assess within-year variability in 2019 data by comparing them against single-year CES, and then to assess 2019 data relative to variation across 2017-2019 samples (multi-year CES).

#### *2.3.4.2. Temporal variability*

The collection of three years of data allows for the first assessment of temporal variability in normal range and CES. This approach estimates the normal range of variability over time at a specific location (Arciszewski and Munkittrick 2015), here at the site scale and at the reach scale. For the BMI monitoring plan in the Hay and Slave rivers, where the end goal is to be able to detect impacts from upstream land use when they occur, reach-specific temporal CES will allow for the determination of the magnitude of change required at that location to trigger additional sampling or investigation of possible impacts. These location-specific normal ranges will capture the natural inter-annual variability within the system, and can be adjusted with the addition of new data and with shifts in normal range that occur as a result of climate change.

Critical Effect Size (upper and lower boundaries of the normal range) can be determined using different measures of variability (see Munkittrick et al. 2009 for a review of different approaches). For univariate metrics, the temporal normal range is calculated using a grand mean (mean of means) and standard deviation, with CES calculated as the grand mean ± 2SD (Arciszewski and Munkittrick 2015). The normal range was calculated at the river scale and at the reach scale. At the river scale, the grand mean was calculated as the mean of annual means across all sites in the river, and SD was calculated from the same annual means. At the reach scale, the grand mean was calculated as the mean of annual means across all sites in the reach, and SD calculated from the same annual means.

Temporal CES was plotted to assess site-scale temporal variability relative to the normal range for the river, and to assess reach-scale temporal variability relative to the normal range for the reach. At the site scale, BMI metrics were plotted as the mean (2017-2019 data) ± 2SE (standard error) for each site, and they were compared with the temporal CES for the river (grand mean ± 2SD for the river). At the reach scale, BMI metrics were plotted as the mean (across sites) ± 2SE for each year (2017, 2018, and 2019), and they were compared with the temporal CES for the reach (grand mean ± 2SD for the reach).

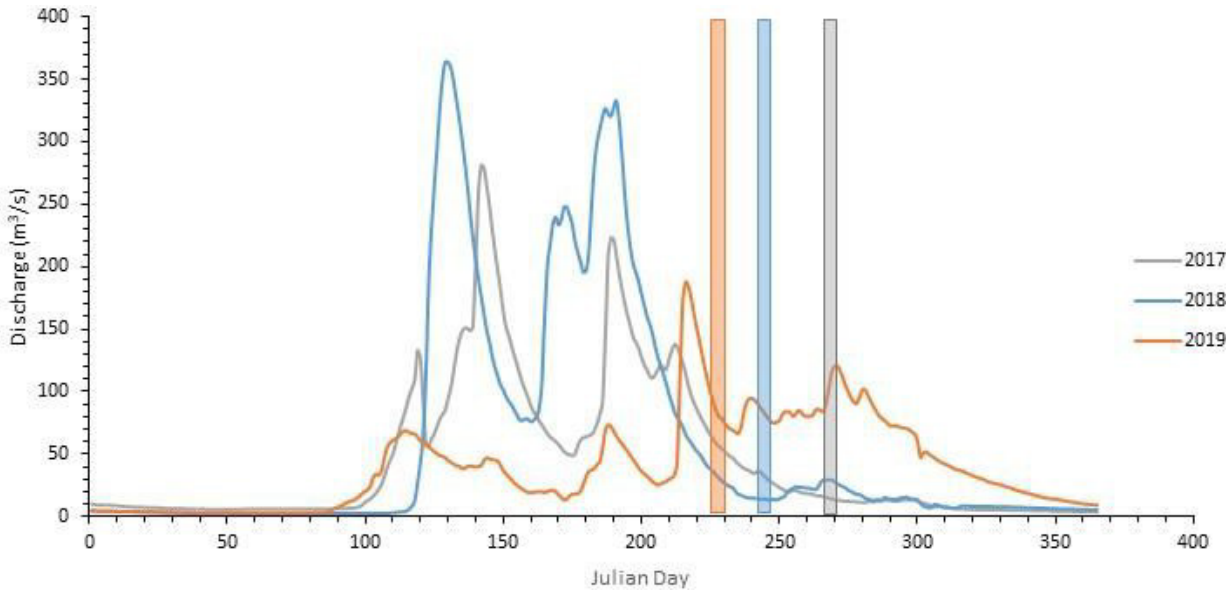


*Figure 5. Hydrographs for the Hay River in 2017 (grey), 2018 (blue), and 2019 (orange), with vertical shaded bars indicating the timing of sampling in each year. Data for Hay River near ALTA/NWT boundary (station 07OB008) from wateroffice.ec.gc.ca.*

Assessment of variability in normal range and changes across the three years of sampling was used to support conclusions and recommendations for future years of sampling.

# 3. Results and Discussion

## 3.1. Hay River

### 3.1.1. Hydrology

Differences in water chemistry and BMI assemblages between 2017 and 2018 were partially attributed to differences in flow between years. In 2017, water levels were low enough to make it difficult to access the reaches downstream of the boat launch, and sandbars throughout the river added to the challenges of sampling. In 2018, sampling was shifted earlier in the year to ensure higher water levels, but water levels in the Hay River were at or below record minimum levels at the end of August 2018 (ECCC gauge Hay River near ALTA/ NWT boundary, station 07OB008; Figure 5), which resulted in lower water levels for sampling than observed the previous year. The timing of sampling was shifted earlier in August in 2019 because water levels were low during the usual spring freshet (Figure 5), and there were concerns that many sites would be inaccessible. However, a surge in discharge prior to sampling led to extremely high water levels at the time of sampling compared to previous years (discharge of approximately 100 $m^3/s$, compared with 16.9 $m^3/s$ and 14.6 $m^3/s$ in 2017 and 2018, respectively). In 2019, some aspects of sampling (e.g., rock walk) could not be completed at some sites where water levels were too high.

The hydrograph from 2019 reflects a change in the timing and magnitude of peak flows, with a flatter hydrograph during the spring freshet and a more peaked and flashy hydrograph in the late summer/early fall (Figure 5). Such a shift in flow timing and magnitude has the potential to affect the composition of BMI found at a site if that site was not under water during low flows in the spring, and

*Table 2. Antecedent hydrology metrics for the Hay River in 2017, 2018, and 2019, including median discharge (Q ($m^3/s$)) and the coefficient of variation (CV) of flow, calculated for 60 days and 30 days prior to sampling in each year.*

| Year | At Sampling | 60 Days Prior to Sampling | | 30 Days Prior to Sampling | |
|---|---|---|---|---|---|
| | Q ($m^3/s$) | Median Q ($m^3/s$) | CV (%) | Median Q ($m^3/s$) | CV (%) |
| 2017 | 16.9 | 42.6 | 67.6 | 23.7 | 31.1 |
| 2018 | 14.6 | 97.6 | 80.9 | 37.5 | 57.0 |
| 2019 | 100 | 37.6 | 84.0 | 44 | 74.8 |

was only submerged in the few weeks prior to sampling. For example, sampling areas of the river bank that were only recently submerged can lead to the collection of primarily colonizing taxa, which are more mobile and can more easily access new habitats, but which may not be representative of the full assemblage. Alternatively, it may be possible to access the sample sites, but water levels may be deeper than usual, potentially resulting in a sample with higher proportions of taxa that thrive in deeper water conditions. Ideally, sampling would wait until high water levels had fully receded, but as indicated in Figure 5, it may not always be possible to achieve ideal water levels during the window of time in which rivers can reasonably be accessed and sampled in the fall. In such situations, sampling may not be possible in some years.

Antecedent hydrologic conditions in the 60 days and 30 days prior to sampling were compared among years by calculating two metrics of flow: the median discharge and the coefficient of variation of discharge, the latter of which provides a standardized measure of variation in flow. When compared across the period of 60 days prior to sampling, median discharge in 2018 was greater than twice as high as that observed in 2017 or 2019, but variability was similar in both 2018 and 2019 (Table 2), reflecting the low water levels and late peak observed in 2019. In the 30 days prior to sampling, median flow was more similar among years, but highest in 2019, and variability in flow was much higher in 2019 compared to previous years (Table 2). These results highlight the highly variable flow in this river among sampling years, and indicate that within-year variability in flow was high prior to sampling in 2019. The variable flow conditions should be considered when interpreting patterns in BMI assemblages among years.

### 3.1.2. Spatial characterization of reaches

#### *3.1.2.1. Chemical and physical habitat*

##### 3.1.2.1.1. Water chemistry

Water chemistry samples were collected at three kick-sites to characterize BMI habitat and variability within and among reaches. These samples represented spot measurements of water chemistry conditions at the time of sampling, and were collected at three sites in each reach to account for local-scale variability in BMI assemblages in response to the chemical environment. Although kick-sites were generally close together in a reach (50-100 m apart), some degree of variation in water chemistry might exist due to differences in velocity or groundwater seepage among sites, and this could impact the abundance and diversity of invertebrates collected at a site. Due to the meandering nature of the river channel, several reaches were on river bends, which led to variation in velocity between sites, and may have contributed to variability in water chemistry within reaches. However, the greatest level of variation in water chemistry was expected to be evident among reaches, which were farther separated

geographically along the river. The longitudinal gradient of Hay River reaches extended from Reach 1 at the south (upstream) to Reach 6 at the north (downstream; Figure 3A). Reaches 4, 5, and 6 were located downstream of the boat launch (upstream sites on Reach 4 were located on the bank opposite the boat launch) and downstream of the inflow from two tributaries, which may have introduced some variability in water chemistry relative to reaches upstream of the launch. Furthermore, a section of large rocks downstream of Reach 4 acts as a barrier during low flow years, and may represent a barrier to fish movement when water levels are low. Analyses considered variation within and among reaches to account for differences due to reach location and location of sites within reaches.

Water samples were analyzed for major ions, nutrients, and physicals (Table 3). Mean levels of ions and a selection of nutrients were compared with Canadian guidelines for short-term and long-term exposure to identify any reaches where water chemistry was indicative of poor water quality (Canadian Council of Ministers of the Environment 2001b). Mean values for ions and nutrients did not exceed CCME guidelines for the protection of aquatic life for any reaches in the Hay River. Reaches were classified as eutrophic (KS1 and KS3 through KS5) or hyper-eutrophic (KS2 and KS6) based on mean total phosphorus (TP) values, which ranged from 0.074 to 0.126 mg/L. TP was higher than observed in 2017 or 2018, and higher than indicated in previous analyses of long-term water chemistry monitoring data (e.g., Stantec Consulting Ltd. 2016, where the Hay River was considered mesotrophic to eutrophic). However, total suspended solids (TSS) were also elevated compared to previous years, and the high levels of TP may have been a reflection of the recent surge in water levels flushing more sediments through the system (Figure 5).

For many water chemistry parameters, the increased water levels in 2019 appeared to have the effect of reducing variability within and among reaches in the Hay River. Variability among sites in the Hay River was extremely low for some water chemistry parameters in 2019. For example, hardness varied between 97.3-102 mg/L, sulphate varied between 43-44 mg/L, and calcium varied between 27.5-28.8 mg/L across all sites in 2019. In 2018, these parameters were more variable and at higher concentrations, ranging from 190-239 mg/L, 73-84 mg/L, and 46.7-56.4 mg/L, respectively. The low variability within reaches is evident in the low standard deviations in Table 3 and the small interquartile ranges in the summary box plots in Figure 6, particularly for alkalinity, calcium, magnesium, and dissolved nitrogen.

Variation in ions, nutrients, and physicals was fairly low among reaches, but because within-reach variability was so low, there was high power to detect statistically significant differences among reaches (at $\alpha\alpha$ = 0.05) for some parameters, even if differences among reaches were not large. For example, there was a statistically significant difference in alkalinity between Reach 4 and Reaches 1, 2, and 6 (Figure 6), but the difference in mean alkalinity between those reaches was less than 2 mg/L (Table 3), which was unlikely to be biologically meaningful. Mean TP was statistically significantly lower in Reach 3 than it was in Reach 2 or 6 (Figure 6), both of which were higher than the threshold for a hyper-eutrophic system (0.100 mg/L; Canadian Council of Ministers of the Environment 2001b). The difference in mean TP between Reach 3 and Reaches 2 and 6 was 0.035 mg/L and 0.052 mg/L, respectively (Table 3), which may have represented a more biologically-meaningful difference. But the highest TP was found in reaches with the highest TSS levels, and there was little difference in dissolved phosphorus (biologically-available phosphorus) between reaches, which suggests a high contribution of phosphorus bound to sediments (Sanderson et al. 2012). With high discharge at the time of sampling and a recent peak in flow, this result would not be unexpected.

*Table 3. Summary of ion, nutrient, and physical water chemistry parameters sampled in the Hay River at six sample reaches, indicating site mean ± standard deviation for each reach. When all sites in a reach were below detection limit, the detection limit is presented. When only a subset of sites in a reach was below detection limit, half the detection limit was used in calculations (number of sites below detection limit indicated in Parameter column). Samples were collected at three sites in each reach and a duplicate sample was collected at two sites.*

| Parameter | HR-KS1 | HR-KS2 | HR-KS3 | HR-KS4 | HR-KS5 | HR-KS6 |
|---|---|---|---|---|---|---|
| Alkalinity (mg/L) | 67.3 ± 0.1 | 68.0 ± 0.3 | 68.6 ± 0.3 | 68.8 ± 0.2 | 68.5 ± 0.2 | 67.8 ± 0.3 |
| Ammonia (mg/L) | < 0.005 | < 0.005 | < 0.005 | < 0.005 | < 0.005 | < 0.005 |
| Calcium (mg/L) | 28.1 ± 0.5 | 28.6 ± 0.1 | 28.8 ± 0.1 | 28.7 ± 0.2 | 28.8 ± 0.1 | 28.6 ± 0.2 |
| Chloride (mg/L) | 1.10 ± 0.00 | 1.10 ± 0.00 | 1.00 ± 0.00 | 0.97 ± 0.06 | 1.03 ± 0.06 | 1.02 ± 0.08 |
| Specific Conductivity (µS/cm) | 229.0 ± 1.7 | 230.0 ± 0.0 | 229.7 ± 0.6 | 231.0 ± 1.0 | 231.0 ± 1.0 | 231.2 ± 0.3 |
| Hardness (mg/L) | 99.1 ± 1.6 | 101.0 ± 0.0 | 101.7 ± 0.6 | 101.0 ± 1.0 | 101.0 ± 0.0 | 100.8 ± 0.3 |
| Magnesium (mg/L) | 7.05 ± 0.09 | 7.10 ± 0.00 | 7.20 ± 0.00 | 7.17 ± 0.06 | 7.20 ± 0.00 | 7.17 ± 0.06 |
| Nitrate (mg/L) | 0.242 ± 0.064 | 0.207 ± 0.006 | 0.210 ± 0.000 | 0.190 ± 0.044 | 0.220 ± 0.010 | 0.240 ± 0.106 |
| Nitrite (mg/L) | < 0.01 | < 0.01 | < 0.01 | < 0.01 | < 0.01 | < 0.01 |
| Nitrate+Nitrite (mg/L) | 0.242 ± 0.064 | 0.207 ± 0.006 | 0.210 ± 0.000 | 0.190 ± 0.044 | 0.220 ± 0.010 | 0.240 ± 0.106 |
| Dissolved N (mg/L) | 0.720 ± 0.010 | 0.717 ± 0.006 | 0.727 ± 0.006 | 0.740 ± 0.010 | 0.733 ± 0.012 | 0.788 ± 0.088 |
| Total N (mg/L) | 0.925 ± 0.013 | 0.957 ± 0.006 | 0.893 ± 0.021 | 0.907 ± 0.021 | 0.917 ± 0.021 | 0.970 ± 0.078 |
| DOC (mg/L) | 27.25 ± 0.28 | 27.07 ± 0.15 | 27.87 ± 0.45 | 27.50 ± 0.00 | 27.33 ± 0.25 | 27.65 ± 0.43 |
| TOC (mg/L) | 28.42 ± 0.03 | 28.47 ± 0.40 | 28.60 ± 0.00 | 28.73 ± 0.12 | 28.70 ± 0.10 | 28.55 ± 0.15 |
| Ortho-Phosphate (mg/L) (4 below DL) | 0.0025 ± 0.0005 | 0.0013 ± 0.0006 | 0.0023 ± 0.0006 | 0.0020 ± 0.0010 | 0.0023 ± 0.0006 | 0.0020 ± 0.0010 |
| pH | 7.68 ± 0.01 | 7.70 ± 0.02 | 7.71 ± 0.02 | 7.73 ± 0.02 | 7.72 ± 0.01 | 7.72 ± 0.01 |
| Dissolved P (mg/L) | 0.010 ± 0.001 | 0.009 ± 0.000 | 0.009 ± 0.000 | 0.011 ± 0.001 | 0.009 ± 0.001 | 0.010 ± 0.001 |
| Total P (mg/L) | 0.097 ± 0.002 | 0.109 ± 0.012 | 0.074 ± 0.003 | 0.084 ± 0.003 | 0.096 ± 0.004 | 0.126 ± 0.039 |
| Potassium (mg/L) | 1.00 ± 0.00 | 1.00 ± 0.00 | 1.00 ± 0.00 | 1.00 ± 0.00 | 1.00 ± 0.00 | 1.00 ± 0.00 |
| Sodium (mg/L) | 8.80 ± 0.00 | 8.80 ± 0.00 | 8.67 ± 0.06 | 8.63 ± 0.06 | 8.80 ± 0.00 | 8.80 ± 0.00 |
| TDS (mg/L) | 165.8 ± 5.8 | 188.7 ± 15.3 | 156.3 ± 14.4 | 171.3 ± 17.0 | 165.0 ± 10.4 | 165.7 ± 8.3 |
| TSS (mg/L) | 48.0 ± 4.6 | 67.0 ± 16.7 | 34.3 ± 9.5 | 45.0 ± 7.5 | 39.0 ± 5.6 | 86.8 ± 50.0 |
| Sulphate (mg/L) | 44.0 ± 0.0 | 44.0 ± 0.0 | 43.0 ± 0.0 | 43.0 ± 0.0 | 44.0 ± 0.0 | 44.0 ± 0.0 |
| Turbidity (NTU) | 58.0 ± 2.0 | 69.1 ± 11.6 | 37.8 ± 0.7 | 46.3 ± 4.0 | 56.5 ± 4.2 | 77.9 ± 30.7 |

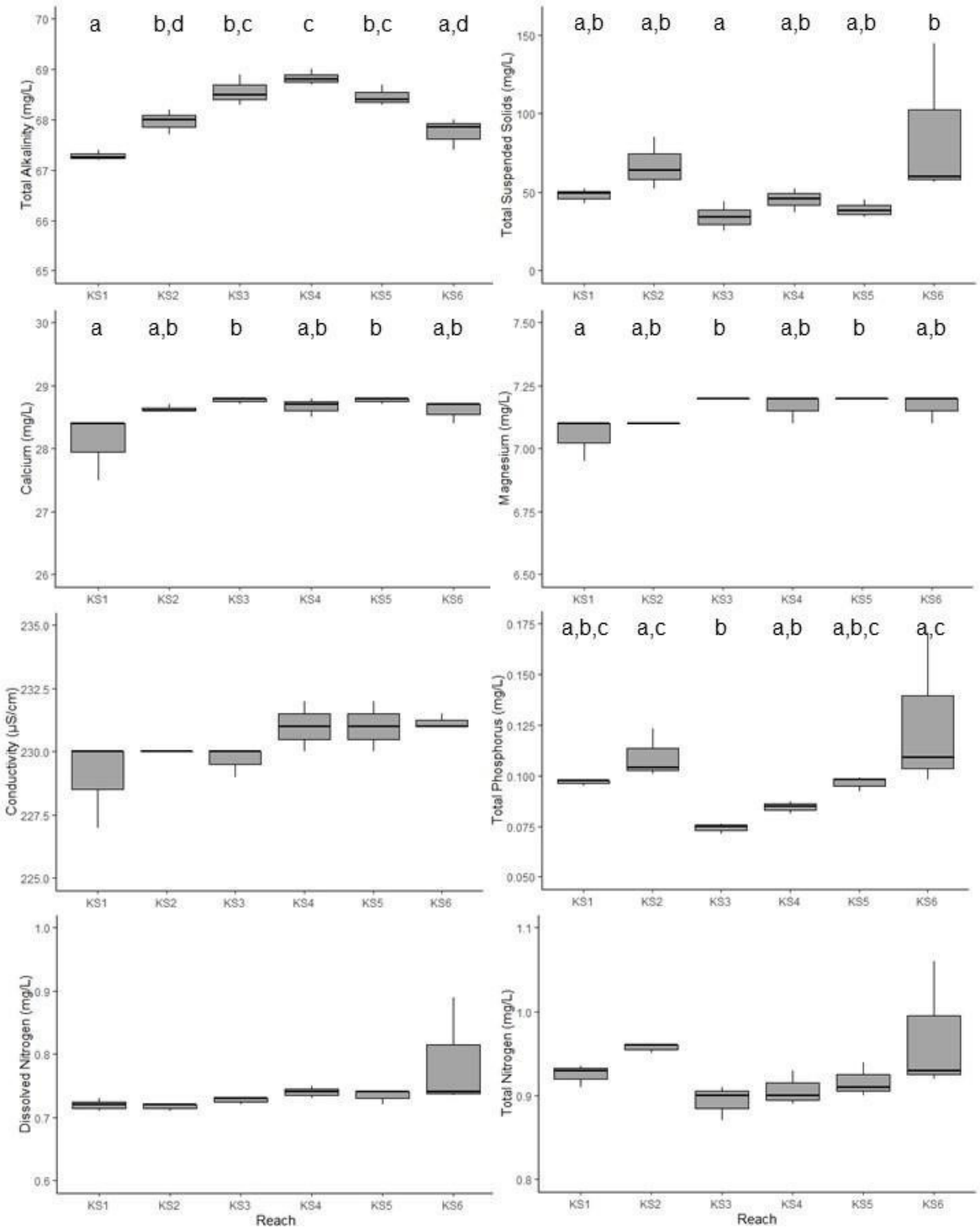


*Figure 6. Box plots of ions, nutrients, and physicals water chemistry concentrations for all reaches sampled in the Hay River in 2019. Plotted is alkalinity, TSS, calcium, magnesium, conductivity, TP, DN, and TN. Box indicates the interquartile range, line through the box indicates the median, and whiskers indicate the lower and upper quartiles. Points indicate statistical outliers. Letters on plots indicate significant differences ($\alpha = 0.05$) from one-way ANOVA and Tukey HSD tests.*

Dissolved and total metals were also tested in water chemistry samples to further characterize the chemical habitat in the water column at the time of sampling. Levels of metals are related to the geology of a watershed, though concentrations of some metals may become elevated with upstream disturbance and have the potential to indicate anthropogenic impacts. Dissolved metals in water are more biologically available to BMI, whereas total metals include those bound to sediments, and may not represent relevant exposure levels for organisms. Some metals, such as aluminum and mercury, are known to be harmful to aquatic organisms at elevated levels, and mercury in particular can accumulate up the food web, impacting the fish that feed on BMI.

Dissolved metals had generally low variability within reaches (between kick-sites) and among reaches (Table 4, Figure 7). Many dissolved metals were below detection limit, or had low standard deviations within reaches. Low variability resulted in high power to detect statistically significant differences among reaches even when actual differences were low, and some statistical differences were evident among reaches for dissolved aluminum, dissolved manganese, and dissolved mercury (Figure 7). However, mean differences between reaches were low and likely not biologically meaningful. Though some dissolved metals varied among reaches, only copper was found to exceed CCME guidelines for the protection of aquatic life (Canadian Council of Ministers of the Environment 2001b). In all reaches, dissolved copper exceeded the long-term exposure guideline of 2.36 µg/L (at a water hardness of 100 mg/L), though all reach means exceeded this guideline by less than 1 µg/L.

*Table 4. Summary of metal water chemistry parameters sampled in the Hay River at six sample reaches, indicating site mean ± standard deviation (for 2 or more samples) for each reach. When all sites in a reach were below detection limit, the detection limit is indicated. When only a subset of sites in a reach was below detection limit, half the detection limit was used in calculations (number of sites below detection limit indicated in Parameter column). Dissolved metal values were excluded when they exceeded total metals. Values in bold were greater than CCME long-term exposure guidelines for the protection of aquatic life (Canadian Council of Ministers of the Environment 2001b). Samples were collected at three sites in each reach and a duplicate sample was collected at two sites.*

| Parameter | HR-KS1 | HR-KS2 | HR-KS3 | HR-KS4 | HR-KS5 | HR-KS6 |
|---|---|---|---|---|---|---|
| Aluminum Diss. (µg/L) | 13.63 ± 0.15 | 13.37 ± 0.21 | 12.00 ± 0.75 | 11.57 ± 0.76 | 12.43 ± 0.32 | 12.75 ± 0.40 |
| Aluminum Total (µg/L) | **892.83 ± 39.52** | **1206.67 ± 236.92** | **586.67 ± 24.58** | **763.00 ± 22.07** | **907.67 ± 57.01** | **1145.00 ± 459.73** |
| Antimony Diss. (µg/L) | 0.10 ± 0.00 | 0.10 ± 0.00 | 0.10 ± 0.00 | 0.10 ± 0.00 | 0.10 ± 0.00 | 0.10 ± 0.00 |
| Antimony Total (µg/L) | 0.20 ± 0.00 | 0.20 ± 0.00 | 0.10 ± 0.00 | 0.10 ± 0.00 | 0.23 ± 0.06 | 0.20 ± 0.00 |
| Arsenic Diss. (µg/L) | 0.73 ± 0.06 | 0.73 ± 0.06 | 0.70 ± 0.00 | 0.70 ± 0.00 | 0.70 ± 0.00 | 0.75 ± 0.05 |
| Arsenic Total (µg/L) | 2.28 ± 0.03 | 2.67 ± 0.29 | 1.80 ± 0.00 | 2.00 ± 0.00 | 2.30 ± 0.10 | 2.63 ± 0.67 |
| Barium Diss. (µg/L) | 35.05 ± 0.83 | 35.53 ± 0.25 | 32.80 ± 2.11 | 31.70 ± 2.25 | 32.27 ± 0.55 | 33.45 ± 1.05 |
| Barium Total (µg/L) | 64.85 ± 1.64 | 75.23 ± 7.07 | 52.37 ± 1.55 | 56.43 ± 0.84 | 61.53 ± 2.35 | 71.62 ± 16.51 |
| Beryllium Total (µg/L) (13 below DL) | < 0.10 | 0.10 ± 0.00 | < 0.10 | < 0.10 | 0.08 ± 0.03 | 0.10 ± 0.09 |
| Bismuth Total (µg/L) | < 0.20 | < 0.20 | < 0.20 | < 0.20 | < 0.20 | < 0.20 |
| Boron Diss. (µg/L) | 28.77 ± 0.72 | 28.77 ± 0.25 | 26.87 ± 1.96 | 26.60 ± 0.62 | 27.27 ± 0.32 | 27.60 ± 1.25 |
| Boron Total (µg/L) | 32.77 ± 1.02 | 34.47 ± 0.51 | 30.33 ± 1.36 | 29.70 ± 0.26 | 31.10 ± 1.00 | 31.52 ± 0.94 |
| Cadmium Diss. (µg/L) | < 0.04 | < 0.04 | < 0.04 | < 0.04 | < 0.04 | < 0.04 |
| Cadmium Total (µg/L) (16 below DL) | <0.10 | 0.07 ± 0.03 | <0.10 | <0.10 | 0.07 ± 0.03 | 0.07 ± 0.03 |
| Cesium Diss. (µg/L) | <0.10 | <0.10 | <0.10 | <0.10 | <0.10 | <0.10 |
| Cesium Total (µg/L) | 0.35 ± 0.05 | 0.43 ± 0.06 | 0.20 ± 0.00 | 0.30 ± 0.00 | 0.33 ± 0.06 | 0.40 ± 0.17 |
| Chromium Diss. (µg/L) | 0.20 ± 0.00 | 0.20 ± 0.00 | 0.17 ± 0.06 | 0.17 ± 0.06 | 0.17 ± 0.06 | 0.20 ± 0.00 |

| Parameter | HR-KS1 | HR-KS2 | HR-KS3 | HR-KS4 | HR-KS5 | HR-KS6 |
|---|---|---|---|---|---|---|
| Chromium Total (µg/L) | 1.63 ± 0.06 | 2.17 ± 0.38 | 1.13 ± 0.06 | 1.43 ± 0.06 | 1.73 ± 0.15 | 2.10 ± 0.78 |
| Cobalt Diss. (µg/L) (11 below DL) | <0.10 | 0.10 ± 0.00 | <0.10 | 0.07 ± 0.03 | 0.07 ± 0.03 | 0.13 ± 0.06 |
| Cobalt Total (µg/L) | 1.15 ± 0.05 | 1.60 ± 0.26 | 0.77 ± 0.06 | 1.00 ± 0.00 | 1.17 ± 0.06 | 1.63 ± 0.76 |
| Copper Diss. (µg/L) | **3.03 ± 0.06** | **3.07 ± 0.06** | **2.80 ± 0.20** | **2.70 ± 0.17** | **2.80 ± 0.00** | **3.07 ± 0.31** |
| Copper Total (µg/L) | **4.93 ± 0.06** | **5.77 ± 0.55** | **4.03 ± 0.15** | **4.40 ± 0.17** | **4.87 ± 0.12** | **5.52 ± 1.25** |
| Iron Diss. (ug/L) | 153.50 ± 2.29 | 151.00 ± 1.00 | 148.67 ± 8.02 | 143.67 ± 10.21 | 138.67 ± 3.06 | 144.00 ± 2.65 |
| Iron Total (µg/L) | **2898.33 ± 95.70** | **3683.33 ± 624.05** | **2020.00 ± 60.00** | **2403.33 ± 30.55** | **2803.33 ± 136.14** | **3625.00 ± 1344.72** |
| Lead Diss. (µg/L) (18 below DL) | 0.37 ± 0.55 | 0.10 ± 0.09 | <0.10 | <0.10 | <0.10 | <0.10 |
| Lead Total (µg/L) | 1.37 ± 0.06 | 1.80 ± 0.26 | 0.97 ± 0.06 | 1.13 ± 0.06 | 1.43 ± 0.06 | 1.73 ± 0.67 |
| Lithium Diss. (µg/L) | 9.05 ± 0.23 | 9.27 ± 0.12 | 8.73 ± 0.70 | 8.60 ± 0.50 | 8.63 ± 0.06 | 8.80 ± 0.26 |
| Lithium Total (µg/L) | 10.47 ± 0.32 | 11.33 ± 0.31 | 9.73 ± 0.23 | 9.70 ± 0.10 | 10.23 ± 0.15 | 10.53 ± 0.84 |
| Manganese Diss. (µg/L) | 4.88 ± 0.37 | 15.63 ± 4.27 | 3.83 ± 1.00 | 9.57 ± 4.16 | 3.87 ± 0.64 | 12.95 ± 7.06 |
| Manganese Total (µg/L) | 87.13 ± 2.24 | 129.67 ± 24.42 | 59.63 ± 1.72 | 77.87 ± 3.21 | 85.33 ± 4.92 | 135.60 ± 65.95 |
| Mercury Diss. (UL) (ng/L) | 3.53 ± 0.67 | 4.13 ± 0.21 | 3.17 ± 0.06 | 3.10 ± 0.00 | 3.17 ± 0.06 | 3.30 ± 0.10 |
| Mercury Total (UL) (ng/L) | 10.00 ± 0.10 | 15.80 ± 1.93 | 9.07 ± 1.77 | 8.87 ± 0.74 | 9.40 ± 0.61 | 13.52 ± 3.76 |
| Molybdenum Diss. (µg/L) | 0.78 ± 0.03 | 0.80 ± 0.00 | 0.73 ± 0.06 | 0.70 ± 0.00 | 0.70 ± 0.00 | 0.80 ± 0.00 |
| Molybdenum Total (µg/L) | 0.95 ± 0.05 | 1.00 ± 0.10 | 0.83 ± 0.06 | 0.87 ± 0.06 | 0.93 ± 0.06 | 0.93 ± 0.06 |
| Nickel Diss. (µg/L) | 3.80 ± 0.10 | 3.87 ± 0.06 | 3.50 ± 0.30 | 3.40 ± 0.26 | 3.53 ± 0.06 | 3.63 ± 0.15 |
| Nickel Total (µg/L) | 6.18 ± 0.13 | 7.17 ± 0.64 | 5.07 ± 0.21 | 5.43 ± 0.06 | 6.07 ± 0.21 | 6.88 ± 1.45 |
| Rubidium Diss. (µg/L) | 0.63 ± 0.06 | 0.60 ± 0.00 | 0.63 ± 0.06 | 0.57 ± 0.06 | 0.60 ± 0.00 | 0.60 ± 0.00 |
| Rubidium Total (µg/L) | 3.58 ± 0.10 | 4.57 ± 0.81 | 2.53 ± 0.06 | 3.03 ± 0.06 | 3.50 ± 0.20 | 4.42 ± 1.50 |
| Selenium Diss. (µg/L) (11 below DL) | 0.28 ± 0.13 | 0.28 ± 0.13 | 0.20 ± 0.09 | 0.20 ± 0.09 | < 0.30 | 0.31 ± 0.09 |
| Selenium Total (µg/L) (19 below DL) | 0.33 ± 0.14 | < 0.50 | < 0.50 | < 0.50 | < 0.50 | < 0.50 |
| Silver Total (µg/L) | < 0.10 | < 0.10 | < 0.10 | < 0.10 | < 0.10 | < 0.10 |
| Strontium Diss. (µg/L) | 90.07 ± 1.96 | 90.33 ± 0.67 | 85.60 ± 6.06 | 82.10 ± 5.48 | 84.13 ± 0.31 | 86.10 ± 2.49 |
| Strontium Total (µg/L) | 96.10 ± 3.03 | 99.93 ± 2.76 | 90.47 ± 3.31 | 88.67 ± 0.96 | 91.07 ± 2.18 | 92.53 ± 2.40 |
| Thallium Total (µg/L) | < 0.10 | < 0.10 | < 0.10 | < 0.10 | < 0.10 | < 0.10 |
| Tin Total (µg/L) | < 0.10 | < 0.10 | < 0.10 | < 0.10 | < 0.10 | < 0.10 |
| Titanium Diss. (µg/L) | 0.32 ± 0.03 | 0.33 ± 0.06 | 0.30 ± 0.00 | 0.30 ± 0.00 | 0.33 ± 0.06 | 0.38 ± 0.03 |
| Titanium Total (µg/L) | 11.00 ± 0.50 | 14.10 ± 2.43 | 8.27 ± 0.47 | 9.87 ± 0.21 | 11.50 ± 0.82 | 13.47 ± 3.67 |
| Uranium Diss. (µg/L) | 0.40 ± 0.00 | 0.40 ± 0.00 | 0.33 ± 0.06 | 0.30 ± 0.00 | 0.33 ± 0.06 | 0.37 ± 0.06 |
| Uranium Total (µg/L) | 0.50 ± 0.00 | 0.60 ± 0.00 | 0.43 ± 0.06 | 0.50 ± 0.00 | 0.50 ± 0.00 | 0.55 ± 0.09 |
| Vanadium Diss. (µg/L) | 0.20 ± 0.00 | 0.20 ± 0.00 | 0.20 ± 0.00 | 0.20 ± 0.00 | 0.20 ± 0.00 | 0.20 ± 0.00 |
| Zinc Diss. (µg/L) (19 below DL) | < 0.40 | < 0.40 | < 0.40 | 0.53 ± 0.58 | < 0.40 | < 0.40 |
| Zinc Total (µg/L) | 9.47 ± 0.32 | 12.93 ± 2.33 | 6.30 ± 0.17 | 8.03 ± 0.40 | 10.53 ± 0.68 | 12.85 ± 5.55 |

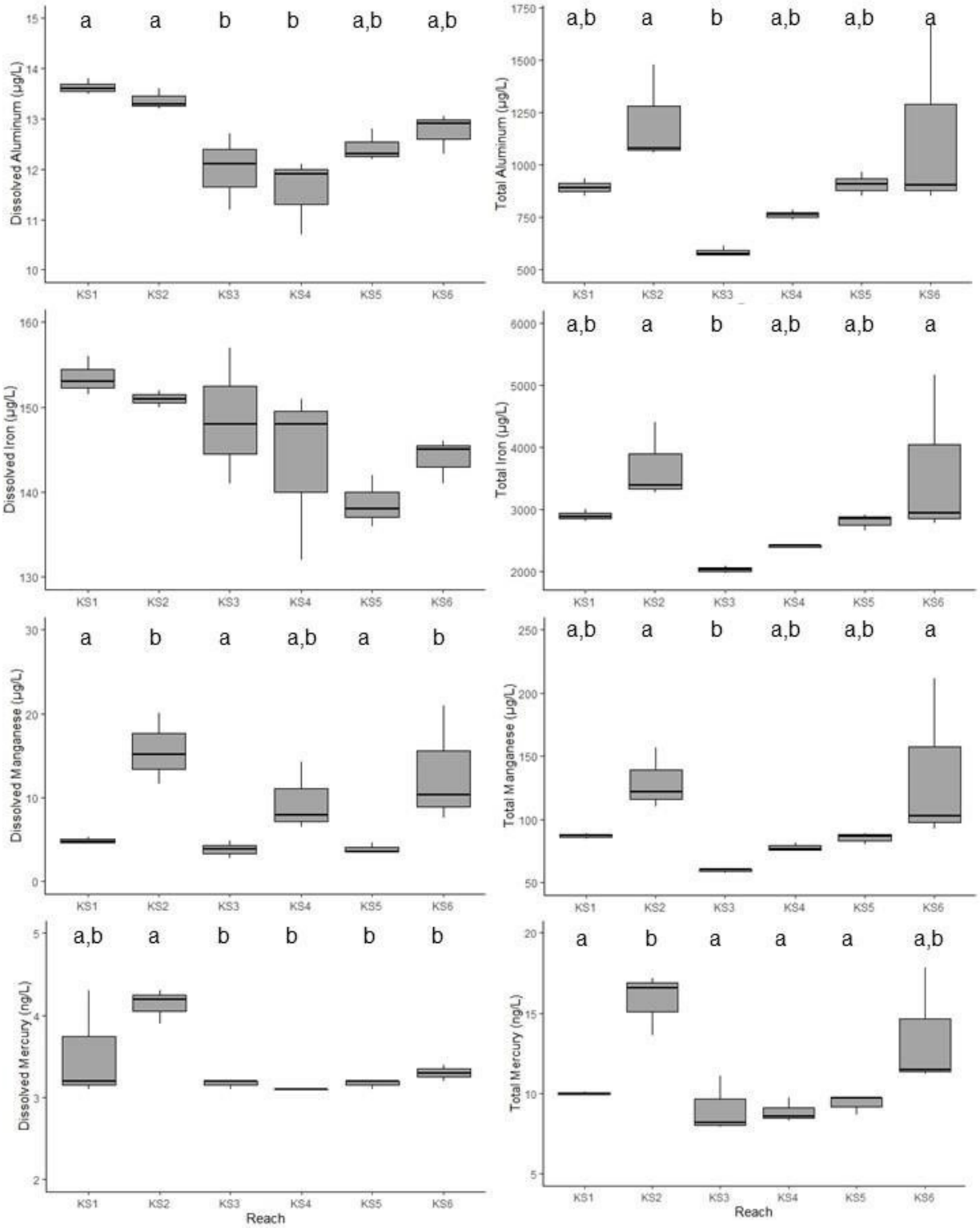


*Figure 7. Box plots of dissolved and total metal concentrations for all reaches sampled in Hay River in 2019. Plotted is (left column, top to bottom) dissolved aluminum, dissolved iron, dissolved manganese, and (right column, top to bottom) total aluminum, total iron, and total manganese, all measured in µg/L. Box indicates the interquartile range, line through the box indicates the median, and whiskers indicate the lower and upper quartiles. Points indicate statistical outliers. Letters on plots indicate significant differences ($\alpha\alpha$ = 0.05) from one-way ANOVA and Tukey HSD tests.*

Total metals were somewhat more variable than dissolved metals, and there were high levels of some total metals that were due to higher TSS levels in the system (as total metals can be elevated due to sorption of metals to sediment particles). Total copper exceeded the long-term guideline (Canadian Council of Ministers of the Environment 2001b), but remained fairly low (< 6 µg/L) across all reaches. Total aluminum was elevated in all reaches, well above the guideline of 100 µg/L for a pH ≥ 6.5, but this likely reflected sorption to suspended sediment particles. Total iron was also higher than CCME guidelines (300 µg/L; Canadian Council of Ministers of the Environment 2001b) in all reaches. The river has naturally high levels of some metals including iron, and the observed levels (ranging on average from 2020 to 3683 mg/L), although higher than what was observed in 2018, were much lower than the levels described in long-term monitoring of the Hay River (90th percentile for iron in open water season = 6434 µg/L; Stantec Consulting Ltd. 2016).

#### 3.1.2.1.2. Physical Habitat

Measurements were taken at each site to characterize the physical habitat in BMI sampling locations, including variables such as velocity, river width, streamside vegetation, in-stream periphyton cover, and substrate composition (Table 5). Not all physical habitat variables were collected in the Hay River in 2019 due to high water levels at some sites. For example, water levels were too high at sites HR-KS1-5A,

*Table 5. Physical habitat variables measured in the Hay River in 2019, summarized by reach. Velocity (spot measurement), bankfull width, and wetted width are presented as mean ± standard deviation (calculated based on 5 sites per reach); dominant streamside vegetation and periphyton coverage are presented as the most common category in each reach across 5 sites; substrate composition is presented as the sum of rock counts for each reach (20 rocks measured per site).*

| Parameter | HR-KS1 | HR-KS2 | HR-KS3 | HR-KS4 | HR-KS5 | HR-KS6 |
|---|---|---|---|---|---|---|
| Velocity (m/s) | 0.37 ± 0.31 | 0.25 ± 0.08 | 0.29 ± 0.14 | 0.49 ± 0.13 | 0.47 ± 0.10 | 0.28 ± 0.13 |
| Bankfull width (m) | 146.2 ± 14.3 | 125.0 ± 7.2 | 144.6 ± 17.0 | 128.3 ± 1.0 | 108.5 ± 15.9 | 127.6 ± 3.2 |
| Wetted width (m) | 136.0 ± 17.0 | 112.5 ± 9.4 | 135.2 ± 18.0 | 116.0 ± 4.6 | 102.1 ± 16.0 | 117.0 ± 4.9 |
| Dominant streamside vegetation | shrubs | shrubs | ferns/ grasses | shrubs | shrubs | ferns/ grasses |
| Periphyton coverage | < 0.5 mm thick | < 0.5 mm thick | < 0.5 mm thick | < 0.5 mm thick | < 0.5 mm thick | < 0.5 mm thick |
| Substrate - sand (%) | 0 | 0 | 0 | 0 | 0 | 0 |
| Substrate - gravel (%) | 4 | 5 | 8 | 27 | 26 | 13 |
| Substrate - pebble (%) | 66 | 74 | 62 | 71 | 54 | 75 |
| Substrate - cobble (%) | 10 | 21 | 10 | 2 | 0 | 12 |
| Substrate - boulder (%) | 0 | 0 | 0 | 0 | 0 | 0 |
| Substrate - bedrock (%) | 0 | 0 | 0 | 0 | 0 | 0 |

HR-KS3-5A, and HR-KS5-5B to conduct the rock walk, and substrate information is missing for those sites.

Velocity was high at Hay River sites in 2019, ranging from 0.25 to 0.49 m/s on average (Table 5). This is in contrast to 2018, when velocity ranged from 0.14 to 0.21 m/s. Higher velocities reflected the higher discharge at the time of sampling, which was more than six times the discharge at the time of sampling in 2017 and 2018 (Figure 5). Wetted width was also much higher in 2019 than in 2018, with increases of 10 to 48 m wetted width in reaches in 2019. Reaches were generally dominated by substrates in the pebble size class, and downstream reaches (Reaches 4, 5, and 6) had a higher proportion of substrates in the gravel size class than upstream reaches.

A notable result of the higher discharge and water levels in 2019 was a change to estimates of periphyton coverage. While periphyton coverage in the typically slow-flowing river included 0.5-1 mm thick and 1-5 mm thick across reaches in 2018, all sites sampled in 2019 were classified as having < 0.5 mm periphyton coverage (the lowest coverage category in CABIN sampling). This shift from variability in thickness and appearance of periphyton in previous years to an apparent absence of visible periphyton in 2019 could reflect temporary habitat being sampled, if high water levels forced lateral shifts in sample site location. But it may also reflect scouring by high flows that disrupted the algal community at these sites. Sampling took place one week after peak flows, and discharge was still declining in the river at the time of sampling. The high discharge also appeared to contribute to higher turbidity, which affects light penetration through the water column and may have limited algal growth. There may not have been sufficient time, flow stability, and light penetration for algal communities to get re-established to the extent that they were found in previous sampling years.

#### 3.1.2.1.3. Characterization of chemical and physical habitat

Principal Component Analysis (PCA) was used as an exploratory analysis to characterize water chemistry and physical habitat conditions within and among reaches. In this analysis, a large suite of water chemistry parameters and field-measured habitat parameters was included to characterize the abiotic habitat for all sites, and the spatial arrangement of sites in the resulting PCA plot was used to identify abiotic gradients in the data and important variables for biotic-abiotic analysis. In the ordination plot, sites located on the same end of gradient vectors had similar chemical and physical habitats, while those at opposite ends of gradient vectors were negatively correlated with respect to one or more abiotic parameters. The analysis is correlation-based, and thus the degree of separation among sites and parameters reflects differences in correlation, rather than differences in the magnitude of measured variables. Given the low variability in chemical parameters among reaches of the Hay River in 2019, it is important to recognize that dissimilarity in the ordination does not imply large differences in parameter values.

The ordination of chemical and physical habitat variables indicated high similarity within reaches, with sites from the same reach generally plotting close together along the same gradient (Figure 8). One exception was site KS6-5, which was positively correlated along the first axis with TSS, turbidity, TP, TN, and most total metals. The other sites in Reach 6 were instead positively correlated with several different dissolved metals (Figure 8). Sites in Reach 2 were intermediary to the two axis, and were positively correlated with both total and dissolved metals along the first axis of the ordination. The separation of KS6-5 and the sites in Reach 2 on the positive end of the first axis from the other Hay River sites on the negative end of the axis explained 52.8% of the variation among sites (Figure 8). Reach 2

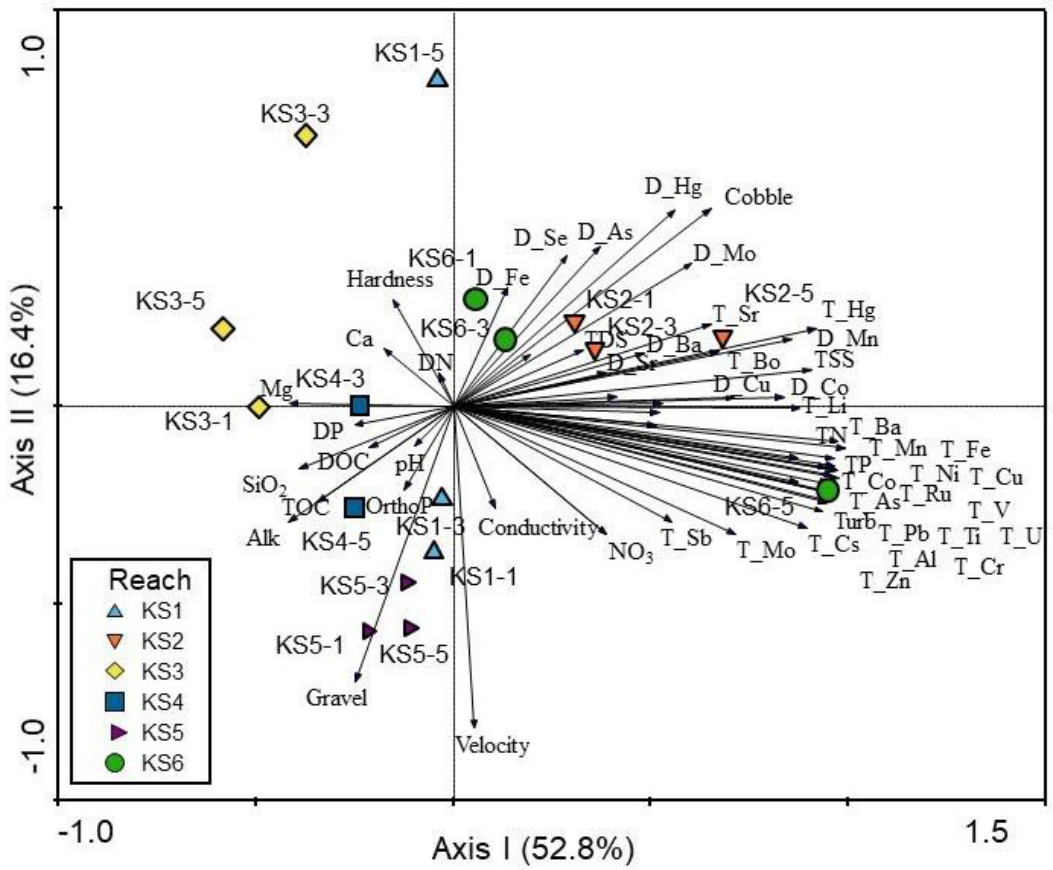


*Figure 8. PCA ordination of water chemistry and habitat variables at Hay River kick-sites, with sites colour-coded based on reach number. Arrows point in the direction of increasing values of parameters, and correlations of sites with parameters are indicated by the location of kick-site points in proximity to arrows. Kick-sites on the same end of a gradient are positively correlated, whereas samples on opposite ends of gradients are negatively correlated. Kick-sites and parameters at right angles through the origin are uncorrelated. Parameters near the origin are not labelled for ease of interpretation. Kick-site points located near the origin have similar correlations with all measured parameters. "D-" in front of metals indicates dissolved form, and "T-" indicates total metals.*

and Reach 6 had elevated levels of dissolved and total metals compared to other reaches, and these differences were statistically significant for some metals (Figure 7), consistent with the positive correlations of these reaches with metals in the ordination.

Reach 1 displayed separation among sites in the ordination that was due to a negative correlation of KS1-5 with velocity along the second axis, which explained 16.4% of the variation among sites (Figure 8). The other sites in Reach 1 and sites in Reach 5 were positively correlated with velocity and the relative abundance of gravel along this axis. Velocity and substrate size parameters had higher loadings on the PCA axes than many ions, nutrients, and physical water chemistry parameters, due in part to the low variability in water chemistry among sites.

#### 3.1.2.1.4. Sediment chemistry

Sediment chemistry samples were collected from two sites in each reach (sites 1 and 5) and analyzed for metals and polycyclic aromatic hydrocarbons (PAHs). PAHs have the potential to impact the environment and human health if present in sufficient quantities, and in particular, they have the

*Table 6. Summary of sediment chemistry parameters sampled in the Hay River in 2019, indicating site mean ± standard deviation for each reach (2 sites sampled per reach). When both sites in a reach were below detection limit, the detection limit is indicated (note that detection limits differed among sites for some parameters). When only one site in a reach was below detection limit, half the detection limit was used in calculations (number of sites below DL indicated in Parameter column). Values were compared with CCME sediment quality guidelines for the protection of aquatic life (Canadian Council of Ministers of the Environment 2001a), and values in bold were greater than interim freshwater sediment quality guidelines (ISQGs) whereas values in red were greater than probable effect levels (PELs).*

| Parameter | HR-KS1 | HR-KS2 | HR-KS3 | HR-KS4 | HR-KS5 | HR-KS6 |
|---|---|---|---|---|---|---|
| **Metals (mg/kg)** | | | | | | |
| Antimony (Sb) | 0.425 ± 0.035 | 0.235 ± 0.021 | 0.325 ± 0.064 | 0.480 ± 0.467 | 0.200 ± 0.085 | 0.420 ± 0.071 |
| Arsenic (As) | **10.85 ± 1.35** | 5.70 ± 0.16 | **8.40 ± 1.01** | **13.04 ± 8.72** | **7.18 ± 0.86** | **11.12 ± 1.82** |
| Barium (Ba) | 205.5 ± 108.2 | 208.0 ± 73.5 | 302.0 ± 43.8 | 130.5 ± 20.5 | 96.2 ± 33.7 | 243.0 ± 12.7 |
| Beryllium (Be) | 0.440 ± 0.226 | 0.405 ± 0.064 | 0.615 ± 0.389 | 0.240 ± 0.141 | 0.190 ± 0.085 | 0.595 ± 0.134 |
| Cadmium (Cd) | **0.688 ± 0.028** | 0.357 ± 0.185 | 0.361 ± 0.008 | 0.388 ± 0.281 | 0.287 ± 0.081 | **0.609 ± 0.174** |
| Chromium (Cr) | 29.2 ± 16.1 | **59.8 ± 45.4** | 20.7 ± 13.9 | **37.6 ± 31.1** | 7.2 ± 1.0 | **69.4 ± 21.8** |
| Cobalt (Co) | 8.49 ± 2.70 | 7.32 ± 0.62 | 8.49 ± 3.13 | 6.16 ± 1.70 | 4.60 ± 1.27 | 11.05 ± 2.62 |
| Copper (Cu) | 14.7 ± 5.5 | 13.3 ± 1.4 | 17.4 ± 13.2 | 8.6 ± 7.3 | 4.2 ± 3.1 | 17.8 ± 2.8 |
| Lead (Pb) | 7.76 ± 3.17 | 6.72 ± 1.28 | 8.97 ± 4.86 | 4.23 ± 2.17 | 3.67 ± 1.66 | 9.63 ± 1.23 |
| Mercury (Hg) | 0.047 ± 0.030 | 0.034 ± 0.005 | 0.044 ± 0.010 | 0.044 ± 0.038 | 0.045 ± 0.022 | 0.067 ± 0.019 |
| Molybdenum (Mo) | 3.945 ± 1.959 | 5.195 ± 3.882 | 1.470 ± 0.184 | 6.605 ± 0.841 | 1.285 ± 0.219 | 6.535 ± 3.401 |
| Nickel (Ni) | 28.1 ± 4.9 | 42.2 ± 21.6 | 24.2 ± 14.0 | 29.2 ± 11.7 | 10.3 ± 2.7 | 52.3 ± 15.6 |
| Selenium (Se) (1 below DL) | 0.675 ± 0.290 | 0.540 ± 0.141 | 0.580 ± 0.255 | 1.255 ± 1.478 | 0.245 ± 0.205 | 0.820 ± 0.184 |
| Silver (Ag) (4 below DL) | 0.170 ± 0.085 | 0.075 ± 0.035 | 0.140 ± 0.057 | 0.125 ± 0.106 | 0.050 ± 0.000 | 0.195 ± 0.035 |
| Thallium (Tl) (1 below DL) | 0.193 ± 0.028 | 0.136 ± 0.000 | 0.137 ± 0.042 | 0.202 ± 0.209 | 0.058 ± 0.046 | 0.191 ± 0.025 |
| Tin (Sn) | < 1 | < 1 | < 1 | < 1 | < 1 | < 1 |
| Uranium (U) | 1.312 ± 0.464 | 1.235 ± 0.205 | 1.385 ± 0.375 | 1.935 ± 1.096 | 1.045 ± 0.035 | 1.400 ± 0.028 |
| Vanadium (V) | 27.9 ± 4.3 | 20.0 ± 0.8 | 33.2 ± 18.1 | 18.0 ± 8.2 | 10.7 ± 3.3 | 30.8 ± 6.0 |
| Zinc (Zn) | 90.5 ± 11.8 | 63.1 ± 23.1 | 68.1 ± 13.1 | 48.8 ± 23.5 | 40.8 ± 12.0 | 82.5 ± 10.5 |
| **Polycyclic Aromatic Hydrocarbons (PAHs) (mg/kg)** | | | | | | |
| 2-Methylnaphthalene | < 0.01 | < 0.01 | < 0.01 | < 0.01 | < 0.01 | < 0.01 |
| Acenaphthene | < 0.005 | < 0.005 | < 0.005 | < 0.005 | < 0.005 | < 0.005 |
| Acenaphthylene | < 0.005 | < 0.005 | < 0.005 | < 0.005 | < 0.005 | < 0.005 |
| Anthracene | < 0.004 | < 0.004 | < 0.004 | < 0.004 | < 0.004 | < 0.004 |
| Benz(a)anthracene | < 0.01 | < 0.01 | < 0.01 | < 0.01 | < 0.01 | < 0.01 |
| Benzo(a)pyrene | < 0.01 | < 0.01 | < 0.01 | < 0.01 | < 0.01 | < 0.01 |
| Benzo(b&j)fluoranthene | < 0.01 | < 0.01 | < 0.01 | < 0.01 | < 0.01 | < 0.01 |
| Benzo(g,h,i)perylene | < 0.01 | < 0.01 | < 0.01 | < 0.01 | < 0.01 | < 0.01 |
| Benzo(k)fluoranthene | < 0.01 | < 0.01 | < 0.01 | < 0.01 | < 0.01 | < 0.01 |
| Chrysene (11 below DL) | < 0.01 | < 0.01 | 0.008 ± 0.004 | < 0.01 | < 0.01 | < 0.01 |
| Dibenz(a,h)anthracene | < 0.005 | < 0.005 | < 0.005 | < 0.005 | < 0.005 | < 0.005 |
| Fluoranthene | < 0.01 | < 0.01 | < 0.01 | < 0.01 | < 0.01 | < 0.01 |
| Fluorene | < 0.01 | < 0.01 | < 0.01 | < 0.01 | < 0.01 | < 0.01 |
| IACR (CCME) | < 0.15 | < 0.15 | < 0.15 | < 0.15 | < 0.15 | < 0.15 |
| Indeno(1,2,3-c,d)pyrene | < 0.01 | < 0.01 | < 0.01 | < 0.01 | < 0.01 | < 0.01 |
| Naphthalene | < 0.01 | < 0.01 | < 0.01 | < 0.01 | < 0.01 | < 0.01 |
| Phenanthrene | < 0.01 | < 0.01 | < 0.01 | < 0.01 | < 0.01 | < 0.01 |
| Pyrene | < 0.01 | < 0.01 | < 0.01 | < 0.01 | < 0.01 | < 0.01 |
| Quinoline | < 0.01 | < 0.01 | < 0.01 | < 0.01 | < 0.01 | < 0.01 |

potential to be carcinogenic (Canadian Council of Ministers of the Environment 2010). PAHs are persistent and have been detected not only in freshwater sediments (Sanderson et al. 2012), but also in a number of freshwater organisms, including invertebrates (Rabodonirina et al. 2015) and fish (Ohiozebau et al. 2016, Ohiozebau et al. 2017). Although there are natural sources for PAHs (e.g., forest fires and volcanos), they are prevalent in the environment primarily due to anthropogenic sources, including oil spills, refineries, waste disposal sites, and sewage (Canadian Council of Ministers of the Environment 2010). Concentrations in sediment samples from 2018 were compared with sediment quality guidelines for the protection of aquatic life (Canadian Council of Ministers of the Environment 2001a), which include interim freshwater sediment quality guidelines (ISQGs) and probably effect levels (PELs). In addition, the Index of Additive Cancer Risk (IACR), which is a human health guideline based on carcinogenic effects (Canadian Council of Ministers of the Environment 2010), was compared with the guideline level for the protection of drinking water. All sediment chemistry results are presented as dry weight.

Mean values of all PAHs were below detection limit in Hay River sediment samples, with the exception of chrysene, which was above the detection limit in one sample in Reach 3 (Table 6). Because most PAHs were below detection limit, the IACR (which is calculated as the sum of a number of PAHs) was also below detection limit, which indicated low risk to drinking water quality (Table 6).

Some metal levels in sediment samples were above ISQGs, but none were above PELs (Table 6), which indicated low risk for biota. Arsenic was above the ISQG of 5.9 mg/kg (Canadian Council of Ministers of the Environment 2001a) in all reaches except Reach 2, and levels of this metal were similar to those found in 2018. Cadmium was above the ISQG of 0.6 mg/kg (Canadian Council of Ministers of the Environment 2001a) in Reach 1 and Reach 6, but values were close to the guideline level (Table 6). Chromium exceeded the ISQG of 37.3 mg/kg in Reach 2, but was notably lower in other reaches than was observed in 2018, when concentrations in the other reaches ranged from 60.7 to 273.0 mg/kg (Lento 2020). Levels of other metals, including mercury, were lower than CCME guidelines (Table 6).

Sediment chemistry data collected in 2018 had high variability within reaches that appeared to have been related to higher silt content of some samples. Particle size information was not obtained from sediment chemistry samples in 2019, but standard deviations for reaches were generally low, suggesting higher precision among paired samples than was found in 2018 samples.

#### *3.1.2.2. Benthic macroinvertebrates*

##### 3.1.2.2.1. Variation within and among reaches

Biotic metrics were calculated for kick sample data to summarize compositional differences among kick-sites and reaches. These metrics also provided a means to estimate normal range and CES for the BMI assemblage in each river (see section 2.3.4). Biotic metrics examined differences in total abundance and taxonomic richness. There were also metrics for specific taxonomic groups, including the relative abundance and richness of EPT, Chironomidae, Diptera + Oligochaeta, and Mollusca. EPT are generally considered to be sensitive to pollutants and disturbance, whereas Chironomidae are generally considered to be more tolerant of pollutants and disturbance and are also extremely tolerant of the cold temperatures and harsh environmental conditions characteristic of northern rivers. The Diptera + Oligochaeta metric also includes a number of taxa tolerant of cold, harsh environmental conditions and

*Table 7 Summary of biotic metrics for kick-site reaches sampled in the Hay River in 2019, including the mean ± standard deviation for BMI abundance and taxonomic richness metrics. EPT is the sum of Ephemeroptera, Plecoptera, and Trichoptera orders; Chironomidae is a family of Diptera; Diptera + Oligochaeta includes all true flies and segmented worms; and Mollusca includes bivalves (clams) and gastropods (snails).*

| Biotic Metric | HR- KS1 | HR-KS2 | HR-KS3 | HR-KS4 | HR-KS5 | HR-KS6 |
|---|---|---|---|---|---|---|
| Total abundance | 1731 ± 1201 | 818 ± 447 | 1416 ± 712 | 1093 ± 1217 | 1719 ± 797 | 1957 ± 491 |
| EPT abundance | 880 ± 656 | 478 ± 273 | 586 ± 250 | 227 ± 219 | 419 ± 105 | 513 ± 209 |
| Chironomidae abundance | 547 ± 375 | 231 ± 123 | 413 ± 332 | 597 ± 920 | 708 ± 397 | 499 ± 180 |
| Diptera + Oligochaeta abundance | 777 ± 541 | 305 ± 179 | 677 ± 511 | 799 ± 1059 | 1230 ± 750 | 1047 ± 555 |
| Mollusca abundance | 46 ± 52 | 14 ± 9 | 93 ± 175 | 38 ± 60 | 10 ± 8 | 242 ± 387 |
| Percent EPT | 43.8 ± 15.6 | 54.3 ± 14.2 | 44.1 ± 14.6 | 21.8 ± 12.0 | 27.7 ± 10.9 | 28.1 ± 14.7 |
| Percent Chironomidae | 37.4 ± 15.1 | 31.0 ± 8.7 | 26.3 ± 9.8 | 48.0 ± 21.4 | 39.3 ± 7.8 | 25.3 ± 3.7 |
| Percent Diptera + Oligochaeta | 49.8 ± 13.3 | 40.2 ± 11.2 | 45.4 ± 12.6 | 67.9 ± 19.0 | 67.3 ± 13.8 | 52.1 ± 17.2 |
| Percent Mollusca | 3.7 ± 4.2 | 2.4 ± 2.1 | 6.4 ± 9.4 | 6.6 ± 10.1 | 0.7 ± 0.6 | 11.8 ± 19.0 |
| Taxonomic richness | 33.2 ± 5.9 | 36.4 ± 3.7 | 41.0 ± 3.4 | 38.0 ± 9.9 | 41.2 ± 10.5 | 37.2 ± 4.9 |
| EPT richness | 7.8 ± 1.8 | 7.8 ± 3.1 | 11.0 ± 1.6 | 8.8 ± 1.3 | 10.4 ± 1.9 | 8.0 ± 2.5 |
| Chironomidae richness | 11.0 ± 1.7 | 13.0 ± 2.0 | 12.2 ± 1.1 | 12.2 ± 4.1 | 13.6 ± 4.2 | 12.4 ± 2.1 |
| Diptera + Oligochaeta richness | 18.0 ± 2.9 | 20.6 ± 2.3 | 20.8 ± 1.3 | 20.2 ± 7.3 | 22.4 ± 6.4 | 18.8 ± 2.4 |
| Mollusca richness | 2.4 ± 1.1 | 1.8 ± 0.4 | 2.2 ± 0.8 | 2.0 ± 1.4 | 1.6 ± 1.1 | 2.6 ± 1.5 |

pollutants, and it was included as an additional measure of the abundance and richness of tolerant organisms. The richness and relative abundance of Mollusca was included as a summary metric due to a high contribution of this taxonomic group in some sites, though it was primarily excluded from statistical analyses of metrics because abundance and richness remained low in most reaches.

In past years of sampling, the Hay River has shown a clear longitudinal gradient in abundance, with higher abundance of BMI in the three upstream reaches, and lower abundance in the three downstream reaches. However, mean abundance was similar between Reach 1, Reach 2, Reach 5, and Reach 6 in 2019, and there was no evidence of a pattern in total abundance moving from upstream to downstream reaches (Table 7; Figure 9). This may have been due in part to higher water levels, as the section of rocks below Reach 4 did not represent a barrier to movement in 2019.

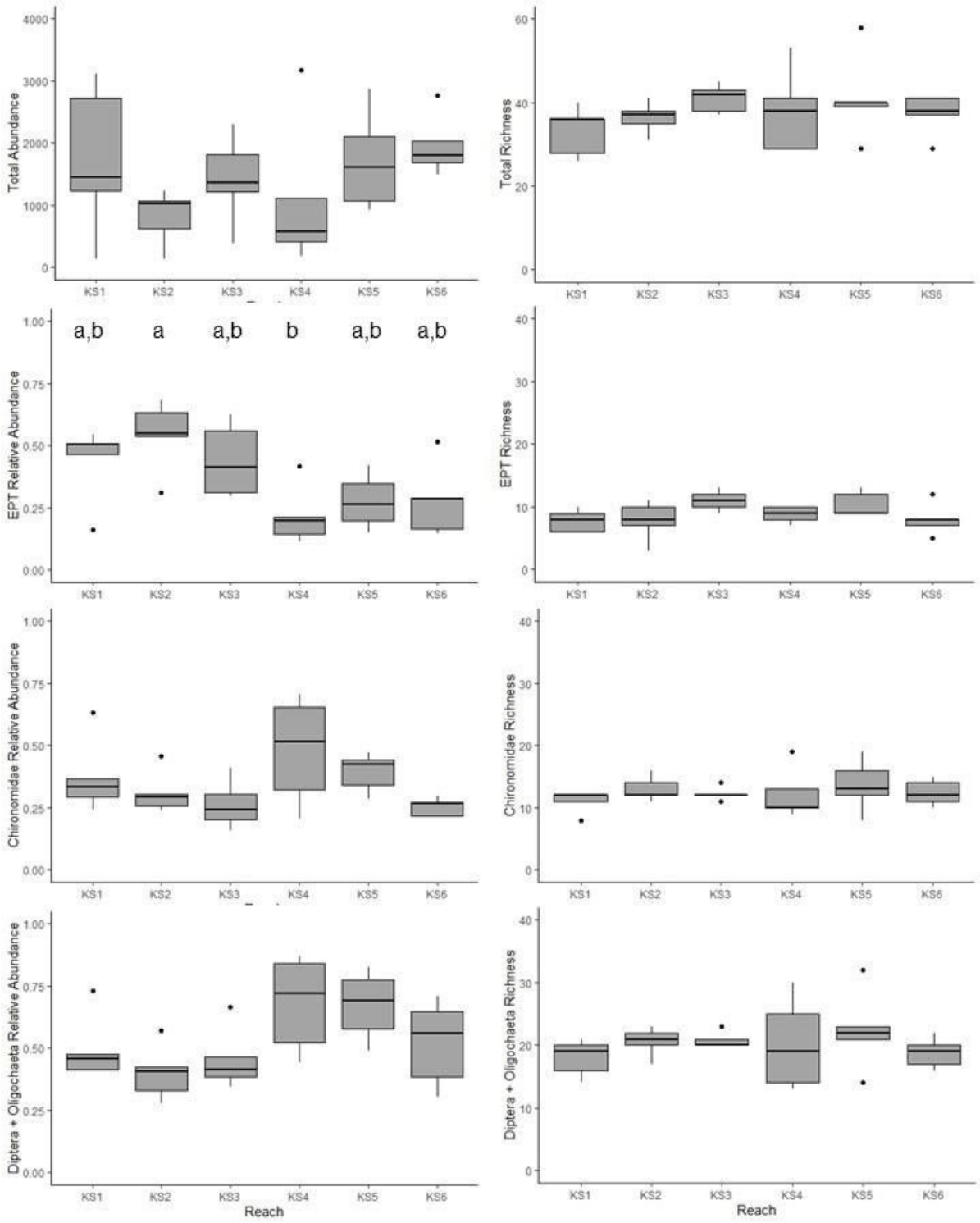


*Figure 9. Box plots of BMI metrics for the Hay River reaches sampled in 2019. Metrics include overall abundance and richness, and relative abundance and richness of Ephemeroptera, Plecoptera, and Trichoptera (EPT), Chironomidae (midges), and Diptera (true flies) + Oligochaeta (segmented worms). Box indicates the interquartile range, line through the box indicates the median, and whiskers indicate the lower and upper quartiles. Points indicate statistical outliers. Letters on plots indicate significant differences ($\alpha\alpha = 0.05$) from one-way ANOVA and Tukey HSD tests.*

Differences between upstream and downstream reaches were still evident when relative abundance of taxonomic groups was considered, though the differences were not generally strong enough to be statistically significant. There was higher relative abundance of EPT in the upstream reaches, though the difference was only statistically significant when Reach 2 and Reach 4 were compared (Table 7; Figure 9). Relative abundance of Chironomidae was somewhat higher in downstream reaches (particularly Reach 4) than in upstream reaches, but the differences were not statistically significant. The patterns of the relative abundance of Diptera + Oligochaeta mirrored those of Chironomidae in Reach 1 through Reach 4, but there were elevated levels for this metric in Reach 5 and Reach 6 (Figure 9). Diptera + Oligochaeta made up 52-67% of the total sample on average in these two downstream reaches, whereas Chironomidae only made up 29-35% of the sample, which indicated a higher abundance of non-chironomid Diptera and/or Oligochaeta at these two downstream reaches.

For most richness metrics, there was a high degree of similarity within and among reaches (Figure 9). Mean richness (total and group-specific) was similar across all reaches (Table 7) and interquartile ranges were small, particularly for EPT and Chironomidae (Figure 9). Total richness ranged from 33 to 41 taxa on average across all reaches, with an average of 7 to 11 EPT taxa and 11 to 14 Chironomidae taxa per reach (Table 7). Richness of Diptera + Oligochaeta taxa was somewhat more variable within reaches than EPT or Chironomidae, particularly in Reach 4 (Figure 9), but mean richness remained similar among reaches for this metric.

#### 3.1.2.2.2. Multivariate assessment of BMI assemblage composition

Multivariate analysis was used to characterize the biotic assemblage of the Hay River and evaluate similarities and differences in assemblage composition among reaches and sites. BMI relative abundance data were assessed at the family/subfamily level for this analysis (subfamily for Chironomidae and family or higher for all other taxa). The PCA was intended to assess correlations within and among reaches, to identify taxa driving similarity/dissimilarity among sites and indicate any potential outliers or gaps in sample sites. PERMANOVA and analysis of homogeneity of multivariate dispersions provided a statistical assessment of compositional differences both among reaches and within reaches.

The PCA of assemblages in the Hay River had no strong outliers (Figure 10A), which suggested that no sites were ecological outliers with respect to assemblage composition. The first axis of the PCA, which explained 44% of variation among sites, represented a gradient separating sites in Reach 1 and Reach 2 from the three downstream reaches, with sites in Reach 3 primarily located near the origin, uncorrelated with the primary gradient (Figure 10A). The mayfly family Leptophlebiidae, which was primarily found in the three upstream reaches, was most strongly correlated with the first axis gradient (Figure 10B). This taxon prefers slow-flowing waters or pools (McCafferty 1998, Monk et al. 2018). There were few other strong associations with particular taxa along the first axis gradient. Sites in Reach 1 and Reach 2 were positively correlated with several molluscs (Physidae, Planorbidae, Valvatidae), as well as segmented worms (Enchytraeidae) and other families of Ephemeroptera, and were negatively associated with some Diptera, Trichoptera, and Plecoptera families (Figure 10B). On the negative end of the first axis gradient, sites in Reach 5 were positively correlated with the chironomid subfamily Diamesinae and several taxa with a preference for fast flows (Monk et al. 2018), including families of Plecoptera (the large-bodied Pteronarcidae and Perlodidae) and Trichoptera (Lepidostomatidae and the

net-spinning caddisfly Hydropsychidae). These taxon associations are consistent with the higher average velocity recorded in this reach (Table 5).

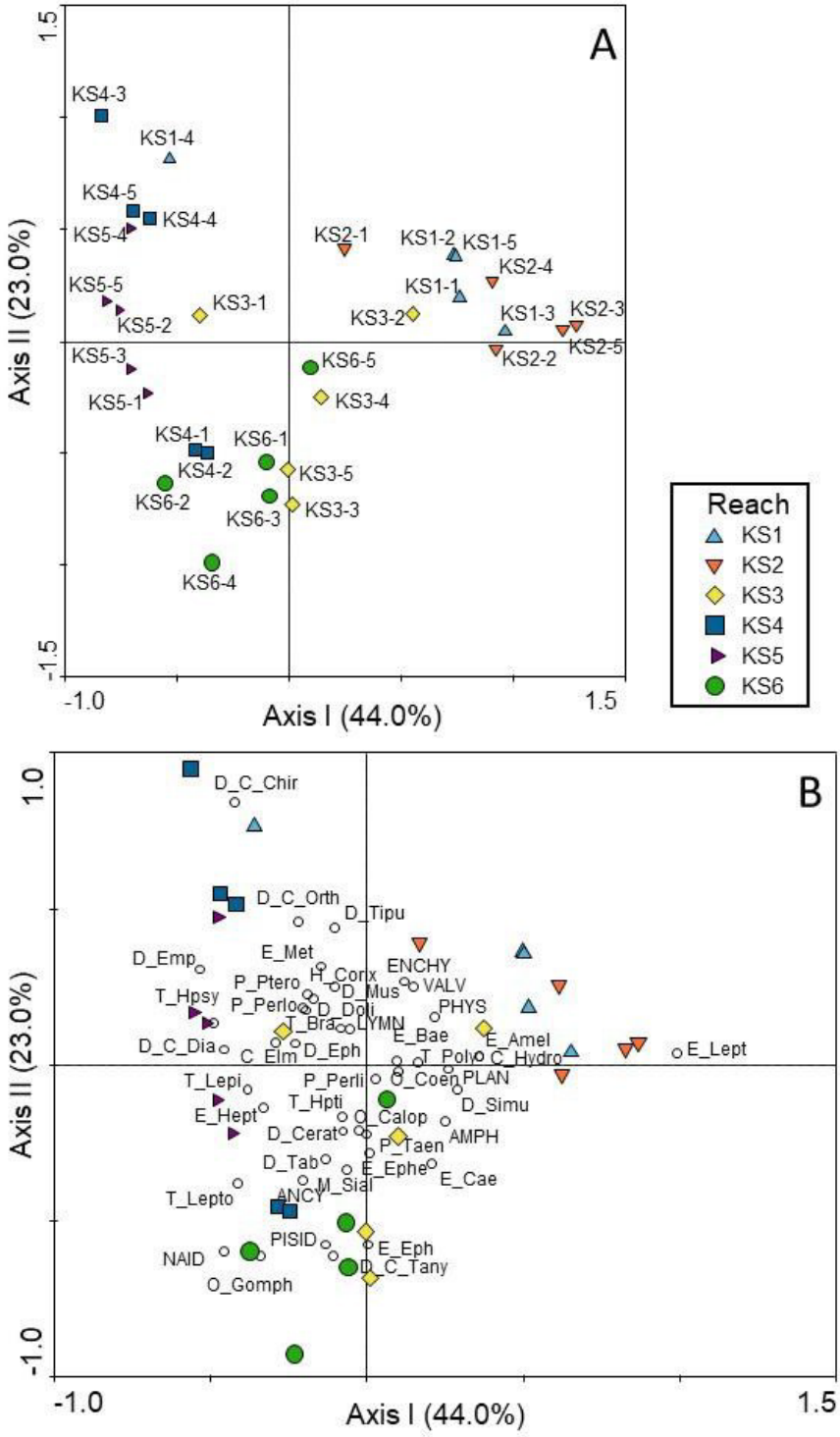

*Figure 10. Multivariate analysis of BMI from kick samples in Hay River in 2019, including (A) PCA of BMI data showing labelled sample points, and (B) PCA biplot of BMI data showing sample points and labelled taxa, both with sample points coloured by reach. Kick-sites in close proximity have similar assemblages, whereas samples on opposite ends of gradients have differences in their assemblages. Samples at right angles through the origin are uncorrelated. Kick-sites are located close to taxa with which they are positively associated. Taxa near the origin are not labelled for ease of interpretation. Taxonomic abbreviations are listed in the appendices.*

*Table 8 Results of pairwise PERMANOVA comparing assemblage dissimilarity among reaches of Hay River, showing pairwise p-values for each comparison. FDR-corrected $\alpha\alpha$ was calculated for each pairwise comparison based on p-value rank, and p-values less than the FDR-corrected $\alpha\alpha$ (marked with *) indicate a significant difference in assemblage composition between reaches based on a dissimilarity matrix.*

| | KS1 | KS2 | KS3 | KS4 | KS5 | KS6 |
|---|---|---|---|---|---|---|
| **KS1** | | | | | | |
| **KS2** | 0.638 | | | | | |
| **KS3** | 0.031 | 0.014* | | | | |
| **KS4** | 0.057 | 0.006* | 0.099 | | | |
| **KS5** | 0.005* | 0.004 | 0.14 | 0.155 | | |
| **KS6** | 0.02* | 0.009* | 0.3 | 0.05 | 0.007* | |

The second axis of the ordination, which explained 23% of variance among sites, largely separated the sites in Reach 4, Reach 5, and Reach 6 (Figure 10A). On the positive end of the second axis gradient, sites in Reach 4 were positively correlated with the chironomid subfamilies Chironominae and Orthocladiinae, as well as Tipulidae (crane flies). Site KS1-4 did not plot out with other sites in Reach 1, but instead was located near site KS4-3, positively associated with the second axis in the ordination, suggesting that this site shared a strong positive correlation with Chironominae (Figure 10B). On the negative end of the second axis gradient, sites in Reach 6 were positively correlated with the dragonfly Gomphidae, the segmented worm Naididae, the bivalve Pisidiidae, the chironomid Tanypodinae, and the mayfly Ephemeridae, all of which have a preference for slow-flowing water (Monk et al. 2018). Reach 6 had slower flow velocity relative to Reach 4 or Reach 5 (Table 5), and the taxon associations in the ordination were consistent with this slower flow. Sites in Reach 3 (KS3-3, KS3-4, and KS3-5) were positively correlated with Reach 6 and had similar flow velocity.

The PERMANOVA indicated that there were significant differences in assemblage composition among reaches in Hay River (based on assessment of a dissimilarity matrix; $F = 3.99$, $p = 0.001$). Pairwise PERMANOVA identified which reaches had statistically significantly different assemblages (significant at an FDR-corrected $\alpha\alpha$-level, based on the rank of each $p$-value). The upstream reaches (Reach 1 and Reach 2) were found to differ significantly from the farthest downstream reaches (Reach 5 and Reach 6, though the comparison between Reach 2 and Reach 5 was not significant at the FDR-corrected $\alpha\alpha$-level; Table 8). The assemblage composition of Reach 2 was also significantly different from that of Reach 3 and Reach 4 (Table 8), consistent with the results of the PCA (Figure 10). Assemblage composition also differed significantly between Reach 5 and Reach 6 (Table 8), possibly reflecting the somewhat orthogonal (uncorrelated) relationship among samples from these reaches in the PCA. Reaches 3 and 4, which had many taxa in common with other reaches, were generally found to be similar to other reaches in the pairwise PERMANOVA.

Each reach of the Hay River displayed a similar magnitude of within-reach variability in assemblage composition, as evidenced by distance to centroid in multivariate space (homogeneity of multivariate dispersions $F = 1.43$, $p = 0.259$). The median distance to centroid was generally low (Figure 11), and similar among all reaches. Reach 5 had the lowest median distance to centroid, indicative of stronger similarity among sites, whereas the median distance to centroid was highest for Reach 2 and Reach 6, which indicated higher within-reach variability.

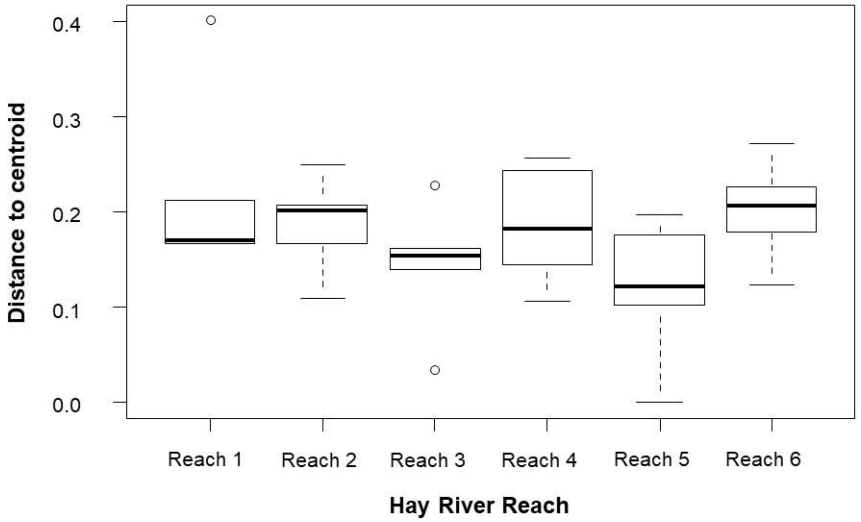


*Figure 11 Results of homogeneity of multivariate dispersions analysis of Hay River BMI assemblages, showing the median distance to centroid for each reach (black bar), 25th and 75th percentiles (lower and upper bounds of box, respectively), minimum and maximum (whiskers), and outliers (points). Distance to centroid represents the spread of sites in multivariate space, where greater distance equals greater dissimilarity among sites. Low distance to centroid indicates similarity within reaches.*

#### 3.1.2.2.3. Biotic-abiotic relationships

Relationships between BMI assemblages and abiotic parameters were tested to explore potential drivers of assemblage structure in the Hay River. Because there appeared to be differences among reaches that related to flow velocity, the relationship between biotic metrics and flow velocity was tested with least-squares linear regression. When the relationship between a metric and velocity appeared to be curvilinear, a polynomial regression model was tested.

Relationships of abundance metrics with velocity were variable, with few examples of a clear biotic response to differences in flow velocity among sites (Figure 12). Total abundance and the relative abundance of Chironomidae appeared to increase with increasing flow, but the relationship was highly variable. When regressions were tested for each of the abundance-based metrics, only total abundance was found to vary significantly as a function of flow velocity (slope $t = 2.12$, $p = 0.044$).

Richness metrics appeared to show a curvilinear (unimodal) response to flow velocity, with the highest richness found in the middle of the velocity range across all sites (Figure 12). Statistical analysis confirmed this pattern, as polynomial models provided a better fit to the data than linear models for all

richness metrics. There was a statistically significant unimodal relationship between total richness and flow velocity (regression $F_{2,26}$ = 6.00, $p$ = 0.007). There was also a statistically significant unimodal relationship between Chironomidae richness and flow velocity (regression $F_{2,26}$ = 5.09, $p$ = 0.014), and between Diptera + Oligochaeta richness and flow velocity (regression $F_{2,26}$ = 3.80, $p$ = 0.036). Although a similar pattern was evident for EPT richness (Figure 12), the results of the polynomial regression were not significant. In general, however, these results indicate that taxonomic richness in the Hay River increases with increasing flow velocity to a point, after which richness begins to decline as velocity increases.

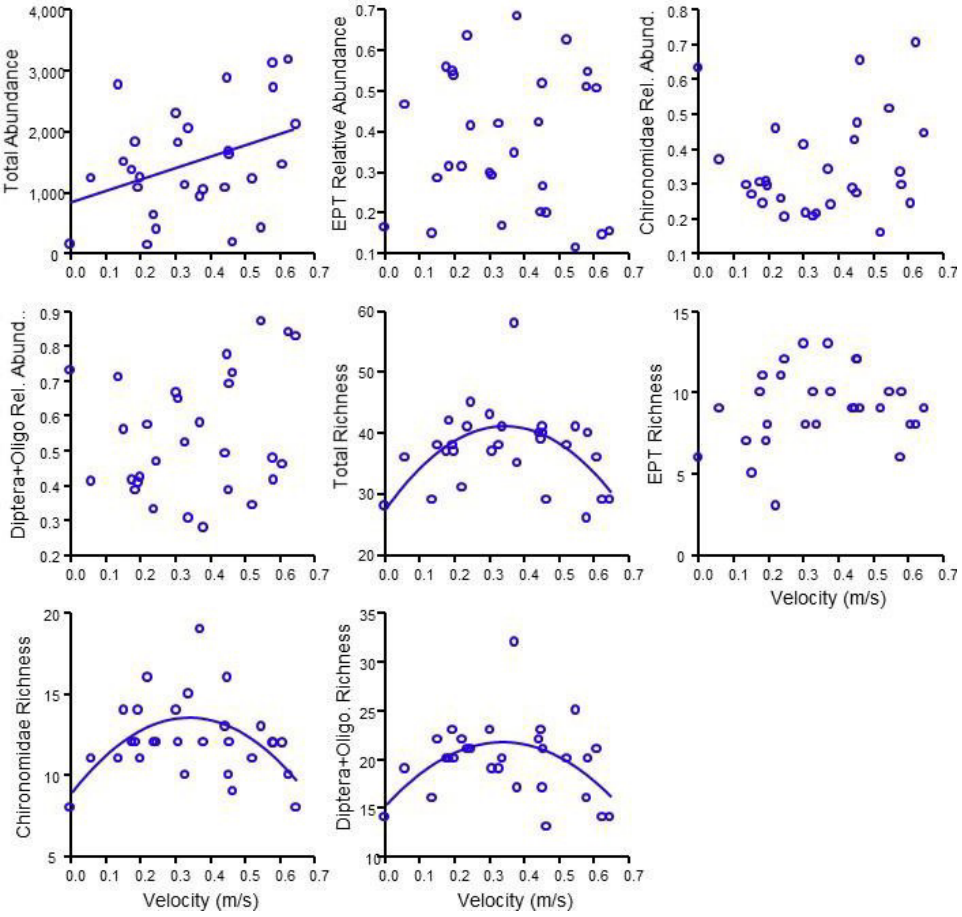


*Figure 12. Relationship between biotic metrics calculated for Hay River sites and flow velocity recorded at each site at the time of sampling, with a linear or polynomial regression line fit to plots where there was a significant relationship with velocity. Each plot has a different metric as the response variable on the y-axis.*

Biotic-abiotic relationships were also assessed in Hay River kick samples using Redundancy Analysis (RDA), a multivariate approach that uses environmental variables to constrain the spatial arrangement of sites based on BMI relative abundance. RDA assesses the amount of variation in the unconstrained ordination (the PCA of BMI samples) that is explained by relating the data to chosen environmental variables and identifies major abiotic gradients in the data. This analysis was completed using water chemistry and physical habitat parameters. Prior to analysis, correlations between environmental

parameters were examined in combination with the abiotic PCA to pick out important drivers of differences among sites that were uncorrelated with each other to avoid multicollinearity in the RDA. This also worked to reduce the number of environmental parameters in the analysis and avoid over-fitting the data. The final RDA included velocity, % gravel, % cobble, alkalinity, conductivity, hardness, dissolved organic carbon (DOC), total organic carbon (TOC), ortho-phosphate (Ortho-P), dissolved phosphorus (DP), dissolved nitrogen (DN), total suspended solids (TSS), dissolved arsenic (D-As), and dissolved iron (D-Fe). Other ions, nutrients, physical measures, and total and dissolved metals were highly correlated with the chosen variables. For example, dissolved iron was strongly positively correlated with a large number of other dissolved metals, whereas TSS was strongly positively correlated with TP, TN, and most total metal concentrations. Thus, any patterns described for these parameters also apply to the correlated parameters.

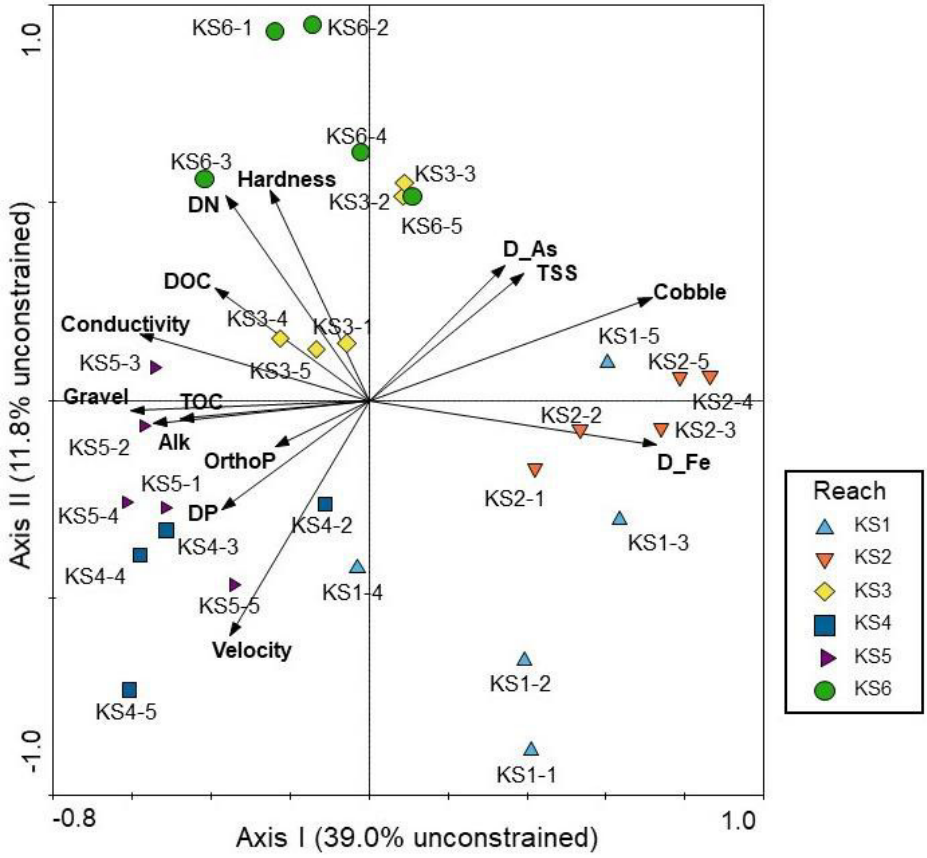


*Figure 13. RDA ordination of Hay River BMI data constrained by physical and chemical habitat data at each site, with sites coloured by reach. Even-numbered sites use average values of chemical parameters from neighbouring odd-numbered sites. Site KS4-1 was omitted due to lack of velocity data. Kick-sites at the same end of a gradient are positively correlated with similar taxa and chemical/physical variables, whereas samples on opposite ends of gradients are negatively correlated. Samples at right angles through the origin are uncorrelated. Vectors indicate direction of change of physical and chemical parameters, and sites are ranked along these vectors based on the strength of their correlation with each parameter.*

All axes of the RDA of BMI relative abundance and chemical and physical parameters were statistically significant (Monte Carlo permutation test: first axis $F = 8.94$, $p = 0002$; all axes $F = 1.76$, $p = 0.026$), and the first three axes explained 87.8% of constrained variation among samples (56% of the unconstrained variation). The dominant gradients in the Hay River RDA were driven by a combination of chemical and physical habitat parameters. Along the first axis, which explained 61.1% of constrained variation in benthic assemblages (39.0% unconstrained variation), sites in Reach 1 and Reach 2 were separated from other reaches due to a positive correlation with the percent cobble, TSS, and concentrations of dissolved metals (As and Fe; Figure 13). Dissolved iron had low variability among most sites and slightly elevated concentrations at a small number of sites, leading to its importance in the ordination. However, even without dissolved iron in the ordination, the same separation among sites was evident, but was instead driven by substrate size (relative abundance of cobble; results not shown). On the negative end of the first axis gradient, sites in Reach 4 and Reach 5 were positively associated with percent gravel, velocity, conductivity, alkalinity, DP, DOC, TOC, and ortho-phosphate (Figure 13).

The second axis of the RDA, which explained 18.5% of constrained variance and 11.8% of unconstrained variance in benthic assemblages, primarily separated sites in Reach 3 and Reach 6 from sites in Reach 1. Sites in Reach 1 were positively correlated with velocity, whereas sites in Reach 3 and Reach 6 were negatively correlated with velocity and positively correlated with hardness, DN, dissolved Ass, and TSS (Figure 13).

The statistical significance of chemical and physical habitat variables in the RDA was tested using Monte Carlo permutational tests. Dissolved iron had the strongest effect on the fit of the model ($F = 7.27$, $p = 0.002$), followed by the percent cobble ($F = 3.64$, $p = 0.004$). Velocity had the third strongest effect on the fit of the model, but it was not statistically significant ($F = 2.07$, $p = 0.076$). No other variables were significant, likely due to the similarity in water chemistry among sites that may have resulted in a lack of explanatory power for water chemistry parameters.

### 3.1.3. Temporal characterization of BMI assemblages

#### *3.1.3.1. Benthic macroinvertebrate composition*

Compositional changes from 2017 to 2019 were summarized at the river level by assessing the average relative abundance of major taxonomic groups across all reaches in each year (Figure 14). Across all reaches, the relative abundance of Diptera (true flies) and Ephemeroptera (mayflies) decreased in 2018, whereas the relative abundance of Oligochaeta (segmented worms) and Bivalvia (bivalve molluscs, which combine with Gastropoda to make up the phylum Mollusca; Figure 14) increased. However, in 2019 the relative abundance of true flies and segmented worms both increased relative to the previous years of sampling, and the relative abundance of bivalve molluscs declined (Figure 14). Relative abundances of other taxonomic groups remained fairly similar among years.

Shifts in the relative abundance of Chironomidae and EPT were evident in the Hay River over the three years of sampling. In 2017, these two groups together made up a large portion of the BMI assemblage, and there were some reaches and sites along the river where one group or the other was clearly dominant. For example, Chironomindae predominated at KS1-4A and at sites in Reach 4 and Reach 5, while EPT predominated in Reach 2 and Reach 3 (Figure 15). In 2018, when the relative abundance of Diptera decreased on average across all sites (Figure 14), there was a more clear upstream-downstream pattern in the relative abundance of EPT and Chironomidae, with EPT predominant in upstream reaches,

and a greater dominance of Chironomidae in downstream reaches (albeit not in all sites in downstream reaches; Figure 15). In 2019, patterns in EPT and Chironomidae relative abundance once again resembled the patterns found in 2017, with similar peaks and troughs in the relative abundance of each taxonomic group. This result suggests that, despite the high water levels in the Hay River in 2019, some aspects of assemblage structure were similar to those found in 2017.

Biotic metric data from all three years were combined into temporal box plots to evaluate general patterns over time within and among reaches (Figure 16). Temporal patterns in total abundance were variable among reaches, with Reach 1 and Reach 2 showing increased abundance in 2018 relative to other years, and Reaches 3, 4, and 5 showing decreased abundance in 2018 and 2019 relative to 2017 (Figure 16). Patterns in relative abundance of particular taxonomic groups were somewhat less variable among reaches. For example, the relative abundance of EPT was lower in 2018 and 2019 than in 2017 in

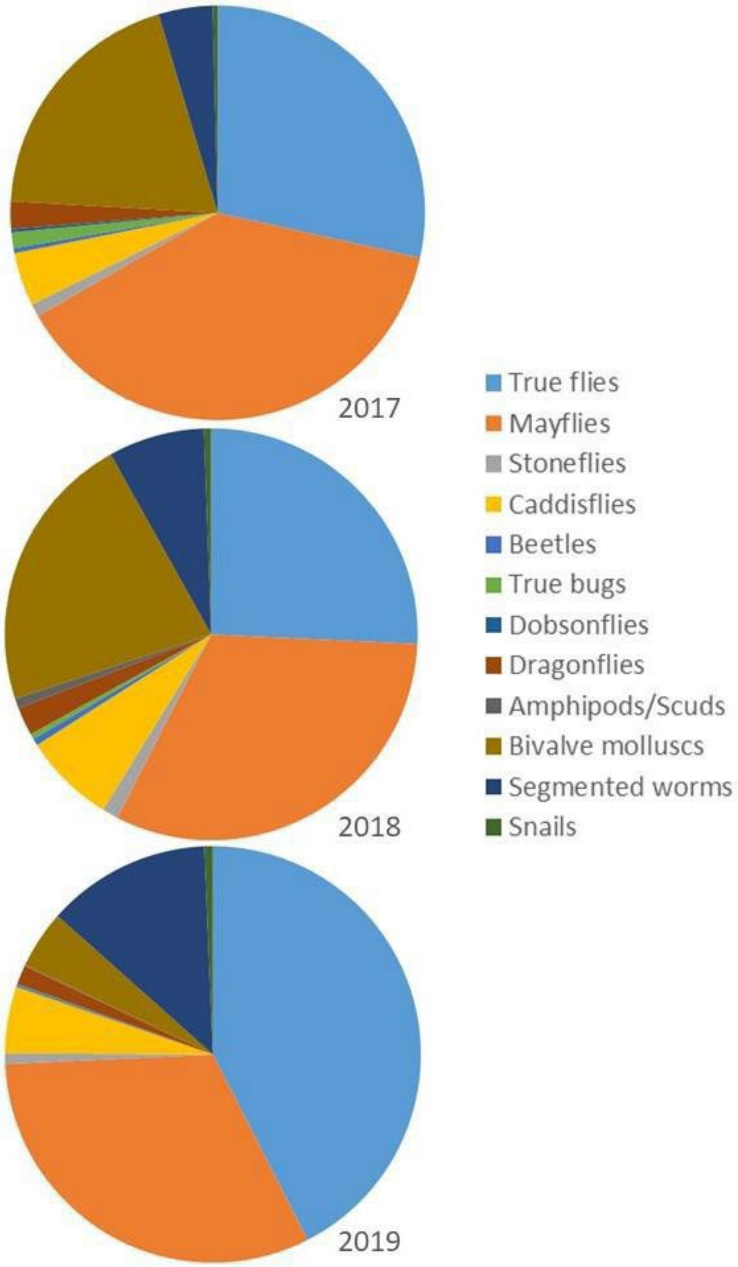


*Figure 14. Average relative abundance of major BMI taxonomic groups in Hay River kick samples collected in (A) 2017 and (B) 2018. Taxa are grouped as true flies (Diptera), mayflies (Ephemeroptera), stoneflies (Plecoptera), caddisflies (Trichoptera), beetles (Coleoptera), true bugs (Hemiptera), dobsonflies (Megaloptera), dragonflies (Odonata), amphipods/scuds (Amphipoda), bivalve molluscs (Bivalvia), segmented worms (Oligochaeta), and snails (Gastropoda)*

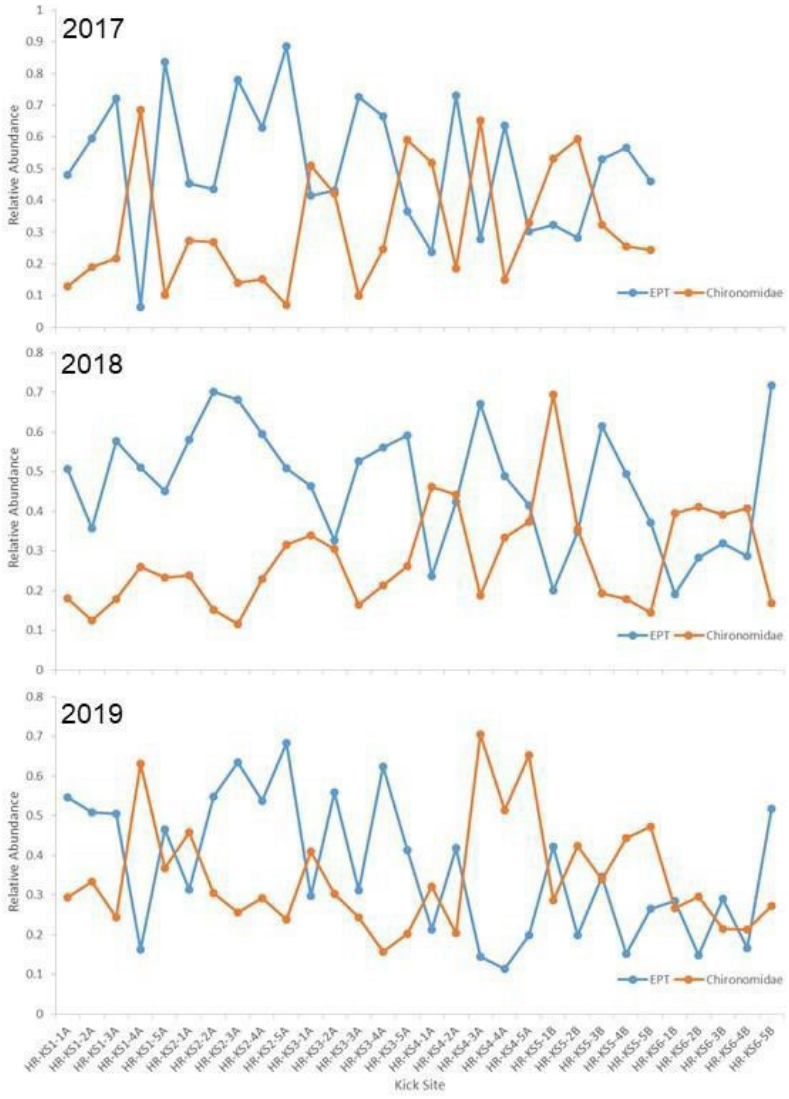


*Figure 15. Relative abundance of EPT (blue lines) and Chironomidae (orange lines) across Hay River sites, with data from 2017, 2018, and 2019 presented. Note that Reach KS6 was not sampled in 2017.*

all reaches. The relative abundance of Chironomidae and of Diptera + Oligochaeta in 2018 was similar to or lower than that found in 2017 for most reaches, but there was a subsequent increase in relative abundance in most reaches in 2019 (Figure 16). Together, these results indicate that a shift in relative proportions of EPT and Diptera/Oligochaeta has occurred in the Hay River since 2017.

Richness metrics also indicated shifts over time that reflected a greater dominance of Chironomidae and other Diptera and Oligochaeta. EPT richness fluctuated over time, but the number of taxa found in 2019 was generally similar to or lower than the number found in 2017 (Figure 16). In contrast, Chironomidae richness and the richness of Diptera + Oligochaeta both increased in 2019 relative to earlier years, and these increases led to a net increase in total richness across all reaches, with the greatest increase observed in Reach 3 (Figure 16).

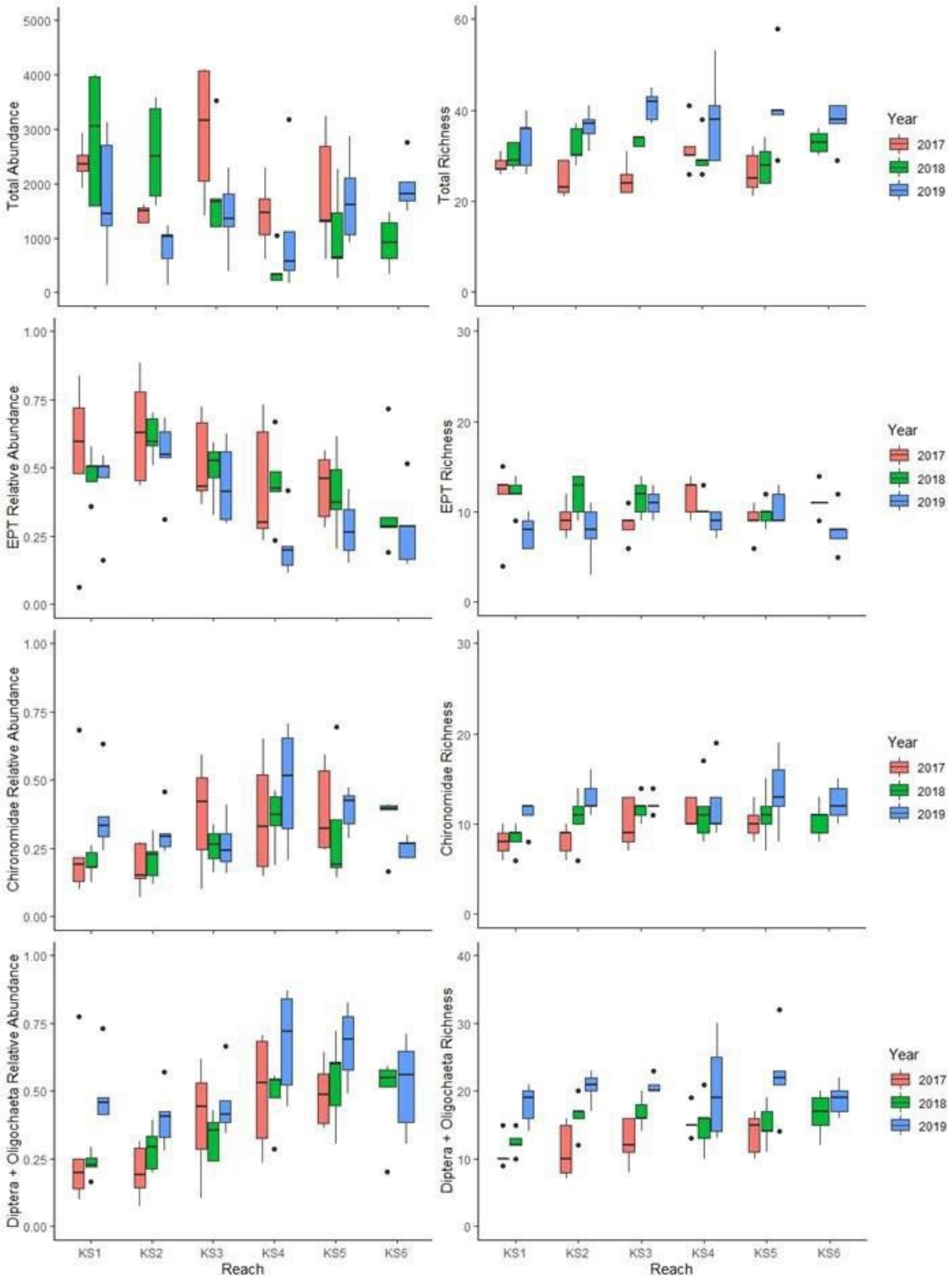


*Figure 16. Box plots of BMI metrics for the Hay River reaches, showing data from 2017, 2018, and 2019 for each reach. Metrics include overall abundance and richness, and relative abundance and richness of Ephemeroptera, Plecoptera, and Trichoptera (EPT), Chironomidae (midges), and Diptera (true flies) + Oligochaeta (segmented worms). Box indicates the interquartile range, line through the box indicates the median, and whiskers indicate the lower and upper quartiles. Points indicate statistical outliers. Note that Reach KS6 was not sampled in 2017.*

The mean ± SE for each biotic metric in each year was plotted with data for all reaches overlain in a single plot to further evaluate change over time in the Hay River (Figure 17). Mean total abundance was most variable among reaches in each year, and patterns over time were also inconsistent among reaches. However, there was greater similarity in mean abundance among reaches in 2019 (Figure 17), possibly reflecting a common response to increased flows in all reaches. Despite some differences in the magnitude of mean relative abundance of taxonomic groups and mean richness among reaches, some general patterns were evident across years, including an increase in relative abundance and richness of Diptera + Oligochaeta over time and a concurrent increase in total taxonomic richness (Figure 17). Though there did appear to be a decline in relative abundance and richness of EPT and an increase in relative abundance and richness of Chironomidae over the three years, these were more subtle changes.

#### *3.1.3.2. Drivers of temporal patterns*

The greatest change that occurred over the sampling period (2017-2019) was related to the flow regime. Changes in the magnitude and timing of peak flows contributed to variation in water levels (ranging from extreme low flows to high flows) and different antecedent hydrologic conditions in each year of sampling. To evaluate the effect of varying flow on biotic metrics, ANCOVA models were tested with velocity as a continuous predictor (as relationships with velocity were evident for some metrics) and year as a categorical predictor and proxy for flow conditions in each year. Analysis was completed with Reaches 1 through 5, because Reach 6 was not sampled in 2017.

The full ANCOVA model for total abundance indicated that the interaction between year and velocity was not significant ($p = 0.458$), and the analysis proceeded with the reduced model. In the reduced model, the year term was significant ($F_{2,71} = 8.07$, $p = 0.001$) and Tukey's HSD indicated that mean abundance across sites, while controlling for velocity, was significantly lower in 2019 than in 2017 ($p < 0.001$) or 2018 ($p = 0.16$). There were no significant differences in total abundance between 2017 and 2018. This result indicates that the higher flows in 2019 contributed to lower abundance across sites.

The full ANCOVA model for total richness also indicated that the interaction between year and velocity was not significant ($p = 0.372$), and the reduced model was used to compare mean richness across years. In the reduced model, the year term was significant ($F_{2,71} = 15.62$, $p < 0.001$) and Tukey's HSD indicated that mean richness across sites, while controlling for velocity, was significantly higher in 2019 than in 2017 ($p < 0.001$) or 2018 ($p = 0.001$). However, there were no significant differences in richness between 2017 and 2018. This result indicates that higher flows in 2019 also contributed to greater taxonomic richness across sites.

### 3.1.4. Normal range and CES

The normal range/CES concept is based on setting boundaries around the normal range of variability in samples, and using those boundaries (which denote the CES) to trigger management action if test samples are impaired (i.e., if they fall outside the range of natural variability, denoted by the upper and lower CES). Normal range is commonly defined as the range within which 95% of samples fall, equivalent to two standard deviations from the mean in a normal distribution (Munkittrick et al. 2009). While it is possible for samples to fall outside the CES, there is a low probability (5% chance) of this happening if the sample is representative of the normal range. Thus, where sites have been exposed to anthropogenic impacts, samples outside of the CES may be an indication of impairment in a system.

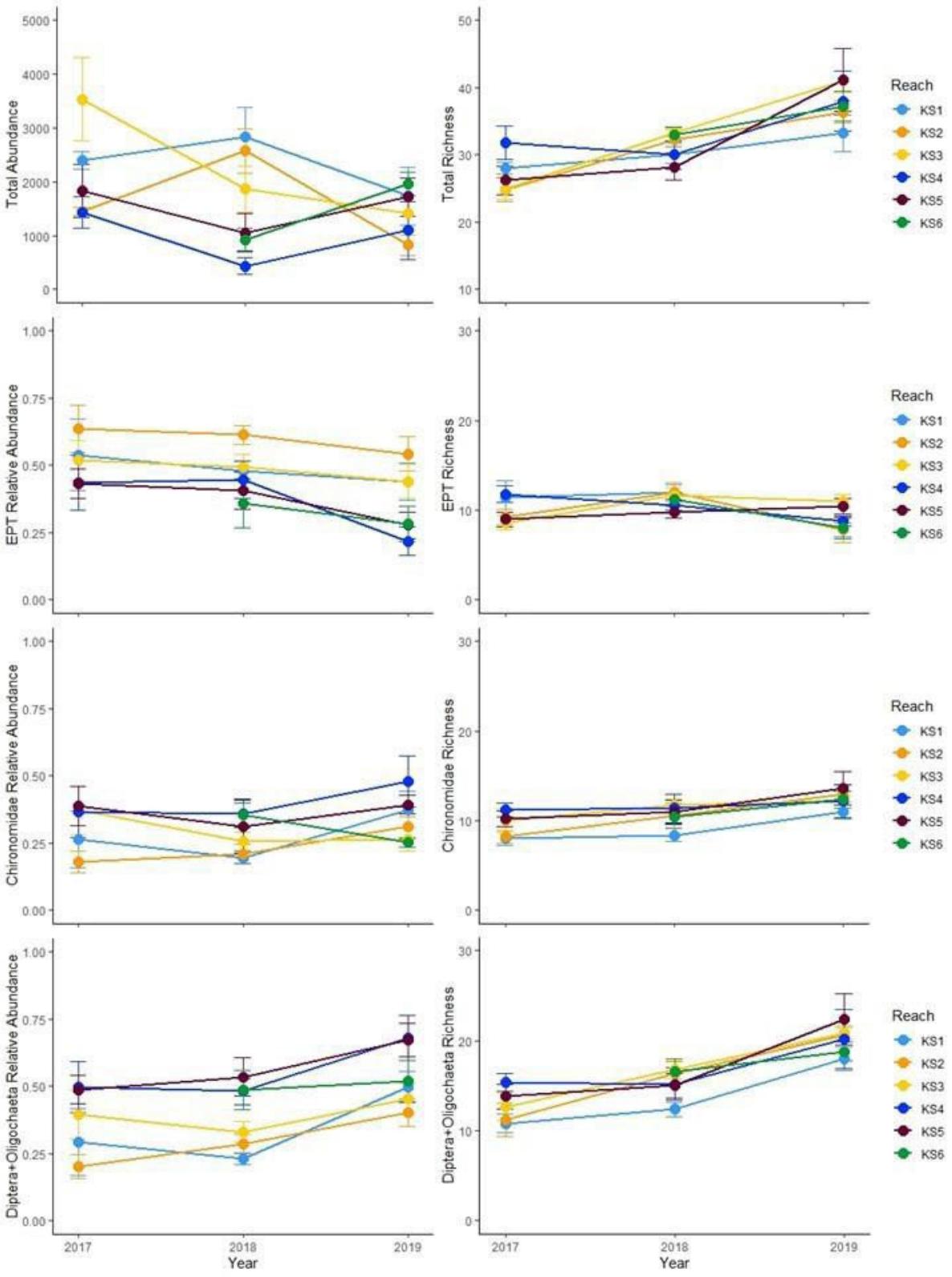


*Figure 17. Line plots of changes over time in biotic metrics in the Hay River, showing the mean ± SE for each reach in 2017, 2018, and 2019. Note that Reach KS6 was not sampled in 2017.*

The normal range and CES is based on variability in the data, and changes in habitat conditions that result from natural variability (i.e., due to shifts in flow, timing of the spring freshet, water temperature, etc.) may affect the normal range from one year to the next. Furthermore, sites that were within the normal range in one year may fall outside the normal range in the next year if they are strongly affected by natural variability in the system. Monitoring of assemblages over several years can therefore be used to get a better, more accurate estimate of the CES or normal range in a system that accounts for this natural variability. Three years of data allows for initial determination of a normal range and CES boundaries, but more years of data (5-10 or more, depending on variability in the system) are needed before greater precision is achieved and there can be greater confidence in the use of these measures to detect potential impairment.

Within-year variability among sites (within-year normal range) was assessed in previous reports using 2017 and 2018 data. This approach considers the variability across all data collected in the current sampling year. With the collection of 2019 data, the analysis of normal range can be expanded to include temporal normal range and CES at the site scale and at the reach scale, for the calculation of boundaries that better reflect site- and reach-specific conditions.

This analysis was used to quantify the normal range of variability (within-year and temporal) and critical effect size based on several BMI metrics: total abundance, relative abundance of EPT, relative abundance of Chironomidae, relative abundance of Diptera + Oligchaeta, total taxonomic richness, richness of EPT, richness of Chironomidae, and richness of Diptera + Oligochaeta.

#### *3.1.4.1. Within-year variability*

For the analysis of within-year variability, mean values of each metric and standard deviations across all sites in the river were calculated, and CES was set to ± 2SDs from the mean. Two sets of within-year CES were calculated: the single-year CES, based on only the 2019 data to identify any sites that appeared to be outliers in this year, and the multi-year CES, based on the mean and standard deviation of combined 2017-2019 data. Single-year and multi-year CES boundaries were compared with site data from 2019. The multi-year CES boundaries build the foundation for temporal assessment of normal range by providing an initial assessment of temporal variation at the river scale.

Samples collected in 2019 generally fell within the CES boundaries developed using only 2019 data (Figure 18). Total abundance was low in three sites in 2019 (KS1-4, KS2-1, and KS4-5), and approached the lower CES bounds for this metric based on 2019 data. In contrast, relative abundance of Chironomidae was high and near the upper CES bounds in two sites (KS4-3 and KS4-5; Figure 18). EPT richness was lower than the single-year CES boundary at KS2-1, and high total richness was found in Reach 4 and Reach 5, reflecting richness levels for Chironomidae and Diptera + Oligochaeta that exceeded the upper CES.

Deviations from normal range were more apparent when data from 2019 were compared with the multi-year CES that was developed based on data from 2017-2019 (Figure 19). These exceedances reflected high variation in metrics in 2019 relative to the variation that was observed across three years of sampling. Total abundance in 2019 was below the lower bounds of the multi-year CES in sites in Reach 1, Reach 2, Reach 3, and Reach 4 (Figure 19). However, some sites in Reach 1 and Reach 4 had a total abundance above the upper bounds of the CES. Relative abundance of taxonomic groups in 2019 also fell outside the multi-year CES in several sites, reflecting lower relative abundance of EPT and higher

relative abundance of Chironomidae and Diptera + Oligochaeta. Relative abundance of EPT was particularly low in the three downstream reaches, where 8 out of 15 sites were below the multi-year CES (Figure 19). In a complementary pattern, many of the same sites in downstream reaches were above the multi-year CES for the relative abundance of Diptera + Oligochaeta metric.

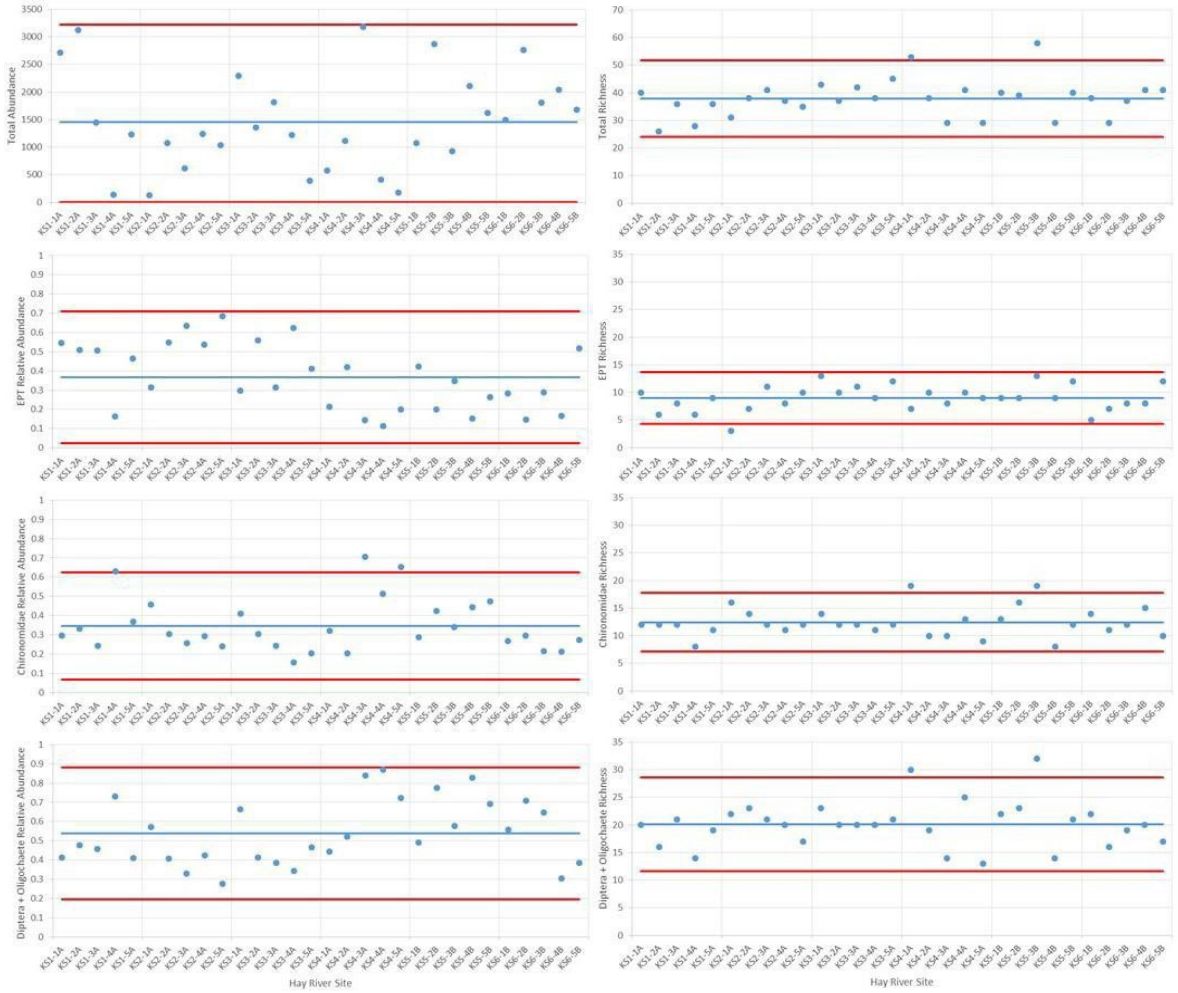


*Figure 18. Biotic metrics plotted for each site in the Hay River with 2019 mean (blue line) and the upper and lower single-year critical effect size (CES; red lines), calculated as mean ± 2SD (calculated based on 2019 data). Each point represents a kick-site, moving from reach 1, site 1 (far left) to reach 6, site 5 (far right) on each plot. Metrics include (left column) total abundance, EPT relative abundance, Chironomidae relative abundance, Diptera + Oligochaeta relative abundance, and (right column) total taxonomic richness, EPT richness, Chironomidae richness, and Diptera + Oligochaeta richness.*

The normal range for richness metrics was much narrower, reflecting lower variability in these metrics from 2017-2019. Total richness in 2019 was above the upper CES boundary in a number of sites, which reflected higher richness of Chironomidae and Diptera + Oligochaeta (higher than CES in most of the same sites; Figure 19). In contrast, low richness of EPT was evident at sites in Reach 1, Reach 2, and Reach 6.

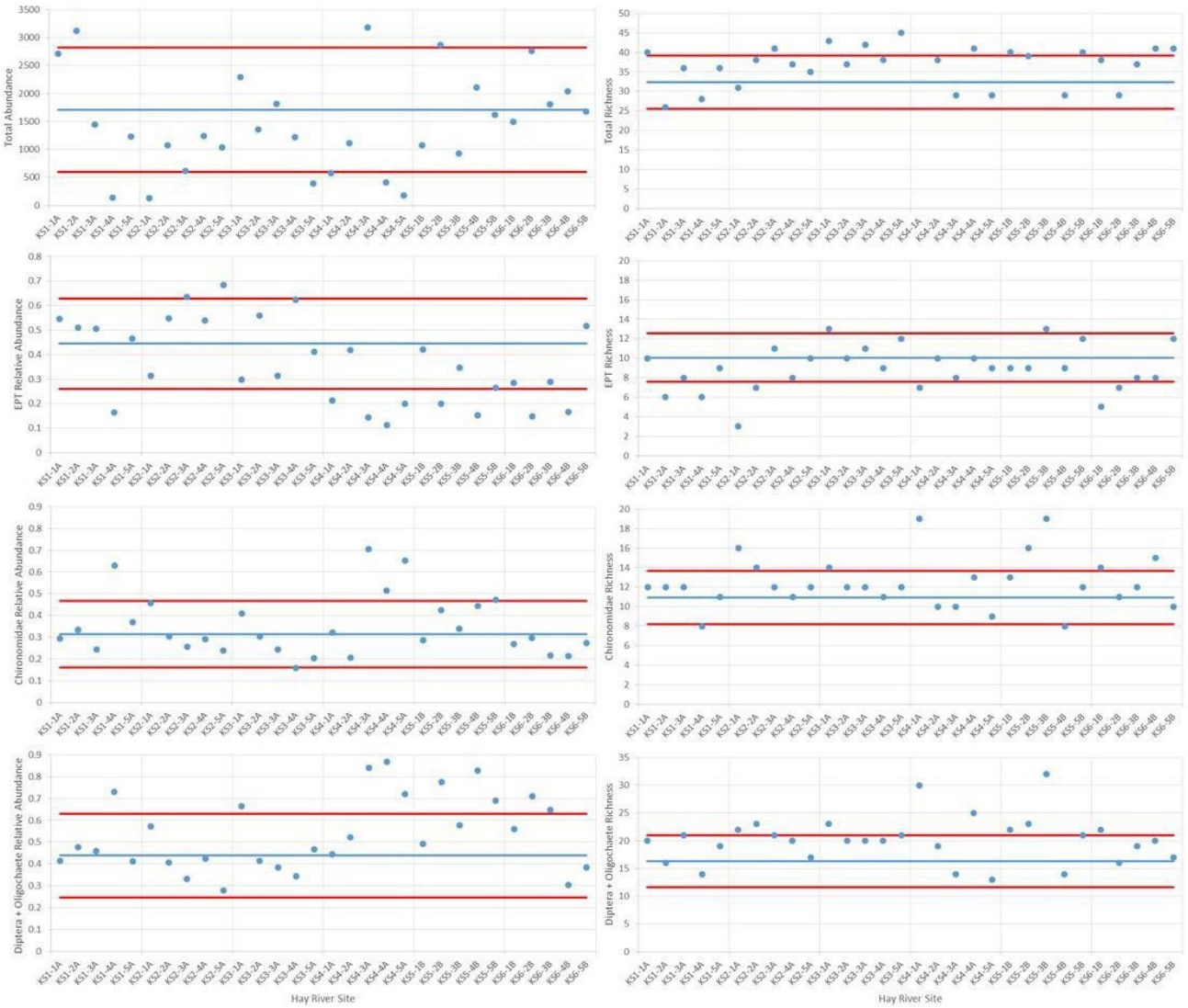


*Figure 19. Biotic metric data for Hay River sites from 2019, with a temporal mean (mean of 2017, 2018, and 2019 data; blue line) and the upper and lower multi-year critical effect size (CES; red lines), calculated as mean ± 2SD (calculated based on 2017, 2018, and 2019 data). Each point represents a kick-site, moving from reach 1, site 1 (far left) to reach 6, site 5 (far right) on each plot. Metrics include (left column) total abundance, EPT relative abundance, Chironomidae relative abundance, Diptera + Oligochaeta relative abundance, and (right column) total taxonomic richness, EPT richness, Chironomidae richness, and Diptera + Oligochaeta richness.*

#### *3.1.4.2. Among-year variability*

##### 3.1.4.2.1. Site-scale variability

Temporal variation at the site scale was assessed by comparing the 2017-2019 mean ± SE with the normal range for the river, which was calculated as the grand mean for the river (mean of 2017, 2018, and 2019 means of all sites) ± 2SD. This analysis visualizes temporal variability within sites relative to temporal variability across all sites, and represents one way in which future data may be compared with the expected normal range in this system.

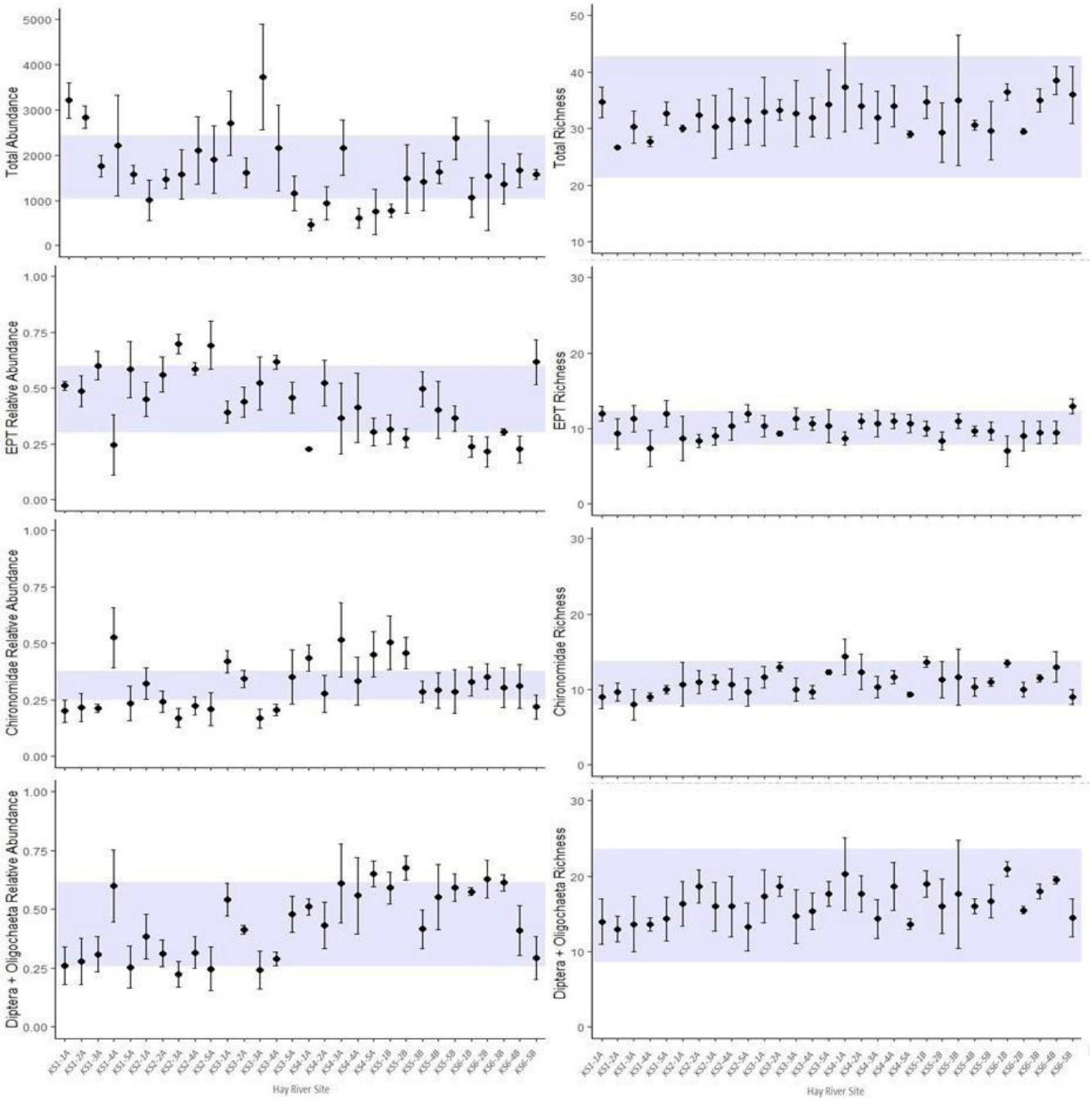


*Figure 20. Site-scale temporal variability in biotic metrics in the Hay River, showing mean ± SE for 2017-2019 for each site, with the grand mean (mean of annual means for the river) ± 2SD (normal range for the river) indicated by the shaded area. Metrics include (left, top to bottom) total abundance, EPT relative abundance, Chironomidae relative abundance, and Diptera + Oligochaeta relative abundance, and (right, top to bottom) total richness, EPT richness, Chironomidae richness, and Diptera + Oligochaeta richness.*

Total abundance in the Hay River was extremely variable within sites (wide error bars, representing high temporal variability within a site; Figure 20). Abundance also varied among sites, but annual means were similar enough that the normal range based on the grand mean for this metric was narrow. Several sites fell outside the initial estimate of normal range, particularly in Reach 4, where most sites were below the lower CES. Given the wide fluctuations in total abundance across the three years of sampling, this result is not unexpected, and suggests that additional years of data will be required before the CES for this metric accurately reflects the true normal range of variability over time.

A large number of sites fell outside the initial estimates of normal range for relative abundance metrics (Figure 20). In particular, sites in the downstream reaches were below CES for EPT relative abundance, while upstream reaches were below CES for Chironomidae relative abundance, reflecting the longitudinal patterns that were particularly evident in these metrics in 2018. The high variability in abundance-based metrics among sites and among years suggests that these metrics may be less useful for developing monitoring thresholds, particularly at the site-scale. However, additional years of sampling will indicate if the normal range can be refined. Collecting additional years of data will improve accuracy and precision of estimates and allow for the refinement of the CES range to better reflect inter-annual variability in the sampled metrics.

The initial estimates of normal range for richness metrics provided a much better fit to the data, and most sites fell within the CES boundaries for all richness metrics (Figure 20). The wider normal range for total richness and Diptera + Oligochaeta reflected inter-annual variation in these metrics across years, and additional years of data may help to narrow these boundaries. The normal range of EPT richness was particularly narrow, which suggested that this metric would be useful for developing triggers for increasing monitoring activities or taking management action.

##### 3.1.4.2.2. Reach-scale variability

Temporal variability at the reach scale was quantified by estimating the reach-specific normal range and developing CES boundaries based on variability among years. The normal range for each reach was calculated based on the grand mean (mean of annual means for the reach from 2017, 2018, and 2019) ± 2SD. Mean metric values ± SE for each reach in each year (averaged across sites, which are treated as replicates in this analysis) were compared with the calculated normal range. This approach develops location-specific CES that can be used in continued monitoring at each reach to identify when there are samples within the reach that are unusual or outside the range of expected variability, leading to large within-reach variation. Initial evaluation of these boundaries focused on their width, as a normal range may not be useful for detecting future impairment if it encompasses too wide a range of possible values.

The initial estimate of normal range for total abundance was wide in many reaches, particularly in Reach 3, where the CES boundaries covered a range of over 4000 individuals (Figure 21). Such a wide normal range would not be useful in identifying impaired samples, as it would be difficult for a sample to fall outside of the wide and all-encompassing CES boundaries. The normal range of variability in total abundance was more narrow in Reach 4 and Reach 5, but encompassed an abundance of 0 individuals in Reach 4 (Figure 21), which would also not be useful for detecting impairment. Future refinement of these ranges with additional data will hopefully improve the usefulness of these estimates of CES.

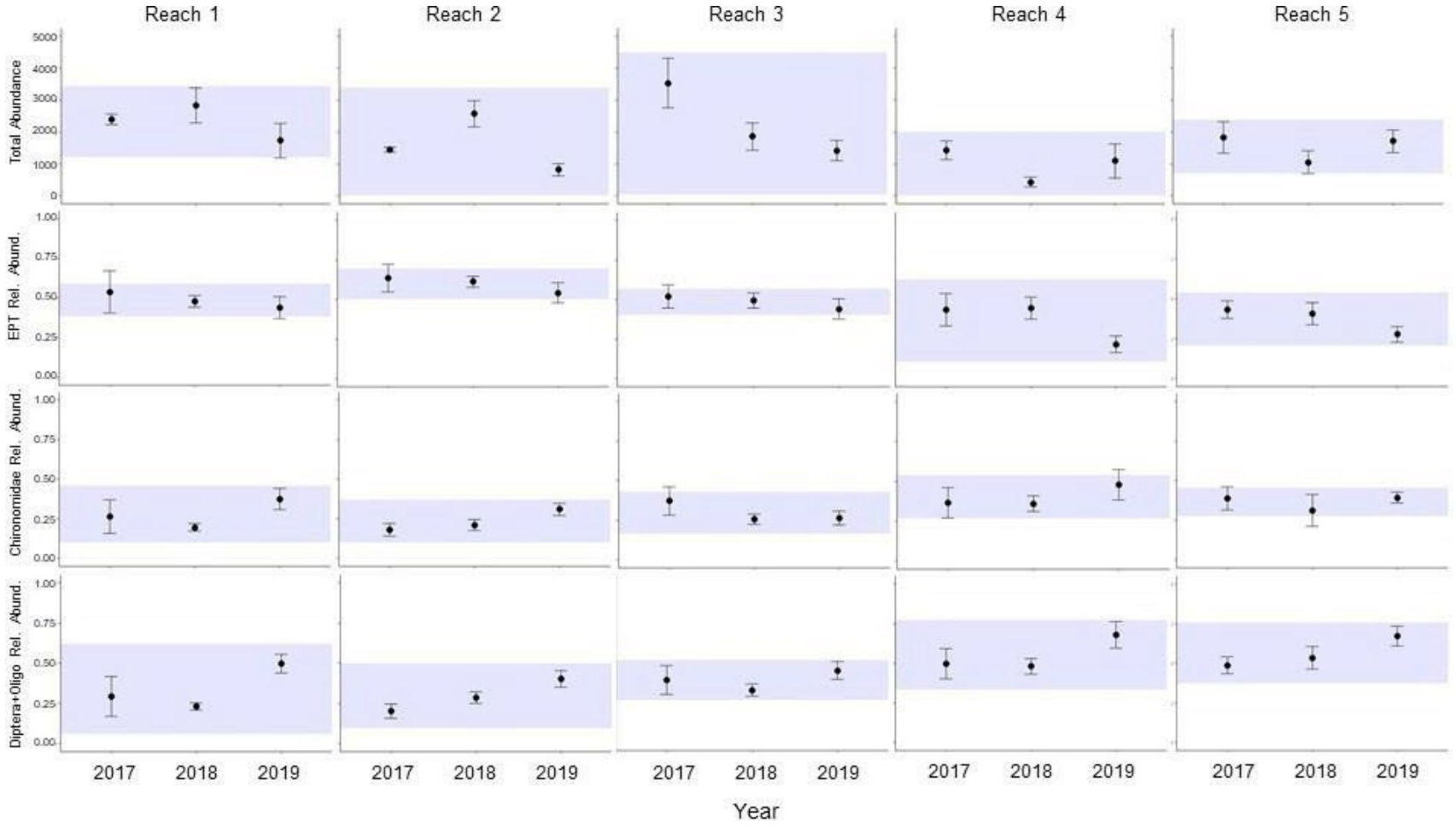


*Figure 21. Reach-scale temporal assessment of normal range and critical effect size for abundance-based metrics in the Hay River, including total abundance, relative abundance of EPT, relative abundance of Chironomidae, and relative abundance of Diptera + Oligochaeta. Points represent the mean ± SE across all sites in a reach, plotted for each year (2017, 2018, and 2019), and the shaded area represents the normal range and CES boundaries for that reach, calculated based on the grand mean (mean of annual means for the reach) ± 2 SD. Each column represents the data for a single reach.*

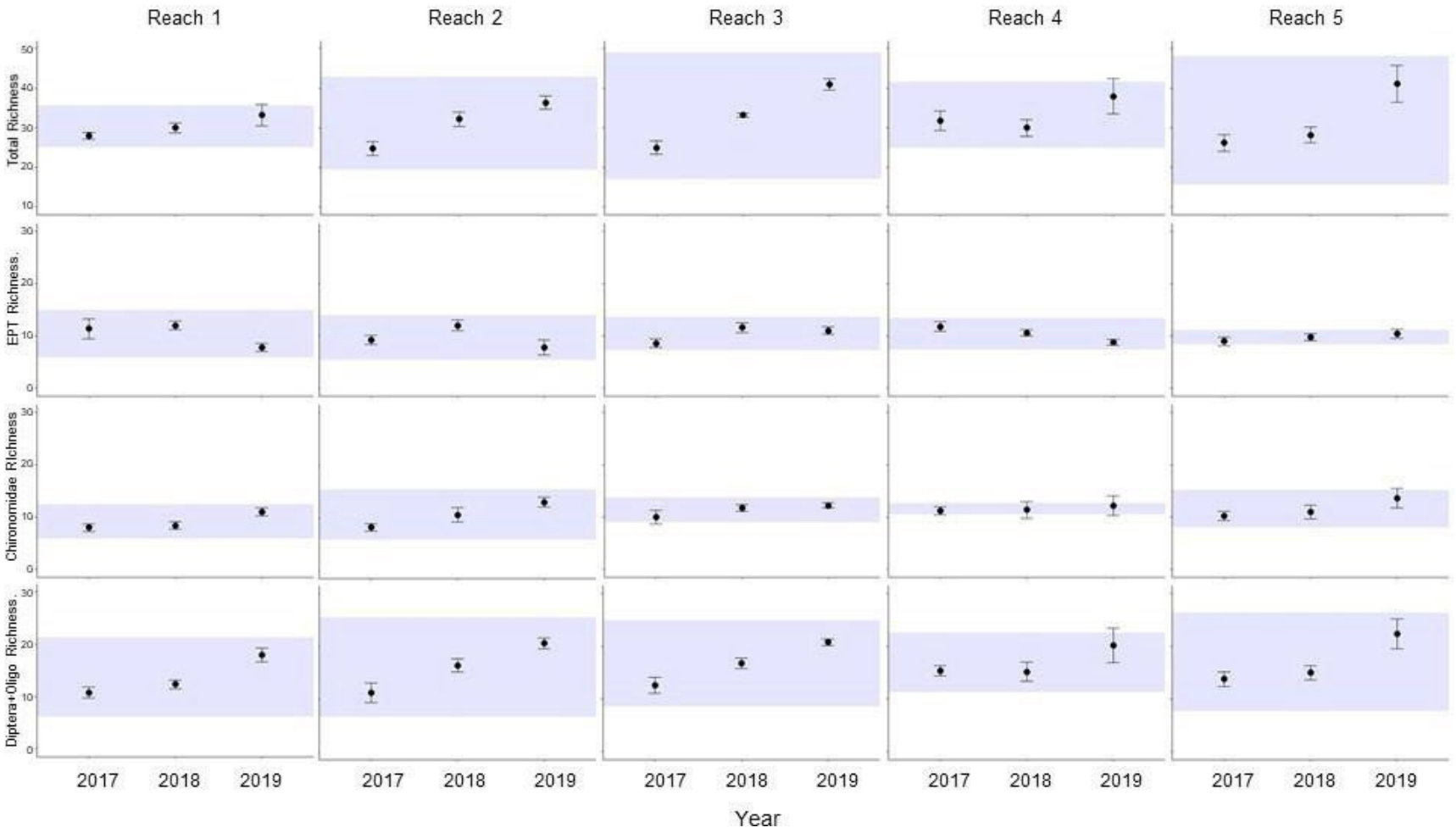


*Figure 22. Reach-scale temporal assessment of normal range and critical effect size for richness-based metrics in the Hay River, including total richness, EPT richness, Chironomidae richness, and Diptera + Oligochaeta richness. Points represent the mean ± SE across all sites in a reach, plotted for each year (2017, 2018, and 2019), and the shaded area represents the normal range and CES boundaries for that reach, calculated based on the grand mean (mean of annual means for the reach) ± 2 SD. Each column represents the data for a single reach.*

Initial estimates of the normal range of variability for the relative abundance of EPT and the relative abundance of Chironomidae were generally more narrow and appeared to be more useful for future detection of impairment in reaches (Figure 21). CES limits were higher in the upstream reaches for EPT, reflecting the generally higher relative abundance of EPT taxa found in those reaches. This speaks to the importance of developing reach-specific normal ranges, as the high relative abundance of EPT that is within the range of natural variability in the upstream reaches may be above what can be expected in the downstream reaches, where Diptera and Oligochaeta are more prevalent. The initial estimate of normal range of variability for the relative abundance of Diptera + Oligochaeta was generally wider than for the other two relative abundance metrics (Figure 21), reflecting the higher inter-annual variability of this metric in some reaches.

As was found with the site-scale analysis, initial estimates of the normal range of variability for richness-based metrics were generally more narrow for EPT and for Chironomidae. Chironomidae richness in Reach 4 was extremely invariable among years, leading to a very narrow normal range (Figure 22). A similar pattern was observed for EPT richness in Reach 5. These results suggest that both richness metrics will be useful for developing management and monitoring triggers.

Total richness and the richness of Diptera + Oligochaeta both had higher inter-annual variability than the other richness metrics, and as a result, the initial estimates of the normal range for each metric were quite wide in some reaches. For example, the CES boundaries for total richness in Reach 3 and Reach 5 covered a range of approximately 30 taxa, which is too wide to be useful in developing triggers. Additional years of sampling will be necessary to improve the estimates of normal range for these metrics.

## 3.2. Slave River

#### *3.2.1.1. Hydrology*

The Slave River is a large, fast-flowing river with high discharge, but flows in this river have been variable across the three years of sampling, similar to what was observed in the Hay River. In 2018, there was a late peak in water levels, occurring only 45 days prior to sampling (Figure 23), and this peak appeared to have influenced the biotic assemblages of the river, leading to strong shifts in abundance of Chironomidae (midges) in particular. The hydrograph in 2019 also differed from what was observed in 2017, this time showing a flatter profile during the typical spring freshet, with a more gradual increase in water levels across the summer, and a more gradual and flashy decline (Figure 23). In both 2018 and 2019, water levels were higher at the time of sampling than in 2017, but in 2019 the hydrograph was generally flatter across the spring/summer than in 2018, with less seasonality to flows. This profile could reflect flows from the Peace River, which is regulated in its upstream reaches in B.C. and which has been shown to impact flows downstream in the Slave River (Sanderson et al. 2012). Antecedent hydrologic conditions were compared among years using metrics summarizing the periods 60 days and 30 days prior to sampling. Over the period 60 days prior to sampling, both 2018 and 2019 had median flows higher than those observed in 2017 by at least 600 $m^3/s$, and both years had higher variability in flow, though 2018 was the most variable year (Table 9). When flow metrics were compared among years for the 30 days prior to sampling, 2018 remained the most variable year, reflecting its flashier flows during that period, but 2019 had the highest median discharge (Table 9). These results indicate that hydrologic conditions in the Slave River were most similar between 2018 and 2019, although water levels were higher in the period immediately prior to sampling in 2019. If high flow did impact benthic assemblages in this river in 2018, these hydrologic metrics suggest that similar patterns may be evident in 2019.

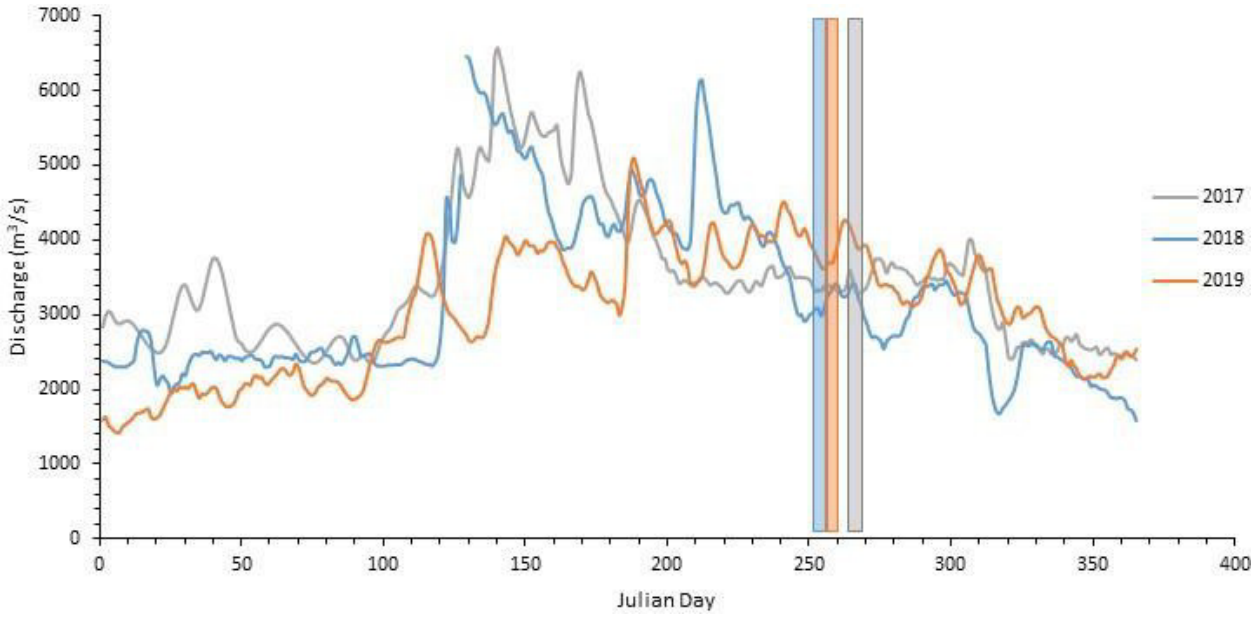


*Figure 23. Hydrographs for the Slave River in 2017 (grey), 2018 (blue), and 2019 (orange), with vertical shaded bars indicating the timing of sampling in each year. Data for Slave River near Fort Fitz (station 07NB001) from wateroffice.ec.gc.ca.*

*Table 9. Antecedent hydrology metrics for the Slave River in 2017, 2018, and 2019, including median discharge (Q ($m^3/s$)) and the coefficient of variation (CV) of flow, calculated for 60 days and 30 days prior to sampling in each year.*

| Year | 60 Days Prior to Sampling | | 30 Days Prior to Sampling | |
|---|---|---|---|---|
| | Median Q ($m^3/s$) | CV (%) | Median Q ($m^3/s$) | CV (%) |
| 2017 | 3430 | 2.7 | 3490 | 3.2 |
| 2018 | 4100 | 19.0 | 3730 | 14.7 |
| 2019 | 4070 | 7.7 | 4070 | 6.1 |

### 3.2.2. Spatial characterization of reaches

#### *3.2.2.1. Chemical and physical habitat*

##### 3.2.2.1.1. Water chemistry

Water chemistry samples were collected in the Slave River to act as supporting variables for the BMI data. These samples represented spot measurements of water chemistry conditions at the time of sampling, and were collected at three sites per reach to account for local-scale variability in BMI assemblages in response to the chemical environment. The Slave River is large (wetted width ~300-600 m compared with ~50-70 m in the Hay River), and habitat conditions and assemblages were expected to differ among reaches, which were far apart geographically. Flow velocity in the channel was fast (velocity was 0.3-0.7 m/s across a number of kick-sites), and some degree of variation in water chemistry among sites was expected due to differences in flow. In their analysis of long-term trends in water quality of the transboundary waters of the Slave River, Sanderson et al. (2012) found that some temporal trends in water chemistry parameters actually reflected temporal change in flow (with summer/fall flows decreasing over time in the river), and correction for flow resulted in the removal of temporal trends in those parameters. Changes in flow and water chemistry patterns over time in this river are a reflection in part of the impacts of the construction of the William A. C. Bennett dam in the upstream Peace River basin in northern British Columbia (Glozier et al. 2009, Sanderson et al. 2012). In the short term, flow differences from 2017 to 2018 and 2019 (Figure 23) may also have contributed to variation in water chemistry parameters between years. Water levels remained high in 2019, but the timing and magnitude of peak flows differed relative to the previous two sampling years.

The longitudinal gradient of Slave River reaches extended from Reach 1 at the south (upstream) to Reach 5 at the north (downstream; Figure 3B), with Reach 6 located upstream of Reach 5. Reach 4 had sampling sites on both banks (Reach 4A and Reach 4B), which were determined in 2017 and 2018 to have different habitat conditions (including different substrate composition). Analyses of all data from the Slave River considered variation within and among reaches to account for differences due to reach location and location of sites within reaches.

Three water samples were collected in each river reach (one sample per odd-numbered site) and analyzed for major ions, nutrients, and physicals. Mean levels of ions and nutrients (Table 10) were compared with Canadian guidelines for short-term and long-term exposure to identify any reaches where water chemistry was indicative of poor water quality (Canadian Council of Ministers of the Environment 2001b).

*Table 10. Summary of ion, nutrient, and physical water chemistry parameters sampled in the Slave River at seven sample reaches, indicating site mean ± standard deviation for each reach. When all sites in a reach were below detection limit, the detection limit is presented. When only a subset of sites in a reach was below detection limit, half the detection limit was used in calculations (number of sites below detection limit indicated in Parameter column). Reaches are ordered from upstream (KS1) to downstream (KS5).*

| Parameter | SR-KS1 | SR-KS2 | SR-KS3 | SR-KS4A | SR-KS4B | SR-KS6 | SR-KS5 |
|---|---|---|---|---|---|---|---|
| Alkalinity (mg/L) | 97.0 ± 0.5 | 97.2 ± 0.4 | 97.8 ± 0.7 | 96.0 ± 0.6 | 97.8 ± 0.6 | 95.9 ± 0.2 | 95.0 ± 0.8 |
| Ammonia (mg/L) | < 0.005 | < 0.005 | < 0.005 | < 0.005 | < 0.005 | < 0.005 | < 0.005 |
| Calcium (mg/L) | 32.1 ± 0.5 | 32.6 ± 0.0 | 32.8 ± 0.1 | 32.5 ± 0.2 | 32.7 ± 0.1 | 32.0 ± 0.1 | 31.6 ± 0.6 |
| Chloride (mg/L) | 3.63 ± 0.05 | 3.67 ± 0.06 | 3.90 ± 0.00 | 4.43 ± 0.06 | 3.87 ± 0.06 | 4.07 ± 0.46 | 3.60 ± 0.00 |
| Specific Conductivity (µS/cm) | 250.3 ± 2.1 | 248.3 ± 0.6 | 249.3 ± 6.4 | 250.3 ± 1.2 | 254.0 ± 2.6 | 249.3 ± 0.6 | 246.0 ± 2.0 |
| Hardness (mg/L) | 112.8 ± 1.5 | 115.0 ± 0.0 | 115.0 ± 0.0 | 114.7 ± 0.6 | 115.0 ± 0.0 | 112.7 ± 0.6 | 111.0 ± 2.0 |
| Magnesium (mg/L) | 8.00 ± 0.12 | 8.10 ± 0.00 | 8.10 ± 0.00 | 8.07 ± 0.06 | 8.10 ± 0.00 | 7.97 ± 0.12 | 7.85 ± 0.10 |
| Nitrate (mg/L) | 0.185 ± 0.026 | 0.190 ± 0.000 | 0.187 ± 0.006 | 0.183 ± 0.006 | 0.187 ± 0.006 | 0.183 ± 0.012 | 0.190 ± 0.000 |
| Nitrite (mg/L) | < 0.01 | < 0.01 | < 0.01 | < 0.01 | < 0.01 | < 0.01 | < 0.01 |
| Nitrate+Nitrite (mg/L) | 0.185 ± 0.026 | 0.190 ± 0.000 | 0.187 ± 0.006 | 0.183 ± 0.006 | 0.187 ± 0.006 | 0.183 ± 0.012 | 0.190 ± 0.000 |
| Dissolved N (mg/L) | 0.350 ± 0.014 | 0.363 ± 0.021 | 0.347 ± 0.012 | 0.340 ± 0.000 | 0.350 ± 0.010 | 0.343 ± 0.006 | 0.340 ± 0.008 |
| Total N (mg/L) | 0.483 ± 0.010 | 0.533 ± 0.084 | 0.480 ± 0.000 | 0.473 ± 0.006 | 0.480 ± 0.000 | 0.480 ± 0.010 | 0.495 ± 0.010 |
| DOC (mg/L) | 12.95 ± 0.13 | 13.10 ± 0.00 | 13.27 ± 0.21 | 12.93 ± 0.06 | 13.23 ± 0.15 | 13.00 ± 0.10 | 12.93 ± 0.13 |
| TOC (mg/L) | 13.20 ± 0.16 | 13.23 ± 0.25 | 13.40 ± 0.17 | 13.00 ± 0.10 | 13.47 ± 0.15 | 13.07 ± 0.12 | 12.90 ± 0.22 |
| Ortho-Phosphate (mg/L) (1 below DL) | 0.0048 ± 0.0010 | 0.0033 ± 0.0021 | 0.0053 ± 0.0012 | 0.0050 ± 0.0000 | 0.0053 ± 0.0006 | 0.0057 ± 0.0006 | 0.0055 ± 0.0013 |
| pH | 8.09 ± 0.01 | 8.08 ± 0.04 | 8.10 ± 0.01 | 8.09 ± 0.00 | 8.10 ± 0.01 | 8.11 ± 0.01 | 8.11 ± 0.01 |
| Dissolved P (mg/L) | 0.006 ± 0.000 | 0.006 ± 0.001 | 0.006 ± 0.000 | 0.006 ± 0.001 | 0.006 ± 0.000 | 0.006 ± 0.001 | 0.006 ± 0.000 |
| Total P (mg/L) | 0.075 ± 0.004 | 0.077 ± 0.011 | 0.066 ± 0.003 | 0.073 ± 0.006 | 0.077 ± 0.003 | 0.086 ± 0.004 | 0.096 ± 0.009 |
| Potassium (mg/L) | 0.90 ± 0.00 | 0.90 ± 0.00 | 0.90 ± 0.00 | 0.90 ± 0.00 | 0.90 ± 0.00 | 0.97 ± 0.12 | 0.90 ± 0.00 |
| Sodium (mg/L) | 7.43 ± 0.05 | 7.43 ± 0.06 | 7.60 ± 0.00 | 7.37 ± 0.06 | 7.57 ± 0.06 | 7.30 ± 0.17 | 7.08 ± 0.05 |
| TDS (mg/L) | 184.0 ± 14.2 | 190.7 ± 8.3 | 177.3 ± 7.6 | 166.7 ± 16.0 | 162.7 ± 3.1 | 153.0 ± 12.1 | 168.0 ± 6.7 |
| TSS (mg/L) | 66.3 ± 5.3 | 58.0 ± 5.3 | 53.7 ± 11.1 | 71.3 ± 20.0 | 65.3 ± 4.2 | 65.0 ± 9.5 | 73.0 ± 5.3 |
| Sulphate (mg/L) | 25.3 ± 0.5 | 25.0 ± 0.0 | 25.0 ± 0.0 | 24.3 ± 0.6 | 24.7 ± 0.6 | 24.3 ± 0.6 | 23.0 ± 0.0 |
| Turbidity (NTU) | 43.8 ± 1.6 | 42.3 ± 2.0 | 41.4 ± 0.7 | 43.0 ± 1.2 | 43.6 ± 2.1 | 52.1 ± 8.5 | 57.3 ± 8.1 |

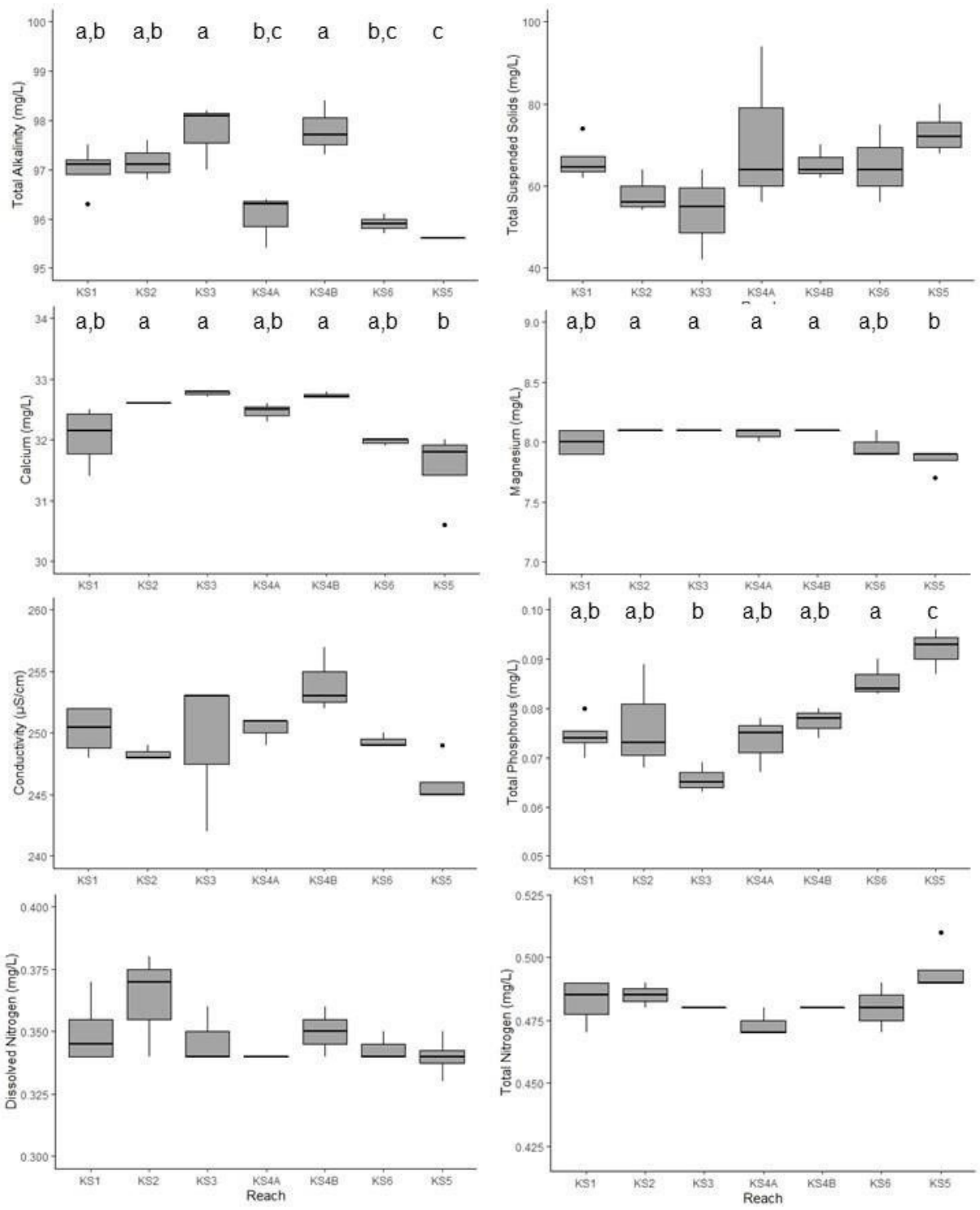


*Figure 24. Box plots of ions, nutrients, and physicals water chemistry concentrations for all reaches sampled in the Slave River in 2019. Plotted is alkalinity, TSS, calcium, magnesium, conductivity, TP, DN, and TN. Box indicates the interquartile range, line through the box indicates the median, and whiskers indicate the lower and upper quartiles. Points indicate statistical outliers. Letters on plots indicate significant differences ($\alpha$ = 0.05) from one-way ANOVA and Tukey HSD tests. Reaches are ordered from upstream (KS1) to downstream (KS5).*

Similar to patterns observed in the Hay River, higher flow in 2019 appeared to have the effect of reducing variability in water chemistry parameters in the Slave River, leading to low standard deviations within reaches (Table 10) and low interquartile ranges (Figure 24), particularly with respect to ions. For example, calcium ranged from 31.6 to 32.8 mg/L on average across all sampled reaches (Table 10). Similarly, magnesium ranged from 7.85 to 8.1 mg/L on average across all reaches. Mean values for ions, nutrients, and physicals did not exceed CCME guidelines for the protection of aquatic life for any reaches in the Slave River (Table 10). TSS levels were lower on average than what was observed in 2018, and lower than long-term (1982-2010) mean of less than 100 mg/L reported for August and September at Fort Smith (Sanderson et al. 2012). Although flow was high in 2019, it was less variable than in 2018, and sediment transport was likely more steady through the summer.

*Table 11. Summary of metal water chemistry parameters sampled in the Slave River at seven sample reaches, indicating site mean ± standard deviation (for 2 or more samples) for each reach. When all sites in a reach were below detection limit, the detection limit is indicated. When only a subset of sites in a reach was below detection limit, half the detection limit was used in calculations (number of sites below detection limit indicated in Parameter column). Dissolved metal values were excluded when they exceeded total metals. Values in bold were greater than CCME long-term exposure guidelines for the protection of aquatic life (Canadian Council of Ministers of the Environment 2001b). Samples were collected at three sites in each reach and a duplicate sample was collected at two sites. Reaches are ordered from upstream (KS1) to downstream (KS5).*

| Parameter | SR-KS1 | SR-KS2 | SR-KS3 | SR-KS4A | SR-KS4B | SR-KS6 | SR-KS5 |
|---|---|---|---|---|---|---|---|
| Aluminum Diss. (µg/L) | 3.60 ± 0.00 | 3.37 ± 0.25 | 3.53 ± 0.15 | 3.43 ± 0.31 | 4.63 ± 1.88 | 3.50 ± 0.10 | 3.13 ± 0.49 |
| Aluminum Tot. (µg/L) | **792.75 ± 42.99** | **766.67 ± 38.08** | **779.33 ± 57.01** | **1096.67 ± 280.42** | **881.67 ± 7.09** | **1049.00 ± 71.51** | **1125.00 ± 85.44** |
| Antimony Diss. (µg/L) | < 0.10 | < 0.10 | < 0.10 | < 0.10 | < 0.10 | < 0.10 | < 0.10 |
| Antimony Tot.(µg/L) | 0.13 ± 0.05 | 0.10 ± 0.00 | 0.13 ± 0.06 | 0.13 ± 0.06 | 0.13 ± 0.06 | 0.10 ± 0.00 | 0.10 ± 0.00 |
| Arsenic Diss. (µg/L) | 0.53 ± 0.05 | 0.60 ± 0.00 | 0.60 ± 0.00 | 0.57 ± 0.06 | 0.70 ± 0.00 | 0.67 ± 0.06 | 0.60 ± 0.08 |
| Arsenic Tot. (µg/L) | 1.28 ± 0.05 | 1.27 ± 0.06 | 1.30 ± 0.10 | 1.57 ± 0.25 | 1.40 ± 0.00 | 1.53 ± 0.06 | 1.53 ± 0.05 |
| Barium Diss. (µg/L) | 52.90 ± 0.00 | 52.93 ± 0.35 | 52.87 ± 0.35 | 53.37 ± 0.15 | 53.10 ± 0.44 | 52.47 ± 0.25 | 48.58 ± 6.45 |
| Barium Tot. (µg/L) | 77.00 ± 1.71 | 76.17 ± 1.93 | 76.33 ± 1.88 | 92.30 ± 13.93 | 80.00 ± 1.45 | 82.03 ± 2.69 | 83.65 ± 2.56 |
| Beryllium Tot. (µg/L) (18 below DL) | < 0.10 | < 0.10 | < 0.10 | 0.08 ± 0.03 | < 0.10 | 0.07 ± 0.03 | 0.08 ± 0.03 |
| Bismuth Tot. (µg/L) (22 below DL) | 0.13 ± 0.05 | < 0.20 | < 0.20 | < 0.20 | < 0.20 | < 0.20 | < 0.20 |
| Boron Diss. (µg/L) | 18.53 ± 0.19 | 18.73 ± 0.21 | 19.13 ± 0.06 | 19.40 ± 0.20 | 19.23 ± 0.15 | 18.83 ± 0.38 | 17.18 ± 1.99 |
| Boron Tot. (µg/L) | 21.05 ± 0.41 | 21.00 ± 0.10 | 21.93 ± 0.29 | 22.60 ± 0.60 | 22.40 ± 0.44 | 21.70 ± 0.46 | 21.73 ± 0.26 |
| Cadmium Tot.(µg/L) | <0.10 | <0.10 | <0.10 | <0.10 | <0.10 | <0.10 | <0.10 |
| Cesium Diss. (µg/L) | <0.10 | <0.10 | <0.10 | <0.10 | <0.10 | <0.10 | <0.10 |
| Cesium Tot. (µg/L) | 0.23 ± 0.05 | 0.23 ± 0.06 | 0.20 ± 0.00 | 0.30 ± 0.10 | 0.27 ± 0.06 | 0.30 ± 0.00 | 0.30 ± 0.00 |
| Chromium Diss. (µg/L) | <0.10 | <0.10 | <0.10 | <0.10 | <0.10 | <0.10 | <0.10 |
| Chromium Tot. (µg/L) | 1.30 ± 0.08 | 1.27 ± 0.06 | 1.30 ± 0.10 | 1.83 ± 0.47 | 1.43 ± 0.06 | 1.70 ± 0.10 | 1.80 ± 0.14 |
| Cobalt Diss. (µg/L) | <0.10 | <0.10 | <0.10 | <0.10 | <0.10 | <0.10 | <0.10 |

| Parameter | SR-KS1 | SR-KS2 | SR-KS3 | SR-KS4A | SR-KS4B | SR-KS6 | SR-KS5 |
|---|---|---|---|---|---|---|---|
| Cobalt Tot. (µg/L) | 0.75 ± 0.06 | 0.73 ± 0.06 | 0.67 ± 0.06 | 1.00 ± 0.26 | 0.80 ± 0.00 | 0.93 ± 0.06 | 0.98 ± 0.10 |
| Copper Diss. (µg/L) | 1.53 ± 0.05 | 1.53 ± 0.06 | 1.50 ± 0.00 | 1.53 ± 0.06 | 1.50 ± 0.00 | 1.60 ± 0.00 | 1.53 ± 0.22 |
| Copper Tot. (µg/L) | **3.00 ± 0.12** | **3.07 ± 0.15** | **3.00 ± 0.17** | **3.73 ± 0.70** | **3.30 ± 0.10** | **3.60 ± 0.20** | **3.68 ± 0.17** |
| Iron Diss. (ug/L) | 42.75 ± 2.22 | 42.33 ± 0.58 | 41.33 ± 0.58 | 38.67 ± 2.52 | 46.00 ± 1.00 | 41.00 ± 2.00 | 35.75 ± 11.30 |
| Iron Tot. (µg/L) | **1775.00 ± 75.06** | **1720.00 ± 91.65** | **1700.00 ± 110.00** | **2406.67 ± 589.69** | **1940.00 ± 52.92** | **2220.00 ± 140.00** | **2345.00 ± 155.88** |
| Lead Diss. (µg/L) (22 below DL) | <0.10 | 0.07 ± 0.03 | <0.10 | <0.10 | <0.10 | <0.10 | <0.10 |
| Lead Tot. (µg/L) | 0.98 ± 0.10 | 0.97 ± 0.06 | 0.97 ± 0.06 | 1.30 ± 0.36 | 1.07 ± 0.06 | 1.23 ± 0.06 | 1.28 ± 0.10 |
| Lithium Diss. (µg/L) | 5.85 ± 0.13 | 5.87 ± 0.06 | 6.00 ± 0.10 | 6.03 ± 0.06 | 6.10 ± 0.10 | 5.97 ± 0.12 | 5.40 ± 0.67 |
| Lithium Tot. (µg/L) | 7.00 ± 0.14 | 6.93 ± 0.06 | 7.20 ± 0.10 | 7.60 ± 0.40 | 7.40 ± 0.10 | 7.40 ± 0.10 | 7.50 ± 0.12 |
| Manganese Diss. (µg/L) | 0.63 ± 0.10 | 0.70 ± 0.10 | 0.57 ± 0.06 | 0.63 ± 0.06 | 0.57 ± 0.12 | 0.50 ± 0.10 | 0.65 ± 0.17 |
| Manganese Tot. (µg/L) | 47.08 ± 2.02 | 45.63 ± 2.50 | 45.67 ± 2.45 | 60.87 ± 13.72 | 51.97 ± 1.53 | 60.63 ± 4.57 | 63.93 ± 4.10 |
| Mercury Diss. (UL) (ng/L) | 1.00 ± 0.22 | 1.07 ± 0.06 | 0.97 ± 0.06 | 0.97 ± 0.06 | 0.97 ± 0.06 | 0.93 ± 0.15 | 0.88 ± 0.13 |
| Mercury Tot. (UL) (ng/L) | 5.43 ± 1.18 | 5.83 ± 1.64 | 6.60 ± 2.82 | 4.93 ± 0.40 | 5.53 ± 0.31 | 7.63 ± 2.57 | 6.10 ± 0.22 |
| Molybdenum Tot. (µg/L) | 0.75 ± 0.06 | 0.70 ± 0.00 | 0.77 ± 0.06 | 0.77 ± 0.06 | 0.73 ± 0.06 | 0.70 ± 0.00 | 0.70 ± 0.00 |
| Nickel Diss. (µg/L) | 1.60 ± 0.00 | 1.60 ± 0.00 | 1.60 ± 0.00 | 1.60 ± 0.00 | 1.60 ± 0.00 | 1.60 ± 0.00 | 1.50 ± 0.20 |
| Nickel Tot. (µg/L) | 3.50 ± 0.12 | 3.43 ± 0.15 | 3.43 ± 0.15 | 4.37 ± 0.85 | 3.77 ± 0.06 | 4.00 ± 0.17 | 4.18 ± 0.21 |
| Rubidium Diss. (µg/L) | 0.60 ± 0.00 | 0.60 ± 0.00 | 0.60 ± 0.00 | 0.60 ± 0.00 | 0.60 ± 0.00 | 0.60 ± 0.00 | 0.58 ± 0.05 |
| Rubidium Tot.(µg/L) | 2.73 ± 0.10 | 2.67 ± 0.12 | 2.63 ± 0.15 | 3.43 ± 0.70 | 2.90 ± 0.00 | 3.33 ± 0.15 | 3.50 ± 0.18 |
| Selenium Tot.(µg/L) (22 below DL) | < 0.50 | 0.33 ± 0.14 | < 0.50 | < 0.50 | < 0.50 | < 0.50 | < 0.50 |
| Silver Tot. (µg/L) | < 0.10 | < 0.10 | < 0.10 | < 0.10 | < 0.10 | < 0.10 | < 0.10 |
| Strontium Diss. (µg/L) | 160.50 ± 1.00 | 160.33 ± 0.58 | 161.67 ± 0.58 | 163.00 ± 1.00 | 161.67 ± 0.58 | 160.33 ± 1.53 | 147.50 ± 20.34 |
| Strontium Tot. (µg/L) | 167.00 ± 0.82 | 166.67 ± 2.52 | 170.00 ± 3.61 | 172.00 ± 2.65 | 170.33 ± 2.52 | 169.33 ± 3.06 | 168.75 ± 1.71 |
| Thallium Tot. (µg/L) | < 0.10 | < 0.10 | < 0.10 | < 0.10 | < 0.10 | < 0.10 | < 0.10 |
| Tin Tot. (µg/L) | < 0.10 | < 0.10 | < 0.10 | < 0.10 | < 0.10 | < 0.10 | < 0.10 |
| Titanium Diss. (µg/L) (1 below DL) | 0.20 ± 0.00 | 0.20 ± 0.00 | 0.20 ± 0.00 | 0.20 ± 0.00 | 0.20 ± 0.00 | 0.20 ± 0.00 | 0.16 ± 0.08 |
| Titanium Tot. (µg/L) | 11.20 ± 0.45 | 10.97 ± 0.71 | 11.30 ± 0.72 | 15.80 ± 3.12 | 12.70 ± 0.44 | 14.37 ± 0.81 | 14.90 ± 0.99 |
| Uranium Diss. (µg/L) | 0.40 ± 0.00 | 0.40 ± 0.00 | 0.40 ± 0.00 | 0.40 ± 0.00 | 0.40 ± 0.00 | 0.40 ± 0.00 | 0.38 ± 0.05 |
| Uranium Tot. (µg/L) | 0.50 ± 0.00 | 0.50 ± 0.00 | 0.50 ± 0.00 | 0.50 ± 0.00 | 0.50 ± 0.00 | 0.50 ± 0.00 | 0.50 ± 0.00 |
| Vanadium Diss. (µg/L) | 0.30 ± 0.00 | 0.30 ± 0.00 | 0.30 ± 0.00 | 0.30 ± 0.00 | 0.30 ± 0.00 | 0.30 ± 0.00 | 0.28 ± 0.05 |
| Vanadium Tot. (µg/L) | 3.00 ± 0.16 | 2.90 ± 0.10 | 2.90 ± 0.20 | 4.00 ± 0.92 | 3.27 ± 0.06 | 3.70 ± 0.30 | 3.95 ± 0.26 |
| Zinc Diss. (µg/L) | < 0.40 | < 0.40 | < 0.40 | < 0.40 | < 0.40 | < 0.40 | < 0.40 |
| Zinc Tot. (µg/L) | 6.65 ± 0.51 | 6.77 ± 0.78 | 6.47 ± 0.29 | 9.63 ± 3.02 | 9.90 ± 3.82 | 8.37 ± 0.57 | 8.73 ± 0.63 |

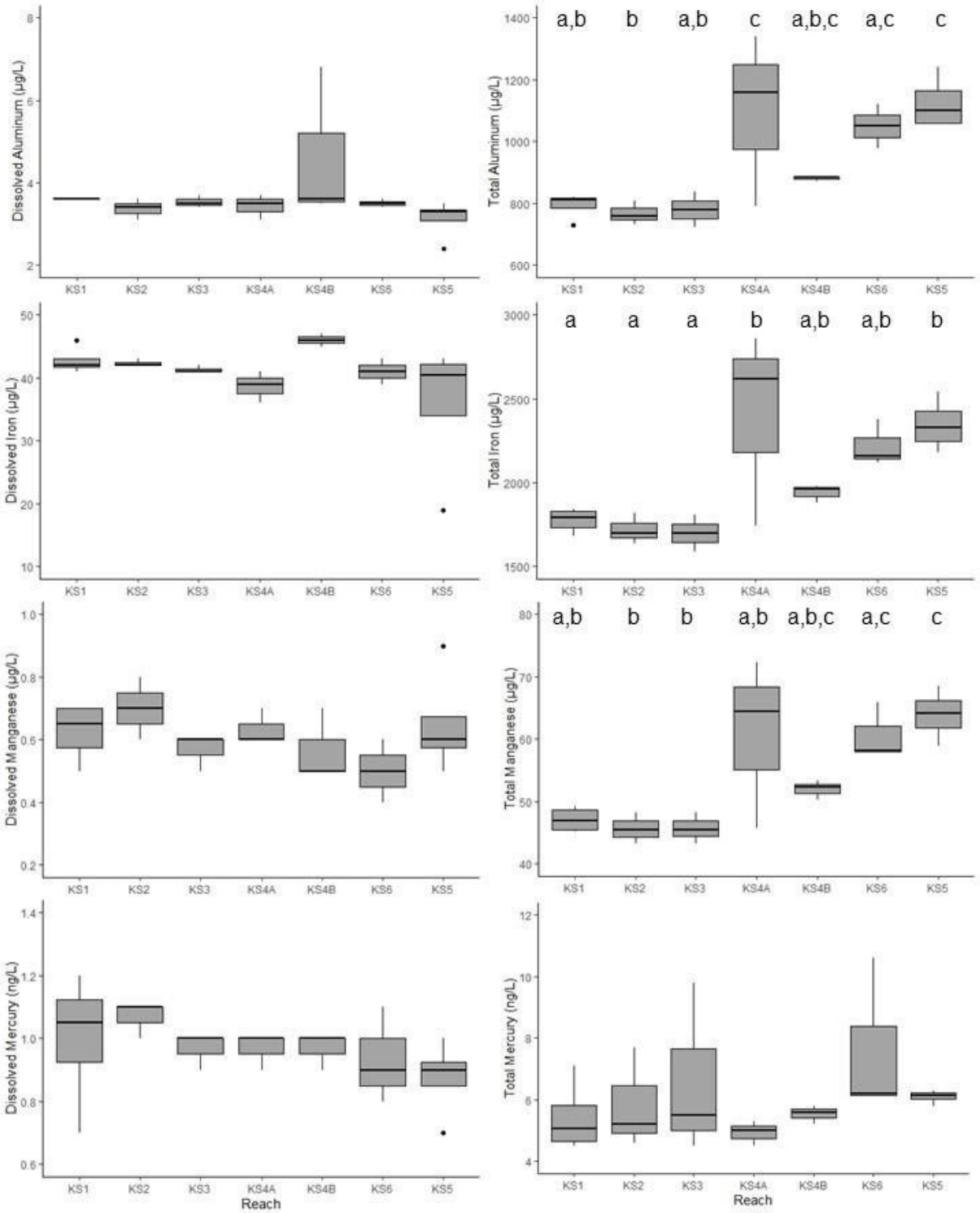


*Figure 25. Box plots of dissolved and total metal concentrations for all reaches sampled in the Slave River in 2019. Plotted is (left column, top to bottom) dissolved aluminum, dissolved iron, dissolved manganese, and (right column, top to bottom) total aluminum, total iron, and total manganese, all measured in µg/L. Box indicates the interquartile range, line through the box indicates the median, and whiskers indicate the lower and upper quartiles. Points indicate statistical outliers. Letters on plots indicate significant differences ($\alpha\alpha = 0.05$) from one-way ANOVA and Tukey HSD tests. Reaches are ordered from upstream (KS1) to downstream (KS5).*

Estimates of mean TP in the Slave River were all lower than 0.100 mg/L, and reaches were classified as eutrophic based on the Canadian Guidance Framework. Analysis of long-term trends in phosphorus (total and dissolved) in the Slave River found elevated levels in the Slave River relative to the Athabasca and Peace Rivers that flow into the Slave (Glozier et al. 2009). The spot measurements of TP collected in the Slave River in 2019 were similar to the median of 0.078 mg/L from long-term routine monitoring data (Glozier et al. 2009), though TP was statistically significantly higher in the furthest downstream reach (Reach 5; Figure 24). Reach 5 had lower levels than other reaches for some parameters, including alkalinity and conductivity, but variability among reaches was generally low (Figure 24).

Total and dissolved metals were also measured in water chemistry samples to quantify the levels to which BMI were exposed at the time of sampling. Dissolved metals provide a more accurate estimate of the relevant exposure of biota than total metals because they are generally more biologically available than the particulate forms, which are included in estimates of total metals (Sanderson et al. 2012). Dissolved metal concentrations were generally low in Slave River reaches, with many metals at or below detection limits (Table 11). As a result, no dissolved metals exceeded long-term exposure water quality guidelines for the protection of aquatic life (Canadian Council of Ministers of the Environment 2001b).

Though total metals were more variable than dissolved metals, concentrations remained low or below detection limit for many metals (Table 11). Total aluminum concentrations exceeded long-term exposure water quality guidelines for (100 μg/L), but reach averages, which ranged from 792 to 1125 μg/L (Table 11), were much lower than the long-term median value of 4360 μg/L reported for the Slave River at Fort Smith (Sanderson et al. 2012). Total aluminum was highest and most variable at Reach 4A, which differed statistically from upstream reaches (Figure 25). Reach 4A also had statistically significantly higher total iron than the upstream reaches (Figure 25), and levels of this metal were higher than CCME guidelines in all reaches (reach means ranged from 1700 to 2406 μg/L, compared with a long-term exposure guideline of 300 μg/L; Table 11). However, total iron remained lower than the long-term median value of 3526 μg/L reported for the Slave River at Fort Smith (Sanderson et al. 2012).

#### *3.2.2.2. Physical Habitat*

*Measurements were taken at each site to characterize they physical habitat in BMI sampling locations, including variables such as velocity, river width, streamside vegetation, in-stream periphyton cover, and substrate composition (*

Table 12). Bankfull width and wetted width were too wide in some reaches to be measured, and these values were omitted from the summary table.

*Velocity ranged from 0.21 to 0.54 m/s on average across reaches (*

*Table 12), and was higher than observed in 2018 (range: 0.17 to 0.38 m/s on average), consistent with the higher discharge at the time of sampling (approximately 3970 $m^3/s$ in 2019 compared with approximately 3600 $m^3/s$ and 3080 $m^3/s$ in 2017 and*

*2018, respectively). Substrate composition in reaches was predominantly a combination of gravel, pebble, and cobble size classes (*

Table 12). Periphyton coverage was recorded as < 0.5 mm thick at all sites, similar to the Hay River, but this is not uncommon for this high-discharge river.

*Table 12. Physical habitat variables measured in the Slave River in 2019, summarized by reach. Velocity (spot measurement) and wetted width are presented as mean ± standard deviation (calculated based on 5 sites per reach); dominant streamside vegetation and periphyton coverage are presented as the most common category in each reach across 5 sites; substrate composition is presented as the sum of rock counts for each reach (20 rocks measured per site). Bankfull width and wetted width were omitted as they could not be recorded at all reaches. Sites are ordered from upstream (KS1) to downstream (KS5).*

| Variable | SR-KS1 | SR-KS2 | SR-KS3 | SR-KS4A | SR-KS4B | SR-KS6 | SR-KS5 |
|---|---|---|---|---|---|---|---|
| Velocity (m/s) | 0.54 ± 0.15 | 0.26 ± 0.06 | 0.41 ± 0.09 | 0.21 ± 0.17 | 0.31 ± 0.05 | 0.43 ± 0.11 | 0.30 ± 0.06 |
| Dominant streamside vegetation | shrubs | shrubs and deciduous trees | shrubs | shrubs | ferns/ grasses | shrubs | ferns/ grasses |
| Periphyton coverage | < 0.5 mm thick | < 0.5 mm thick | < 0.5 mm thick | < 0.5 mm thick | < 0.5 mm thick | < 0.5 mm thick | < 0.5 mm thick |
| Substrate - sand (%) | 0 | 16 | 0 | 22 | 9 | 0 | 8 |
| Substrate - gravel (%) | 21 | 16 | 12 | 36 | 20 | 7 | 28 |
| Substrate - pebble (%) | 55 | 26 | 48 | 48 | 41 | 67 | 46 |
| Substrate - cobble (%) | 23 | 46 | 36 | 15 | 38 | 26 | 25 |
| Substrate - boulder (%) | 1 | 9 | 4 | 1 | 3 | 0 | 1 |
| Substrate - bedrock (%) | 0 | 3 | 0 | 0 | 0 | 0 | 0 |

#### *3.2.2.3. Characterizing the chemical and physical habitat*

Multivariate analysis of abiotic data was used as an exploratory analysis of patterns in water chemistry and physical habitat within and among reaches in the Slave River, and to identify parameters that might be used for analysis of biotic-abiotic relationships. Combining water chemistry and physical habitat data in the ordination allowed for comparison of the relative importance of each in characterizing gradients in the abiotic habitat.

Because variability in water chemistry among sites was very low in the Slave River in 2019, gradients in physical habitat variables were important in the ordination (Figure 26). Notably, a dominant gradient along both the first and second axes was a negative correlation of site KS4-1A with velocity (Figure 26). This site has been identified in previous years as an outlier due to its low velocity, and it was orthogonal to (uncorrelated with) the gradient along which the other Slave River sites varied in the ordination.

The gradient along which the other sites varied was a gradient in substrate size, characterized by a contrast between sites positively correlated with gravel and sand, and those that were positively correlated with cobble and boulder, though a number of water chemistry parameters were also associated with the gradient (albeit with lower weight; Figure 26). The gradient was intermediate to the first and second axes, with gravel and cobble having high loadings on both axes. Among the sites that were positively correlated with gravel and sand, there was also a positive correlation with the majority of total metals along the first axis, which explained 39.7% of the variation among sites (Figure 26). In contrast, sites that were positively associated with larger substrate size were positively correlated with alkalinity, hardness, and several ions (calcium, magnesium, and sodium; Figure 26), contributing to the spread of sites along the second axis, which explained 19.2% of the variation among sites.

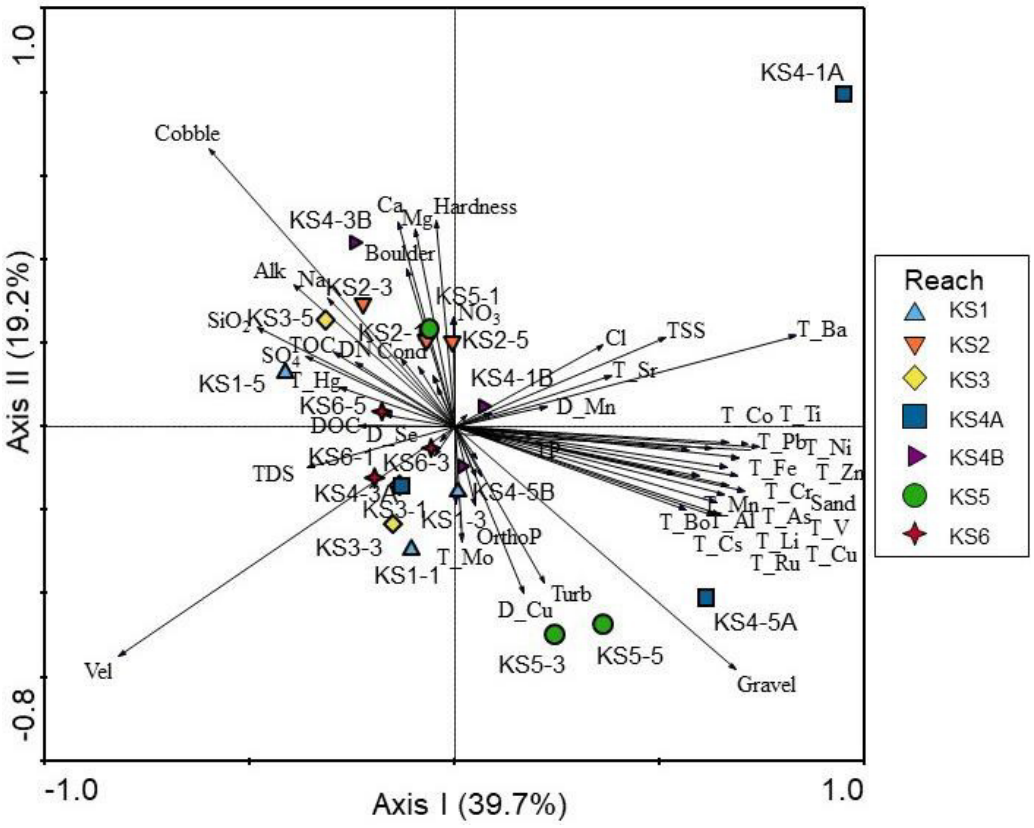


*Figure 26. PCA ordination of water chemistry and habitat variables at Hay River kick-sites, with sites colour-coded based on reach number. Arrows point in the direction of increasing values of parameters, and correlations of sites with parameters are indicated by the location of kick-site points in proximity to arrows. Kick-sites on the same end of a gradient are positively correlated, whereas samples on opposite ends of gradients are negatively correlated. Kick-sites and parameters at right angles through the origin are uncorrelated. Parameters near the origin are not labelled for ease of interpretation. Kick-site points located near the origin have similar correlations with all measured parameters. "D-" in front of metals indicates dissolved form, and "T-" indicates total metals.*

#### 3.2.2.3.1. Sediment chemistry

Sediment chemistry samples were collected from two sites in each Slave River reach (sites 1 and 5) and analyzed for metals and polycyclic aromatic hydrocarbons (PAHs). To determine whether levels of metals or PAHs were elevated beyond recommended levels in Slave River samples, mean values for each site were compared with CCME sediment quality guidelines for the protection of aquatic life (Canadian Council of Ministers of the Environment 2001a), which include interim freshwater sediment quality guidelines (ISQGs) and probably effect levels (PELs). In addition, Benzo[a]pyrene Total Potency Equivalents and the Index of Additive Cancer Risk (IACR) were compared with guideline levels to ensure protection of humans and drinking water, respectively (Canadian Council of Ministers of the Environment 2010).

Average values for several PAHs were above detection limits in the Slave River reaches, though concentrations were low and all PAHs were below guideline levels (Table 13). Some PAHs with potential carcinogenic effects (listed in Canadian Council of Ministers of the Environment 2010) were above detection limit in several reaches, including Benzo(b&j)fluoranthene and chrysene (Table 13). Levels of these PAHs remained fairly low, and were below guideline levels. The B(a)P Total Potency Equivalent, which is a measure of cancer risk to humans, was below detection limit in all reaches. The IACR, which measures threat to drinking water, was above detection limit in Reach 2, but it was much lower than the guideline level of 1.0 (Canadian Council of Ministers of the Environment 2010). Arsenic was the only metal that was above the ISQG in Slave River sediment samples, and these exceedances of the guideline were minor (Table 13). Levels of most metals were low, and variability was generally low, indicating good precision between samples collected in the same reach.

*Table 13. Summary of sediment chemistry parameters sampled in the Slave River in 2019, indicating site mean ± standard deviation for each reach (2 samples collected per reach, with 1 duplicate). When both sites in a reach were below detection limit, the detection limit is indicated. When only one site in a reach was below detection limit, half the detection limit was used in calculations (number of sites below DL indicated in Parameter column). Values were compared with CCME sediment quality guidelines for the protection of aquatic life (Canadian Council of Ministers of the Environment 2001a), and values in bold were greater than interim freshwater sediment quality guidelines (ISQGs) whereas values in red were greater than probable effect levels (PELs). Reaches are ordered from upstream (KS1) to downstream (KS5).*

| Parameter | SR-KS1 | SR-KS2 | SR-KS3 | SR-KS4A | SR-KS4B | SR-KS6 | SR-KS5 |
|---|---|---|---|---|---|---|---|
| **Physicals** | | | | | | | |
| Moisture % | 32.6 ± 1.1 | 32.3 ± 16.5 | 38.9 ± 0.1 | 30.0 ± 6.4 | 33.6 ± 1.2 | 32.7 ± 7.0 | 40.6 ± 5.7 |
| **Metals (mg/kg)** | | | | | | | |
| Antimony (Sb) | 0.410 ± 0.028 | 0.488 ± 0.138 | 0.505 ± 0.078 | 0.385 ± 0.049 | 0.390 ± 0.000 | 0.475 ± 0.120 | 0.485 ± 0.021 |
| Arsenic (As) | **6.67 ± 0.01** | **7.44 ± 1.35** | **8.46 ± 1.47** | **6.51 ± 0.97** | **6.63 ± 0.49** | **8.49 ± 1.94** | **7.96 ± 0.25** |
| Barium (Ba) | 284.5 ± 10.6 | 298.0 ± 7.1 | 334.5 ± 81.3 | 225.5 ± 47.4 | 228.0 ± 1.4 | 316.5 ± 50.2 | 356.5 ± 16.3 |
| Beryllium (Be) | 0.435 ± 0.035 | 0.550 ± 0.156 | 0.580 ± 0.127 | 0.410 ± 0.113 | 0.405 ± 0.021 | 0.555 ± 0.163 | 0.570 ± 0.014 |
| Cadmium (Cd) | 0.533 ± 0.118 | 0.444 ± 0.070 | 0.519 ± 0.088 | 0.401 ± 0.032 | 0.382 ± 0.024 | 0.528 ± 0.074 | 0.468 ± 0.040 |
| Chromium (Cr) | 14.7 ± 0.6 | 16.7 ± 2.4 | 18.5 ± 3.9 | 14.0 ± 3.0 | 14.0 ± 0.3 | 18.6 ± 4.4 | 18.0 ± 0.3 |
| Cobalt (Co) | 7.33 ± 0.07 | 8.08 ± 1.48 | 9.03 ± 1.80 | 7.20 ± 0.83 | 7.63 ± 0.66 | 8.91 ± 1.68 | 8.47 ± 0.30 |
| Copper (Cu) | 13.7 ± 0.1 | 15.7 ± 4.0 | 18.2 ± 3.5 | 13.1 ± 3.4 | 17.4 ± 4.9 | 18.1 ± 4.9 | 16.8 ± 0.6 |

| Parameter | SR-KS1 | SR-KS2 | SR-KS3 | SR-KS4A | SR-KS4B | SR-KS6 | SR-KS5 |
|---|---|---|---|---|---|---|---|
| Lead (Pb) | 7.69 ± 0.31 | 9.44 ± 2.78 | 9.97 ± 1.89 | 7.29 ± 1.71 | 7.97 ± 0.69 | 9.68 ± 2.57 | 9.14 ± 0.28 |
| Mercury (Hg) | 0.050 ± 0.002 | 0.049 ± 0.011 | 0.051 ± 0.005 | 0.044 ± 0.011 | 0.041 ± 0.003 | 0.055 ± 0.012 | 0.049 ± 0.001 |
| Molybdenum (Mo) | 0.910 ± 0.000 | 0.990 ± 0.283 | 1.080 ± 0.269 | 0.760 ± 0.170 | 0.800 ± 0.042 | 1.135 ± 0.389 | 0.990 ± 0.042 |
| Nickel (Ni) | 21.2 ± 0.0 | 23.0 ± 3.6 | 26.0 ± 5.2 | 20.4 ± 2.4 | 20.9 ± 1.0 | 25.9 ± 4.7 | 24.4 ± 0.8 |
| Selenium (Se) | 0.440 ± 0.042 | 0.475 ± 0.134 | 0.575 ± 0.120 | 0.395 ± 0.064 | 0.390 ± 0.014 | 0.535 ± 0.148 | 0.520 ± 0.028 |
| Silver (Ag) (1 below DL) | 0.120 ± 0.000 | 0.155 ± 0.049 | 0.170 ± 0.028 | 0.095 ± 0.064 | 0.110 ± 0.000 | 0.165 ± 0.049 | 0.160 ± 0.014 |
| Thallium (Tl) | 0.134 ± 0.005 | 0.165 ± 0.045 | 0.181 ± 0.031 | 0.125 ± 0.030 | 0.128 ± 0.001 | 0.168 ± 0.045 | 0.159 ± 0.001 |
| Tin (Sn) | < 2.0 | < 2.0 | < 2.0 | < 2.0 | < 2.0 | < 2.0 | < 2.0 |
| Uranium (U) | 0.888 ± 0.066 | 1.043 ± 0.229 | 1.061 ± 0.197 | 0.803 ± 0.142 | 0.891 ± 0.000 | 1.026 ± 0.147 | 1.010 ± 0.014 |
| Vanadium (V) | 26.3 ± 0.9 | 29.4 ± 4.3 | 32.9 ± 6.9 | 25.1 ± 4.5 | 25.3 ± 0.4 | 32.3 ± 7.6 | 31.8 ± 0.3 |
| Zinc (Zn) | 66.2 ± 2.9 | 74.0 ± 11.2 | 83.7 ± 16.4 | 62.3 ± 11.5 | 65.1 ± 2.5 | 85.2 ± 15.8 | 80.6 ± 2.9 |
| **Polycyclic Aromatic Hydrocarbons (PAHs) (mg/kg)** | | | | | | | |
| 2-Methylnaphthalene (2 below DL) | < 0.01 | 0.017 ± 0.008 | 0.012 ± 0.001 | 0.010 ± 0.006 | 0.011 ± 0.001 | 0.009 ± 0.005 | 0.014 ± 0.013 |
| Acenaphthene | < 0.005 | < 0.005 | < 0.005 | < 0.005 | < 0.005 | < 0.005 | < 0.005 |
| Acenaphthylene | < 0.005 | < 0.005 | < 0.005 | < 0.005 | < 0.005 | < 0.005 | < 0.005 |
| Anthracene | < 0.004 | < 0.004 | < 0.004 | < 0.004 | < 0.004 | < 0.004 | < 0.004 |
| B(a)P Total Potency Equivalent (mg/kg) | < 0.02 | < 0.02 | < 0.02 | < 0.02 | < 0.02 | < 0.02 | < 0.02 |
| Benz(a)anthracene | < 0.01 | < 0.01 | < 0.01 | < 0.01 | < 0.01 | < 0.01 | < 0.01 |
| Benzo(a)pyrene | < 0.01 | < 0.01 | < 0.01 | < 0.01 | < 0.01 | < 0.01 | < 0.01 |
| Benzo(b&j)fluoranthene (13 below DL) | < 0.01 | 0.007 ± 0.002 | < 0.01 | 0.008 ± 0.004 | < 0.01 | < 0.01 | < 0.01 |
| Benzo(g,h,i)perylene | < 0.01 | < 0.01 | < 0.01 | < 0.01 | < 0.01 | < 0.01 | < 0.01 |
| Benzo(k)fluoranthene | < 0.01 | < 0.01 | < 0.01 | < 0.01 | < 0.01 | < 0.01 | < 0.01 |
| Chrysene (9 below DL) | < 0.01 | 0.010 ± 0.007 | 0.011 ± 0.001 | 0.009 ± 0.006 | < 0.01 | < 0.01 | 0.010 ± 0.006 |
| Dibenz(a,h)anthracene | < 0.005 | < 0.005 | < 0.005 | < 0.005 | < 0.005 | < 0.005 | < 0.005 |
| Fluoranthene | < 0.01 | < 0.01 | < 0.01 | < 0.01 | < 0.01 | < 0.01 | < 0.01 |
| Fluorene | < 0.01 | < 0.01 | < 0.01 | < 0.01 | < 0.01 | < 0.01 | < 0.01 |
| IACR (CCME) (14 below DL) | < 0.15 | 0.094 ± 0.027 | < 0.15 | < 0.15 | < 0.15 | < 0.15 | < 0.15 |
| Indeno(1,2,3-c,d)pyrene | < 0.01 | < 0.01 | < 0.01 | < 0.01 | < 0.01 | < 0.01 | < 0.01 |
| Naphthalene (12 below DL) | < 0.01 | 0.008 ± 0.004 | < 0.01 | < 0.01 | < 0.01 | < 0.01 | 0.009 ± 0.005 |
| Phenanthrene (2 below DL) | 0.011 ± 0.001 | 0.018 ± 0.008 | 0.015 ± 0.002 | 0.012 ± 0.010 | 0.013 ± 0.001 | 0.010 ± 0.006 | 0.020 ± 0.011 |
| Pyrene (13 below DL) | < 0.01 | 0.007 ± 0.002 | < 0.01 | 0.008 ± 0.004 | < 0.01 | < 0.01 | < 0.01 |
| Quinoline | < 0.01 | < 0.01 | < 0.01 | < 0.01 | < 0.01 | < 0.01 | < 0.01 |

#### *3.2.2.4. Benthic macroinvertebrates*

##### 3.2.2.4.1. Variation within and among reaches

Biotic metrics were used to compare abundance, relative abundance, and taxonomic richness of key organism groups among sites and reaches in the Slave River. Total abundance was low in Slave River samples in 2019, ranging from 125 to 888 individuals on average per reach, with four reaches having fewer than 300 individuals on average (Table 14). Abundance was statistically significantly higher in Reach 1 than in all other reaches, with the exception of Reach 3 (Figure 27). The lowest abundance was found in Reach 2, consistent with results from 2018. EPT abundance followed similar patterns to total abundance because these three orders made up a large proportion of the total assemblage in several reaches (Reaches 1, 3, 4B, and 5, where % EPT was greater than 70%; Table 14). Average EPT relative abundance was statistically significantly higher in Reach 1, Reach 3, and Reach 4B than in Reach 2 (Figure 27). This metric was highly variable within reaches, with large interquartile ranges particularly evident in Reach 2 and Reach 6.

The abundance of Chironomidae, in contrast to EPT, was similar across all reaches, and mean abundance values were extremely low, ranging from only 9 to 36 individuals on average per reach (Table 14). As a result, the average percent composition of Chironomidae in Slave River reaches ranged from 3.4% to 14.5% (Table 14, Figure 27), indicating that they made up only a minor portion of the samples in 2019. This result is consistent with patterns observed in 2018, again in sharp contrast to 2017 when Chironomidae made up 12-63% of the total assemblage. The decline in abundance of Chironomidae in 2018 was suggested to be a result of the flow conditions in 2018 (highly variable, with a peak 45 days prior to sampling; Lento 2020), and the same is likely true for 2019, when water levels were high at the time of sampling and in the antecedent period.

*Table 14. Summary of biotic metrics for kick-site reaches sampled in the Slave River in 2018, including the mean ± standard deviation for BMI abundance and taxonomic richness metrics. EPT is the sum of Ephemeroptera, Plecoptera, and Trichoptera orders; Chironomidae is a family of Diptera; Diptera + Oligochaeta includes all true flies and segmented worms; and Mollusca includes bivalves (clams) and gastropods (snails). Reaches are ordered from upstream (KS1) to downstream (KS5).*

| Biotic Metric | SR- KS1 | SR-KS2 | SR-KS3 | SR-KS4A | SR-KS4B | SR-KS6 | SR-KS5 |
|---|---|---|---|---|---|---|---|
| Total abundance | 888 ± 289 | 125 ± 17 | 560 ± 160 | 222 ± 173 | 189 ± 99 | 468 ± 240 | 286 ± 213 |
| EPT abundance | 662 ± 204 | 53 ± 32 | 407 ± 143 | 124 ± 104 | 129 ± 59 | 344 ± 214 | 204 ± 186 |
| Chironomidae abundance | 38 ± 14 | 18 ± 9 | 18 ± 10 | 16 ± 16 | 9 ± 5 | 15 ± 10 | 36 ± 47 |
| Diptera + Oligochaeta abundance | 59 ± 18 | 56 ± 29 | 45 ± 19 | 31 ± 18 | 18 ± 11 | 40 ± 18 | 66 ± 58 |
| Mollusca abundance | 0 ± 1 | 6 ± 6 | 3 ± 4 | 0 ± 0 | 0 ± 0 | 2 ± 3 | 5 ± 7 |
| Percent EPT | 75.1 ± 8.1 | 41.0 ± 23.4 | 71.5 ± 9.6 | 56.7 ± 12.4 | 72.6 ± 12.6 | 70.0 ± 10.0 | 62.5 ± 20.9 |
| Percent Chironomidae | 4.3 ± 0.7 | 13.8 ± 6.0 | 3.5 ± 2.0 | 11.5 ± 15.7 | 4.6 ± 1.3 | 3.4 ± 1.2 | 14.5 ± 14.5 |
| Percent Diptera + | 6.9 ± 1.6 | 46.6 ± | 8.1 ± 2.8 | 17.9 ± | 9.1 ± 4.1 | 8.7 ± 2.9 | 24.8 ± |

| | | | | | | | |
|---|---|---|---|---|---|---|---|
| Oligochaeta | | 26.4 | | 14.6 | | | 16.0 |
| Percent Mollusca | 0.1 ± 0.2 | 4.2 ± 4.4 | 0.7 ± 1.0 | 0.2 ± 0.4 | 0.0 ± 0.0 | 0.6 ± 1.1 | 1.7 ± 2.1 |
| Taxonomic richness | 21.6 ± 3.5 | 23.0 ± 3.7 | 25.8 ± 5.2 | 20.0 ± 3.7 | 18.4 ± 5.4 | 25.4 ± 3.9 | 25.8 ± 8.6 |
| EPT richness | 9.6 ± 0.9 | 7.0 ± 1.2 | 10.2 ± 1.1 | 7.6 ± 0.5 | 9.0 ± 1.2 | 8.8 ± 1.6 | 8.4 ± 2.6 |
| Chironomidae richness | 4.4 ± 1.1 | 5.2 ± 1.9 | 4.6 ± 1.5 | 5.0 ± 2.7 | 3.8 ± 2.2 | 6.2 ± 2.6 | 8.0 ± 3.7 |
| Diptera + Oligochaeta richness | 7.4 ± 1.7 | 10.0 ± 2.5 | 9.6 ± 3.4 | 9.2 ± 3.1 | 6.2 ± 3.9 | 11.0 ± 3.7 | 12.6 ± 5.5 |
| Mollusca richness | 0.4 ± 0.9 | 1.8 ± 1.3 | 1.0 ± 1.2 | 0.2 ± 0.4 | 0.0 ± 0.0 | 0.4 ± 0.5 | 1.4 ± 1.7 |

The relative abundance of Diptera + Oligochaeta was generally similar to that of Chironomidae, with the exception of Reach 2 (Table 14, Figure 27). Diptera + Oligochaeta made up 46.6% of the samples on average in Reach 2, though samples within the reach were quite variable. This reach also had the lowest and most variable percent composition of EPT, and the shift in relative abundance between these groups indicated that non-chironomid Diptera and Oligochaeta were the more dominant taxa at some sites within the reach.

Taxonomic richness ranged from 18 to 26 taxa on average per reach (Table 14), and though there was some variability among reaches, there were no significant differences found when richness was tested in ANOVA (Figure 27). Variability among reaches was very low for EPT richness and Chironomidae richness, and similar numbers of taxa were found across reaches for each metric (Table 14, Figure 27). However,

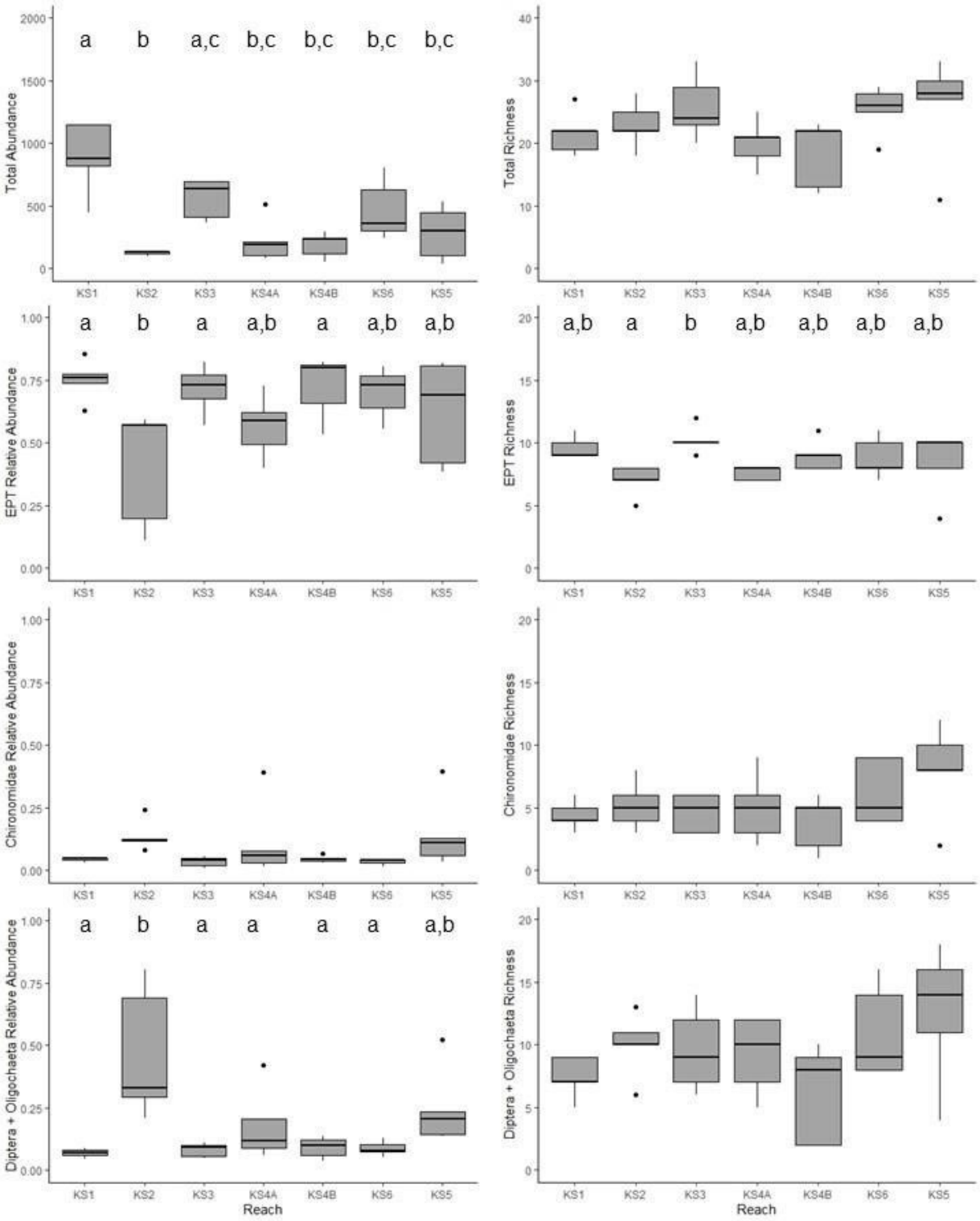


*Figure 27. Box plots of BMI metrics for the Slave River reaches sampled in 2019. Metrics include overall abundance and richness, and percent composition and richness of Ephemeroptera, Plecoptera, and Trichoptera (EPT), Chironomidae (midges), and Diptera (true flies) + Oligochaeta (segmented worms). Box indicates the interquartile range, line through the box indicates the median, and whiskers indicate the lower and upper quartiles. Points indicate statistical outliers. Letters on plots indicate significant differences ($\alpha$ = 0.05) from one-way ANOVA and Tukey HSD tests. Reaches are ordered from upstream (KS1) to downstream (KS5).*

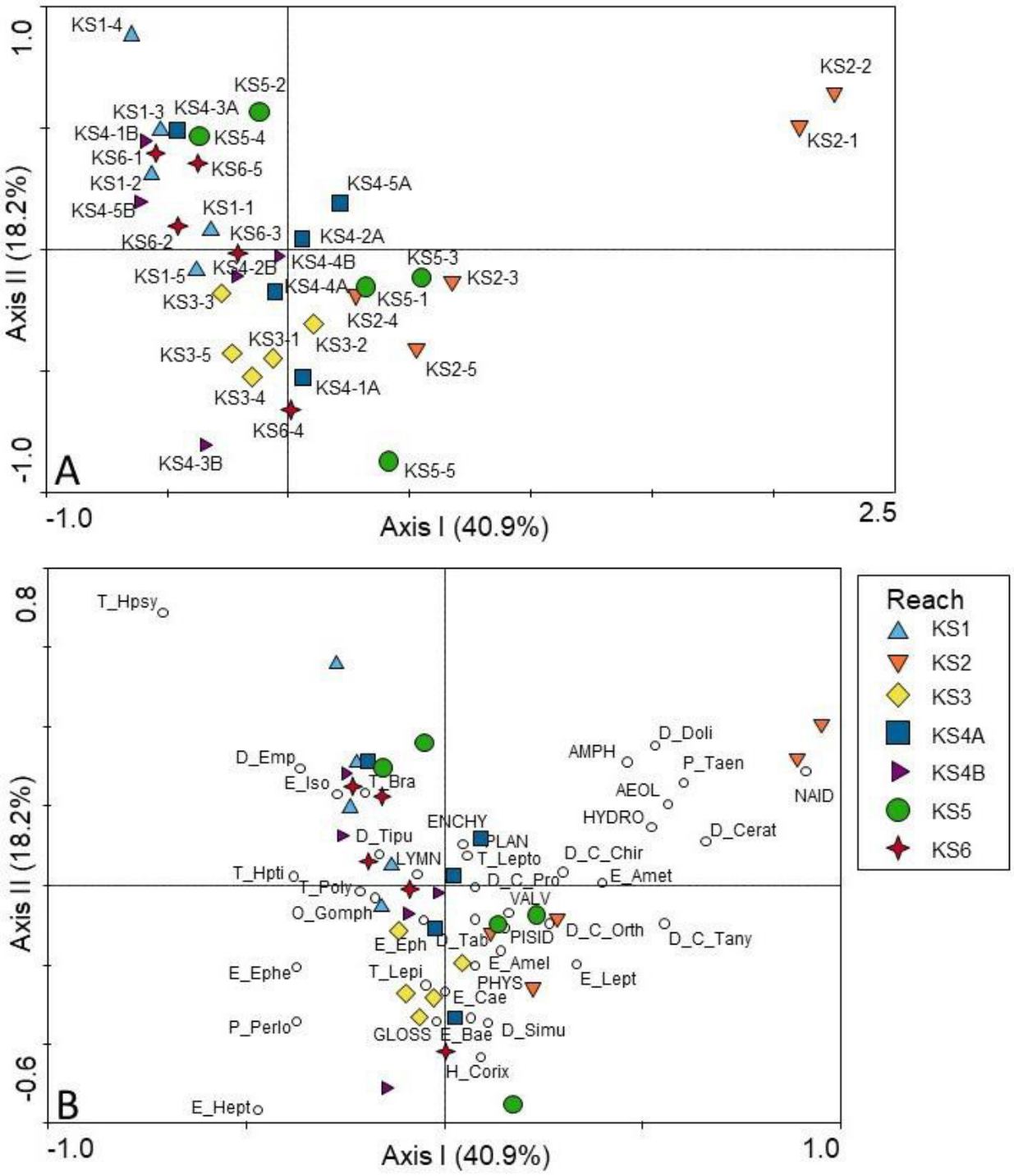


*Figure 28. Multivariate analysis of BMI from kick samples in the Slave River in 2019, including (A) PCA of BMI data with sites labelled, and (B) PCA biplot of BMI data with labelled taxa and with sample points coloured by reach. Kick-sites in close proximity have similar assemblages, whereas samples on opposite ends of gradients have differences in their assemblages. Samples at right angles through the origin are uncorrelated. Kick-sites are located close to taxa with which they are positively associated. Taxonomic abbreviations are listed in the appendices.*

*Table 15. Results of pairwise PERMANOVA comparing assemblage dissimilarity among reaches of the Slave River, showing pairwise p-values for each comparison. FDR-corrected αα was calculated for each pairwise comparison based on p-value rank, and p-values less than the FDR-corrected αα (marked with *) indicate a significant difference in assemblage composition between reaches based on a dissimilarity matrix.*

| | KS1 | KS2 | KS3 | KS4A | KS4B | KS5 | KS6 |
|---|---|---|---|---|---|---|---|
| KS1 | | | | | | | |
| KS2 | 0.009* | | | | | | |
| KS3 | 0.006 | 0.008* | | | | | |
| KS4A | 0.029* | 0.007* | 0.018* | | | | |
| KS4B | 0.02* | 0.012* | 0.017* | 0.451 | | | |
| KS5 | 0.009* | 0.008* | 0.007* | 0.024* | 0.006 | | |
| KS6 | 0.053 | 0.012* | 0.013* | 0.166 | 0.401 | 0.045 | |

variation within reach was also extremely low for EPT richness, and there was high power to detect differences among reaches. As a result, a statistically significant difference in richness was found between Reach 2 (7 taxa on average) and Reach 3 (10.2 taxa on average; Figure 27), though the actual difference in the number of taxa was small. Richness of Diptera + Oligochaeta was more variable within reaches than the other metrics, and though richness was highest on average in Reach 6, no statistically significant differences were found (Figure 27).

#### 3.2.2.4.2. Multivariate assessment of BMI assemblage composition

Multivariate analysis was used to characterize the biotic assemblage of the Slave River and evaluate similarities and differences in assemblage composition among reaches and sites. PCA was intended to assess correlations within and among reaches, and to identify any potential outliers or gaps in sample stations, whereas PERMANOVA and homogeneity of multivariate dispersions assessed similarity in composition among and within reaches. BMI relative abundance data for all taxa were assessed at the family/subfamily level.

*The PCA indicated the presence of two strong outliers: KS2-1 and KS2-2 (Figure 28A). Site KS2-1 had been identified as a potential outlier in previous years due to low abundance and richness at this site, and in 2019 the site was shifted upstream to be closer to site KS2-2. It is therefore interesting that both sites appeared to be outliers in the ordination plot for 2019. The difference between these sites and the remaining Slave River sites contributed to most of the spread along axis I of the PCA ordination, which explained 40.9% of the variation among sites. KS2-1 and KS2-2 were positively correlated with a number of taxa, including the segmented worm families Aeolosomatidae and Naididae, the gastropod Hydrobiidae, and the Diptera families Dolichopodidae and Ceratopogonidae (Figure 28B), all of which have a preference for low flows (Monk et al. 2018). In contrast, the sites were negatively correlated with several taxa that prefer high flows (Monk et al. 2018), including the mayflies Ephemerellidae and Heptageniidae, and the stonefly Perlodidae (Figure 28B). Flow velocity was low in Reach 2 (*

Table 12), consistent with these taxonomic associations.

Remaining sites were primarily spread along the second axis, which explained 18.2% of the variation among sites (Figure 28A). Reach 4A was found to be similar to other reaches, despite the fact that it was a strong outlier in both 2017 and 2018. However, biotic metrics also indicated a greater similarity of this

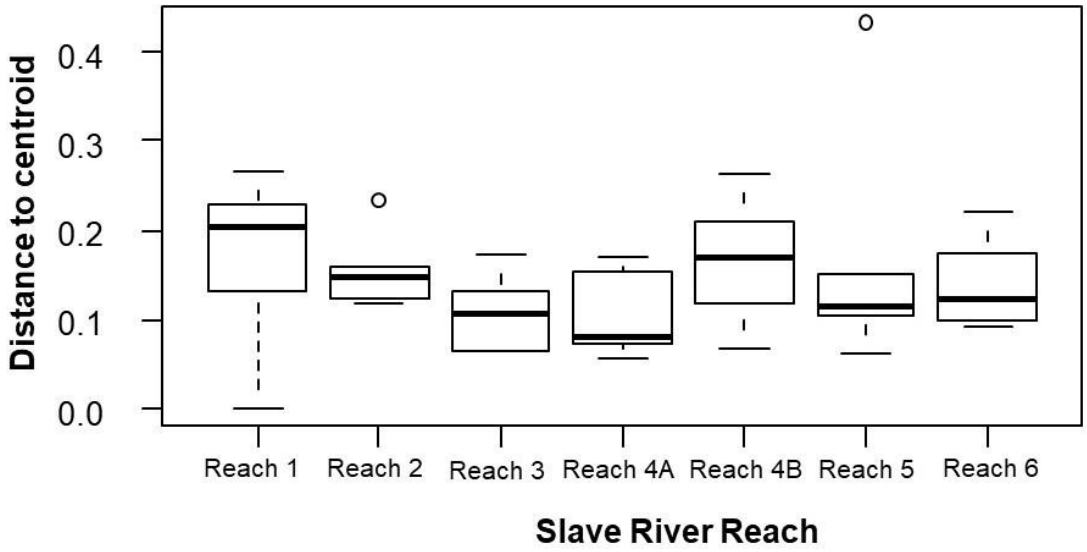


*Figure 29. Results of homogeneity of multivariate dispersions analysis of Slave River BMI assemblages, showing the median distance to centroid for each reach (black bar), 25th and 75th percentiles (lower and upper bounds of box, respectively), minimum and maximum (whiskers), and outliers (points). Distance to centroid represents the spread of sites in multivariate space, where greater distance equals greater dissimilarity among sites. Low distance to centroid indicates similarity within reaches.*

reach to the other Slave River reaches in 2019 (Table 14, Figure 27). Reach 6, which was newly sampled in 2019, plotted out close to Reach 1 in the ordination (Figure 28A). The goal in adding this reach was to add another fast-flowing location that was similar to Reach 1, and the results of the ordination confirm that similar assemblage composition was found between these two reaches. Sites in Reach 1, Reach 6, and Reach 5 found at the positive end of the second axis gradient were associated with the caddisfly families Hydropsychidae and Brachycentridae, the Diptera family Empididae, and the mayfly family Isonychiidae (Figure 28B). On the negative end of the second axis gradient, sites in Reach 3 and Reach 2 (and individual sites from other reaches), were positively associated with taxa including the leech family Glossiphonidae, black flies (Simuliidae), the stonefly family Perlodidae, and several families of mayflies, including Baetidae, Heptogeniidae, and Ephemerellidae (Figure 28B).

Based on a dissimilarity matrix of all sites, the PERMANOVA indicated that there were significant differences in assemblage composition among reaches in the Slave River ($F$ = 3.80, $p$ = 0.001). Pairwise PERMANOVA was used to identify which reaches had statistically significant differences in assemblages (significant at an FDR-corrected $\alpha\alpha$-level, based on the rank of each $p$-value). There was generally stronger pairwise similarity among the downstream reaches (Reaches 4A, 4B, 5, and 6) than among upstream reaches or comparisons between upstream and downstream reaches (Table 15).The reaches that differed the most from the rest of the river included Reach 2 (all pairwise comparisons significant at

FDR-corrected $\alpha\alpha$-level ) and Reach 3 (all pairwise comparisons significant except the comparison with Reach 1;Table 15). In contrast, Reach 6 was the most similar to other reaches, only differing significantly from Reach 2 and Reach 3 (Table 15). Patterns in the pairwise PERMANOVA results were generally consistent with those evident in the PCA (Figure 28), which showed Reach 2 differing from all other

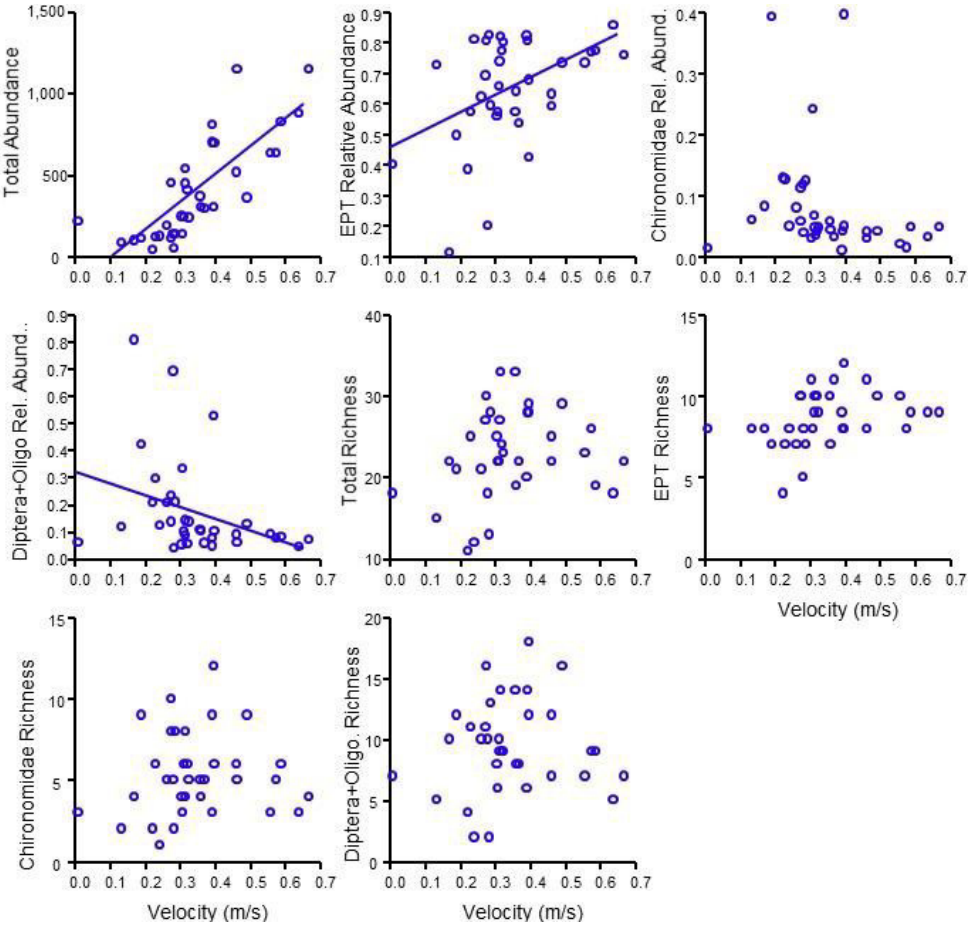


*Figure 30. Relationship between biotic metrics calculated for Slave River sites and flow velocity recorded at each site at the time of sampling. Each plot has a different metric as the response variable on the y-axis. Linear regression lines are plotted for metrics that were significantly associated with velocity.*

reaches along the first axis, Reach 3 differing from most other reaches along the second axis, and a strong overlap of Reach 6 with other sites including those in Reach 1.

Within-reach variability in assemblage composition was similar for each reach of the Slave River (homogeneity of multivariate dispersions $F = 0.551$, $p = 0.796$). The median distance to centroid was similarly low for all reaches, though it was highest in Reach 1 (indicating greater differences among sites) and lowest for Reach 4A (indicating fewer compositional differences among sites; Figure 29). Both Reach 2 and Reach 5 had sites that were outliers with respect to distance to centroid in multivariate space. These outliers represented sites that differed more strongly from the average composition of the other sites in the reach.

#### 3.2.2.4.3. Biotic-abiotic relationships

Relationships between BMI assemblages and abiotic parameters were tested to explore potential drivers of assemblage structure in the Slave River. Because there appeared to be differences among reaches that related to flow velocity, the relationship between biotic metrics and flow velocity was tested with least-squares linear regression. When the relationship between a metric and velocity appeared to be curvilinear, a polynomial regression model was tested.

There was clear evidence of a relationship between total abundance of BMI and flow velocity among sites, with abundance increasing as a function of increasing velocity (Figure 30). Least-squares linear regression analysis confirmed a statistically significant increase in abundance in response to increasing velocity (slope $t = 7.25$, $p < 0.001$). The relative abundance of EPT was also found to increase significantly in response to increasing velocity (slope $t = 2.91$, $p = 0.006$), though the relationship was far more variable than that observed for total abundance (Figure 30). In contrast, the relative abundance of Chironomidae and the relative abundance of Diptera + Oligochaeta both appeared to decrease with increasing flow velocity (Figure 30), though the relationship was only statistically significant for the relative abundance of Diptera + Oligochaeta (slope $t = -2.17$, $p = 0.037$).

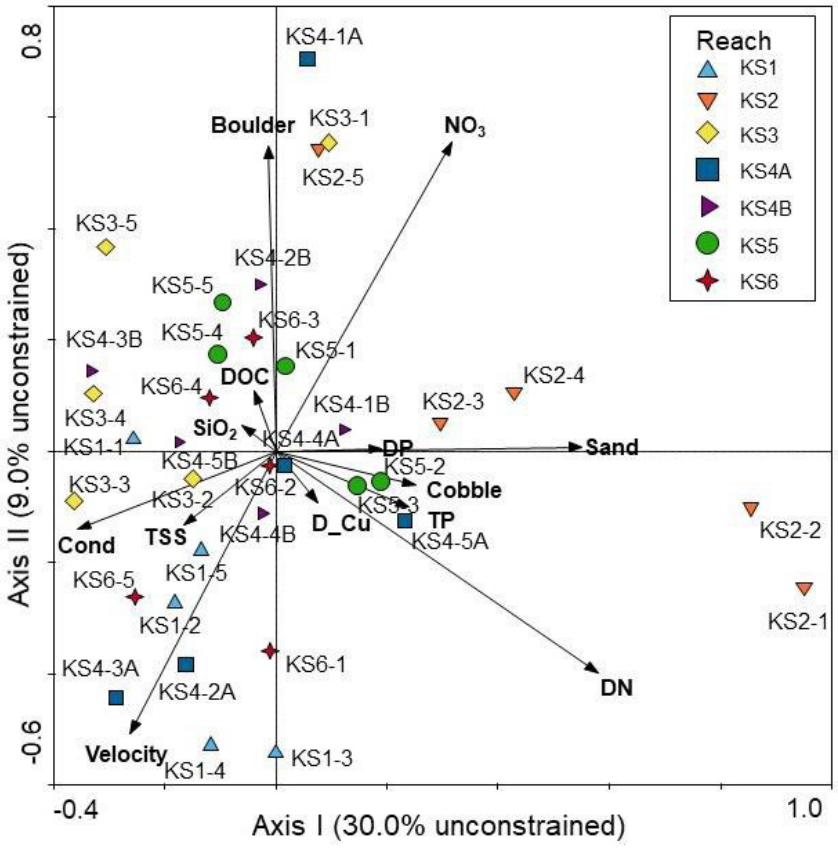


*Figure 31 RDA ordination of Slave River BMI data constrained by physical and chemical habitat data at each site, with sites coloured by reach. Even-numbered sites use average values of chemical parameters from neighbouring odd-numbered sites. Kick-sites at the same end of a gradient are positively correlated with similar taxa and chemical/physical variables, whereas*

*samples on opposite ends of gradients are negatively correlated. Samples at right angles through the origin are uncorrelated. Vectors indicate direction of change of physical and chemical parameters, and sites are ranked along these vectors based on the strength of their correlation with each parameter.*

Total richness metrics appeared to show a curvilinear (unimodal) response to flow velocity, similar to the Hay River, with the highest richness found in the middle of the velocity range across all sites (Figure 30). Statistical analysis confirmed this pattern, as the polynomial model provided a significantly better fit to the data than linear model for total richness (velocity and velocity$^2$ terms both significant at $\alpha\alpha$=0.05), but the unimodal relationship between total richness and flow velocity was not statistically significant (regression $F_{2,32}$ = 3.18, $p$ = 0.055). Although the relationships of other richness metrics with flow velocity appeared to be curvilinear (Figure 30), addition of the polynomial term did not significantly improve the fit of the model to the data, and no other richness metrics were found to have a significant relationship with flow velocity in the Slave River.

Biotic-abiotic relationships were also assessed in Slave River kick samples using Redundancy Analysis (RDA), a multivariate approach that uses environmental variables to constrain the spatial arrangement of sites based on BMI relative abundance. RDA assesses the amount of variation in the unconstrained ordination (the PCA of BMI samples) that is explained by relating the data to chosen environmental variables, and identifies major abiotic gradients in the data. Prior to analysis, correlations between environmental parameters were examined in combination with the abiotic PCAs to pick out important drivers of differences among sites that were uncorrelated with each other (low correlations between environmental parameters were chosen to avoid multicollinearity). This also worked to reduce the number of environmental parameters in the analysis and avoid over-fitting the data. The final RDA for water chemistry and physical habitat variables included velocity, % sand, % cobble, % boulder, conductivity, dissolved organic carbon (DOC), nitrate ($NO_3$), dissolved nitrogen (DN), dissolved phosphorus (DP), total phosphorus (TP), reactive silicate ($SiO_2$), total suspended solids (TSS), and dissolved copper (D_Cu). Other ions, nutrients, physical measures, and total and dissolved metals were highly correlated with the chosen variables. Thus, any patterns described for these parameters also apply to the correlated parameters.

The first axis and all axes of the RDA of BMI relative abundance and chemical and physical parameters were statistically significant (Monte Carlo permutation test: first axis $F$ = 8.26, $p$ = 0.022; all axes $F$ = 1.87, $p$ = 0.008), and the first three axes explained 81.9% of the constrained variation among Slave River samples (43.9% of the unconstrained variation). In the constrained ordination, sites KS2-1 and KS2-2 remained outliers, and the separation of these and other Reach 2 sites from the other reaches along the first axis explained 30% of the unconstrained variation in benthic assemblages (53.7% of constrained variation; Figure 31). Most sites in Reach 2 were positively correlated with sand, nitrate, and DN along the first axis. Each of these variables had high loadings on axis 1 and contributed to strong gradients among sites (Figure 31). Along the second axis, which explained 9% of the unconstrained variation among sites (17.4% of the constrained variation), sites varied along a gradient in velocity and substrate size, with sites in Reach 1, Reach 4A, and Reach 6 positively associated with velocity and individual sites from six of the reaches (all except Reach 1) positively associated with the percent boulder. Sites were generally mixed among other reaches in the ordination, indicating few strong reach-specific gradients in chemical and physical habitat variables.

The statistical significance of chemical and physical habitat variables in the RDA was tested using Monte Carlo permutational tests. Dissolved nitrogen had the strongest effect on the fit of the model ($F$ = 4.66, $p$

= 0.004), followed by the percent sand ($F$ = 4.52, $p$ = 0.002). Conductivity also had a significant effect on the fit of the model ($F$ = 3.07, $p$ = 0.020), and it was positively correlated with velocity in the ordination plot (Figure 31). No other variables were significant, likely due to the similarity in water chemistry among sites that may have resulted in a lack of explanatory power for water chemistry parameters.

### 3.2.3. Temporal characterization of BMI assemblages

#### *3.2.3.1. Benthic macroinvertebrate composition*

Compositional changes from 2017 to 2019 were summarized at the river level for the Slave River by assessing the average relative abundance of major taxonomic groups across all reaches in each year (Figure 32). One of the most dramatic changes from 2017 to 2018 was a sharp decline in the relative abundance of Diptera (true flies) and increase in relative abundance of Trichoptera (caddisflies; Figure 32). Increases in relative abundance of other mobile taxa such as Ephemeroptera (mayflies), Plecoptera (stoneflies), and Hemiptera (true bugs) were also evident in 2018. Average relative abundance of several taxonomic groups were similar in 2019 to what was found in 2018, particularly for true flies. However, there was an increase in relative abundance of EPT groups (mayflies, stoneflies, and caddisflies), and a decrease in true bugs and non-insects (including molluscs, snails, and segmented worms) relative to 2018 (Figure 32). Despite these changes, average relative abundance of different taxonomic groups in 2019 remained more similar to 2018 than to 2017.

At the site scale, large changes were evident when total abundance was compared between 2017 and 2018, but in 2019, abundance was more similar across sites (Figure 33). Changes to total abundance in 2018 included large decreases in some sites (including sites in Reach 2 and Reach 4A) and large increases in other sites (particularly in Reach 3 and Reach 4B; Figure 33). In 2019, abundance exceeded 1000 individuals in only two sites, and only 11 of the 35 sites sampled in 2019 had greater than 500 individuals collected. Changes in abundance over time in Slave River sites suggest that the flow regime in 2019, which included a gradual increase in flow (without a strong spring freshet) and higher water levels at the time of sampling and in the antecedent period, may have contributed to some homogenization of BMI assemblages with respect to abundance of individuals at a site.

Biotic metric data from all three years of sampling in the Slave River were combined into temporal box plots to evaluate general patterns over time within and among reaches (Figure 34). Changes in total abundance in reaches over time reflected the site-scale patterns shown in Figure 33, with increased mean abundance in Reach 3 and Reach 4B in 2018, and decreased mean abundance in all reaches in 2019 (Figure 34). The temporal box plot also indicated lower variability in total abundance within and among reaches in 2019, reflecting greater similarity throughout the sampled extent of the river.

In addition to changes in total abundance, there was strong evidence of changes to the relative abundance of taxonomic groups over the period 2017-2019, with the largest changes occurring between 2017 and 2018 (Figure 34). The most obvious of these changes was the decline in relative abundance of Chironomidae. Changes in abundance of Chironomidae from 2017 to 2018 were extreme, as this taxonomic group went from being dominant to being found at very low abundances and relative abundances across all sites. Over half of the Slave River sites saw a decline in percent composition of Chironomidae of greater than 30% from 2017 to 2018 (Lento 2020). Chironomidae relative abundance declined from 70-80% down to less than 10% of the total abundance in some samples (Lento 2020). In 2017, the maximum % Chironomidae was 85% and 18 sites had > 30% Chironomidae. In contrast, the

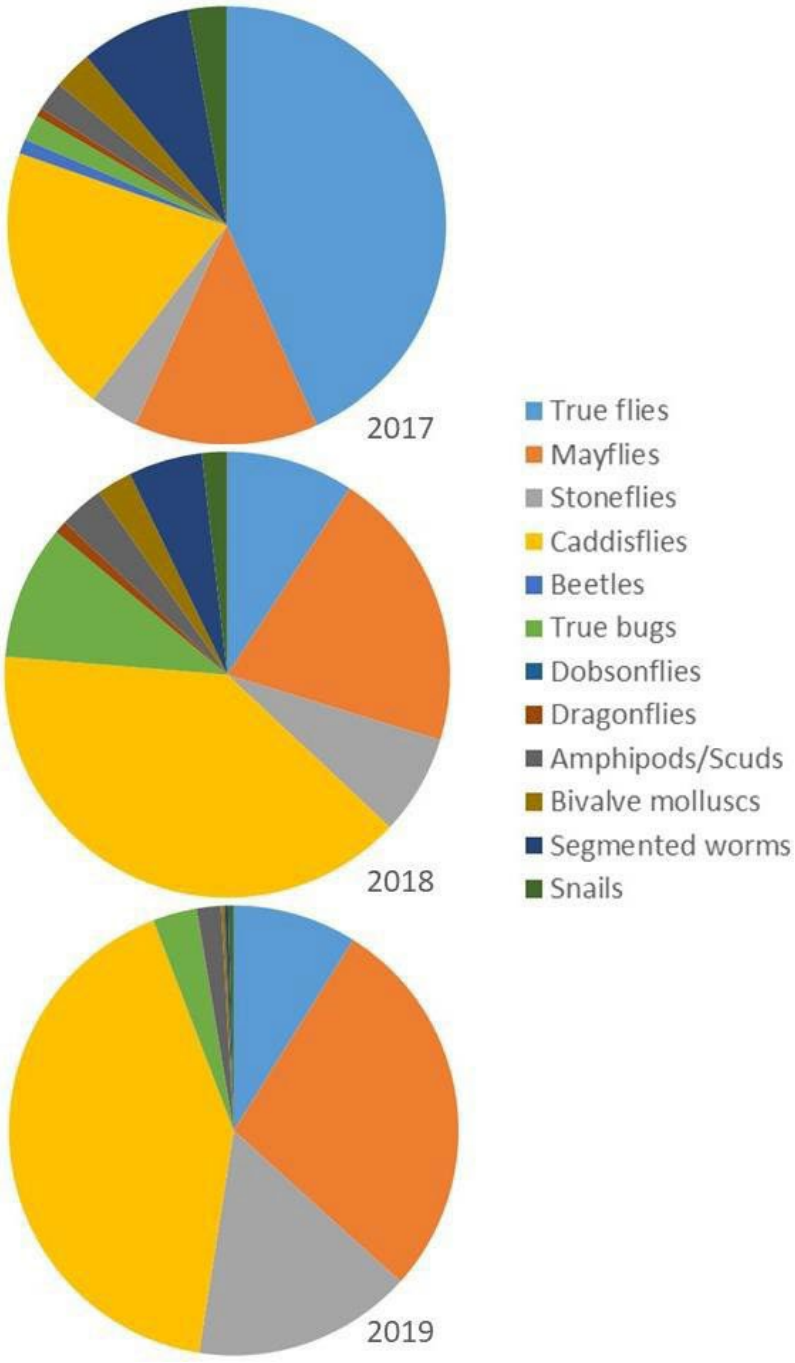


*Figure 32. Average relative abundance of major BMI taxonomic groups in Slave River kick samples collected in (A) 2017 and (B) 2018. Taxa are grouped as true flies (Diptera), mayflies (Ephemeroptera), stoneflies (Plecoptera), caddisflies (Trichoptera), beetles (Coleoptera), true bugs (Hemiptera), dobsonflies (Megaloptera), dragonflies (Odonata), amphipods/scuds (Amphipoda), bivalve molluscs (Bivalvia), segmented worms (Oligochaeta), and snails (Gastropoda).*

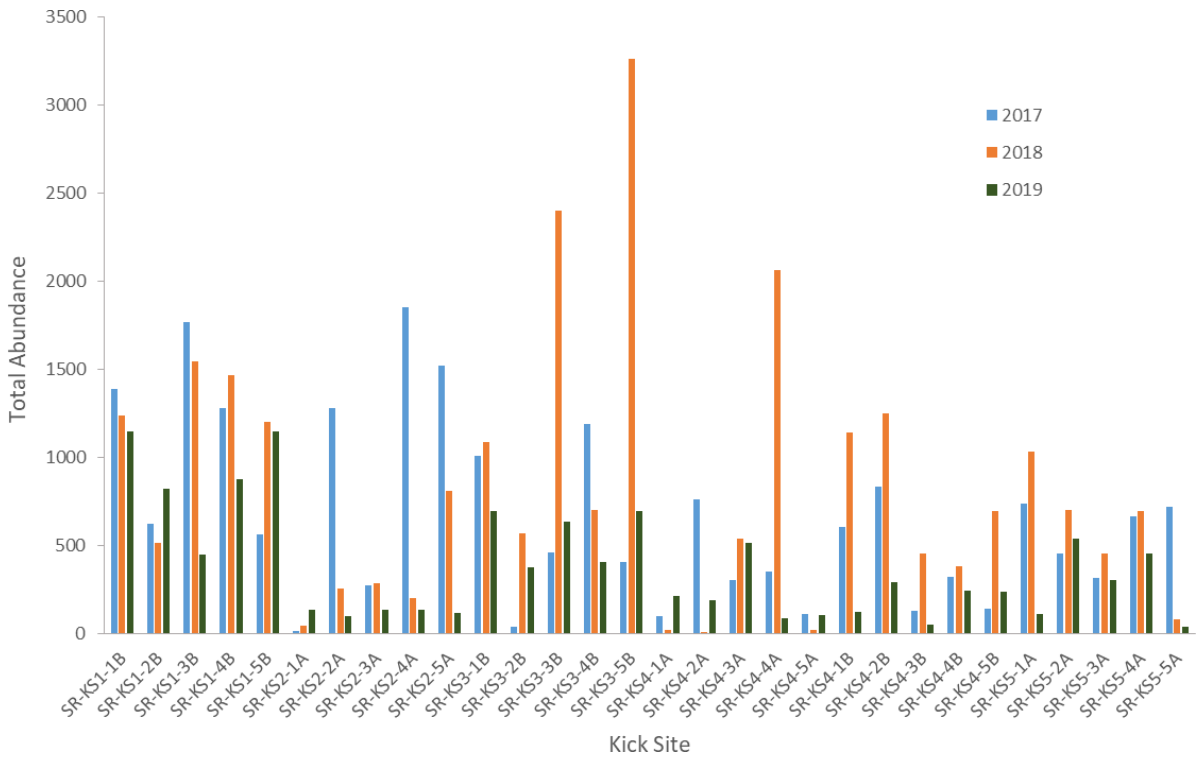


*Figure 33. Total abundance of BMI in Slave River kick sites in 2017 (blue bars), 2018 (orange bars), and 2019 (dark green bars).*

maximum % Chironomidae in 2018 was 29%, and ten sites had a decline of > 200 Chironomidae individuals in 2018 compared to 2017. In 2019, two sites had a higher relative abundance of Chironomidae at 39%, but 27 sites had a relative abundance below 10%, and 33 of the 35 sites sampled in 2019 had fewer than 50 chironomid individuals collected.

The decline in Chironomidae abundance in 2018 may have resulted from sampling temporary habitat, particularly if sampling locations were shifted laterally due to high flows, but it could also reflect ecological processes and flow preferences. The decline in abundance of Chironomidae in 2018 was suggested to be a result of increased flow and a recent peak in flow (45 days prior to sampling in 2018; Lento 2020), and the high flows in 2019 coupled with low abundance of Chironomidae seems to confirm this idea. High flows can cause scouring of benthic communities, and subsequent re-colonization by Chironomidae is typically slower than that by more mobile taxa, such as EPT.

Increased relative abundance of EPT taxa across all sites in 2018 and 2019 relative to 2017 lends further support to the idea that high flows led to a loss of Chironomidae at sample sites (Figure 34). Mean relative abundance of EPT increased relative to 2017 means in all reaches, indicating that the loss of Chironomidae was coupled with a gain of EPT individuals. The shift was most apparent in Reaches 3, 4A, 4B, and 5 (Figure 34). Reach 1 had high relative abundance of EPT and low relative abundance of Chironomidae in 2017, differing from other reaches in this respect, and the relative abundances observed in other reaches in 2018 and 2019 were more similar to those observed in Reach 1 (Figure 34).

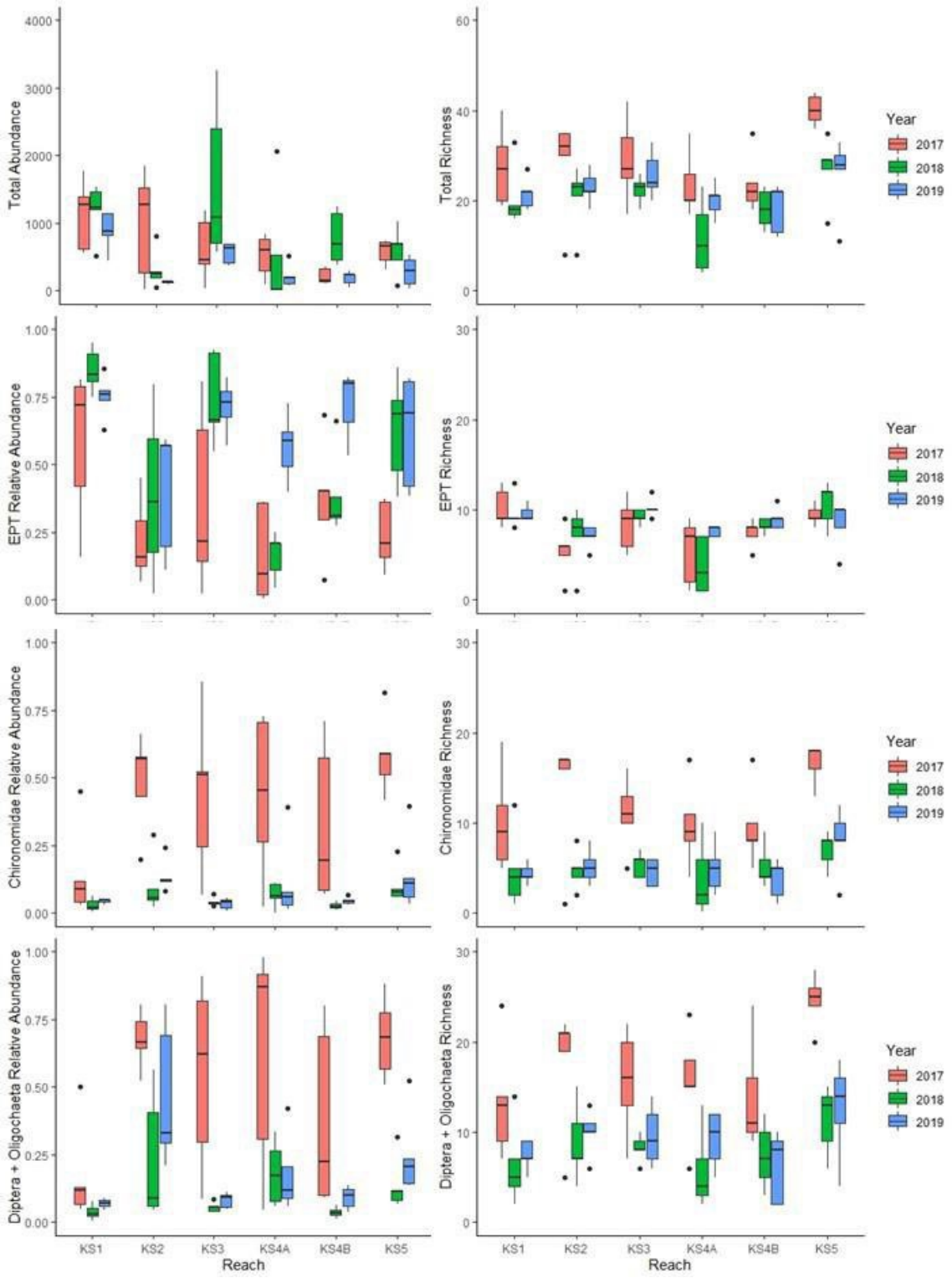


*Figure 34. Box plots of BMI metrics for the Slave River reaches, showing data from 2017, 2018, and 2019 for each reach. Metrics include overall abundance and richness, and relative abundance and richness of Ephemeroptera, Plecoptera, and Trichoptera (EPT), Chironomidae (midges), and Diptera (true flies) + Oligochaeta (segmented worms). Box indicates the interquartile range, line through the box indicates the median, and whiskers indicate the lower and upper quartiles. Points indicate statistical outliers.*

Changes in richness metrics over time primarily reflected the loss of Chironomidae taxa. EPT richness was highly invariable over time and was also similar among reaches (Figure 34), and it therefore had minimal impact on temporal patterns in total richness. In contrast, Chironomidae richness and Diptera + Oligochaeta richness both declined sharply in 2018 and remained at similar low levels in 2019, and this loss of diversity was reflected with lower total richness in 2018 and 2019 relative to 2017 in all reaches (Figure 34).

The mean ± SE for each biotic metric in each year was plotted with data for all reaches overlain in single plots to further evaluate change over time in the Slave River (Figure 35). Mean abundance was variable among reaches in each year of sampling, but means were more similar and there was less variability within reaches in 2019 (Figure 35). Other metrics were also found to be more similar on average among reaches and less variable within reaches in 2019. For example, the mean relative abundance of EPT increased in most reaches in 2018, but was highly variable among reaches (ranging from less than 0.25 to greater than 0.75 among reaches), whereas in 2019, variability among reaches was lower as mean relative abundance became more similar (Figure 35). Interestingly, the two reaches that did not show an increase in mean relative abundance of EPT in 2018 (Reach 4A and Reach 4B) both showed a strong increase in 2019 that brought their mean values more in line with the other reaches. Similar to the relative abundance metric, EPT richness was more variable among reaches in 2018, but became more similar both within and among reaches in 2019 (Figure 35).

Chironomidae and Diptera + Oligochaeta relative abundance and richness metrics showed the expected decline across all reaches in 2018 (Figure 35). Though Chironomidae metrics showed similar means and low variability in 2019, there were some changes evident in the relative abundance of Diptera + Oligochaeta, which increased and was more variable in some reaches (Figure 35). Total richness largely reflected the loss of Chironomidae, other Diptera, and Oligochaeta taxa in 2018, though there was evidence of less variability among reaches in 2019, similar to patterns observed in other metrics.

#### *3.2.3.2. Drivers of temporal patterns*

The greatest change that occurred over the sampling period (2017-2019) was related to the flow regime. Changes in the magnitude and timing of peak flows contributed to variation in water levels (high water levels in both 2018 and 2019) and different antecedent hydrologic conditions in each year of sampling. To evaluate the effect of varying flow on biotic metrics, ANCOVA models were tested with velocity as a continuous predictor (as relationships with velocity were evident for some metrics) and year as a categorical predictor and proxy for flow conditions in each year. Analysis was completed with Reaches 1 through 5, because Reach 6 was not sampled in 2017 or 2018.

The full ANCOVA model for total abundance indicated that there was a significant interaction between year and velocity ($F_{2,84}$ = 4.97, $p$ = 0.009), and the reduced model could not be tested. Differences in mean abundance could not be compared among years while controlling for site velocity, because the response of abundance to site-specific differences in velocity varied across sampling years. Separate regressions of total abundance as a function of velocity for each year indicated that abundance

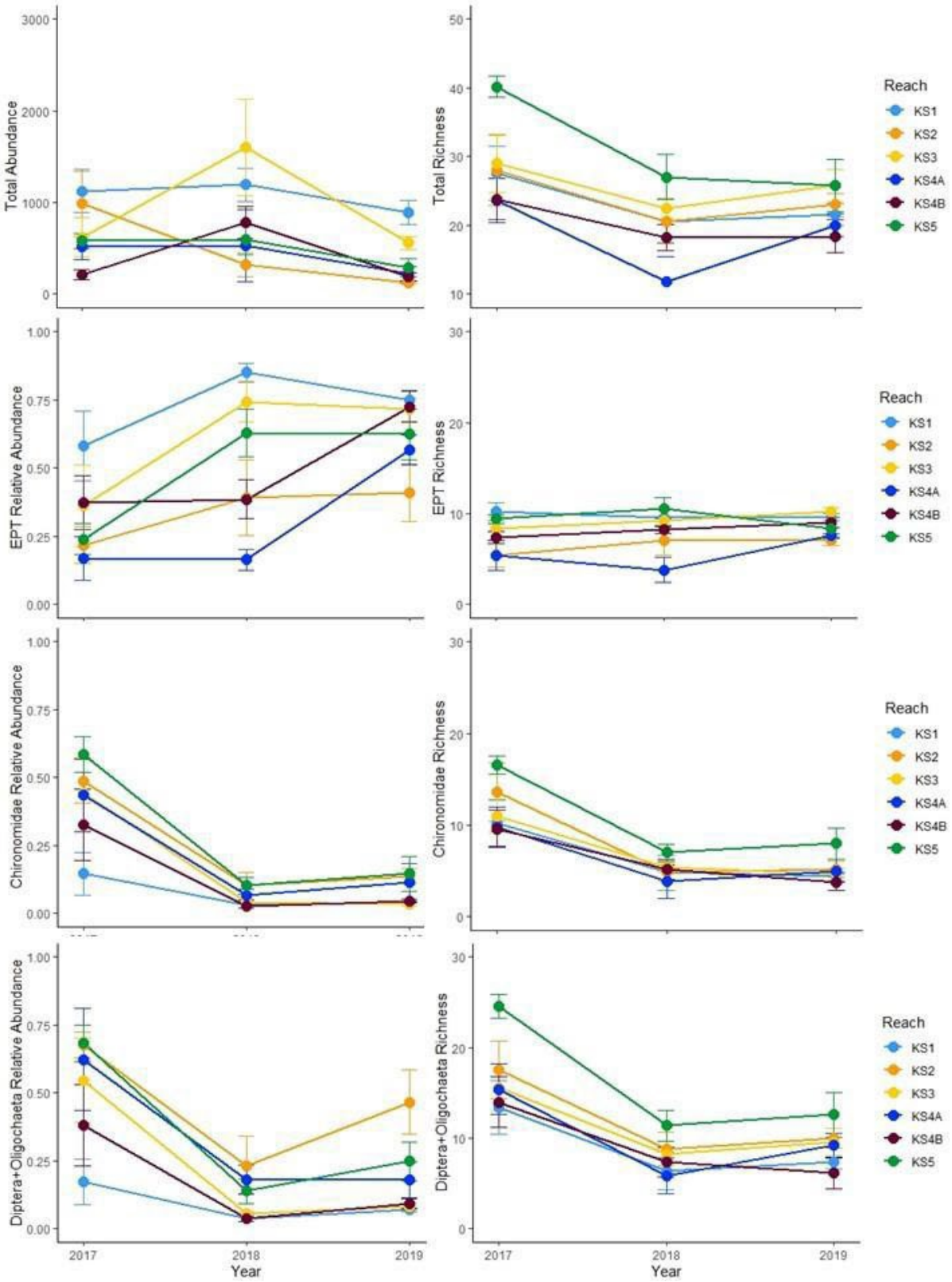


*Figure 35. Line plots of changes over time in biotic metrics in the Slave River, showing the mean ± SE for each reach in 2017, 2018, and 2019.*

increased with increasing velocity in all sites, but the increase occurred at a different rate depending on the year. The most shallow slope was in 2017 (smallest increase in abundance with increasing velocity among years). 2019 had a similar but steeper slope (larger increase in abundance with increasing velocity), and the slope of the relationship in 2018 was twice as steep as that observed in 2019. These results indicate that abundance increased more in response to site-specific differences in velocity in 2018, when the flow regime was more variable and sampling took place shortly after a peak in flow. In 2019, when water levels were higher but the hydrograph was generally more flat, the response of abundance to differences in velocity among sites was weaker and more similar to that observed in 2017.

The full ANCOVA model for total richness indicated that the interaction between year and velocity was not significant ($p = 0.578$), and the reduced model was used to compare mean richness across years. In the reduced model, the year term was significant ($F_{2,86} = 10.74$, $p < 0.001$) and Tukey's HSD indicated that mean richness across sites, while controlling for velocity, was significantly lower in 2018 than in 2017 ($p < 0.001$), and significantly lower in 2019 than in 2017 ($p = 0.001$). However, there were no significant differences in richness between 2018 and 2019. This result indicates that higher flows in 2018 and 2019 contributed to a decline in taxonomic richness across sites.

Because of the large changes observed in the relative abundance of Chironomidae between sampling years, ANCOVA was also run for this metric in the Slave River. The full ANCOVA model indicated that the interaction between year and velocity was not significant ($p = 0.330$), and the reduced model was used to compare Chironomidae relative abundance among years. In the reduced model, the year term was significant ($F_{2,86} = 41.42$, $p < 0.001$) and Tukey's HSD indicated that mean Chironomidae relative abundance across sites, while controlling for velocity, was significantly lower in 2018 and 2019 than it was in 2017 ($p < 0.001$ for both comparisons), whereas there was no significant difference between 2018 and 2019.

### 3.2.4. Normal range and CES

Variation among samples was used to create an initial estimate of the normal range of variability and set preliminary CES boundaries to trigger additional monitoring or management action if test samples are impaired (i.e., if they fall outside the range of natural variability). The normal range is commonly defined as the range within which 95% of samples fall, equivalent to two standard deviations from the mean in a normal distribution (Munkittrick et al. 2009). While it is possible for samples to fall outside the CES, there is a low probability (5% chance) of this happening if the sample is representative of the normal range. Thus, where sites have been exposed to anthropogenic impacts, samples outside of the CES may be an indication of impairment in a system. The normal range and CES is based on variability in the data, and changes in habitat conditions that result from natural variability (i.e., due to shifts in flow, timing of the spring freshet, water temperature, etc.) may affect the normal range from one year to the next. This idea is particularly relevant to the Slave River, where significant changes occurred between sampling years due to changes in the flow regime. With additional sampling, sites that were within the normal range in one year may fall outside the normal range in the next year if they are strongly affected by natural variability in the system. Three years of data represents the minimum time period over which CES can be estimated, but if conditions vary widely in those years, the normal range will be large and CES will not provide an accurate reflection of the limits outside of which management action should be triggered. Monitoring of assemblages over several years and refining normal range estimates can

therefore be used to get a better, more accurate estimate of the CES in a system that accounts for this natural variability.

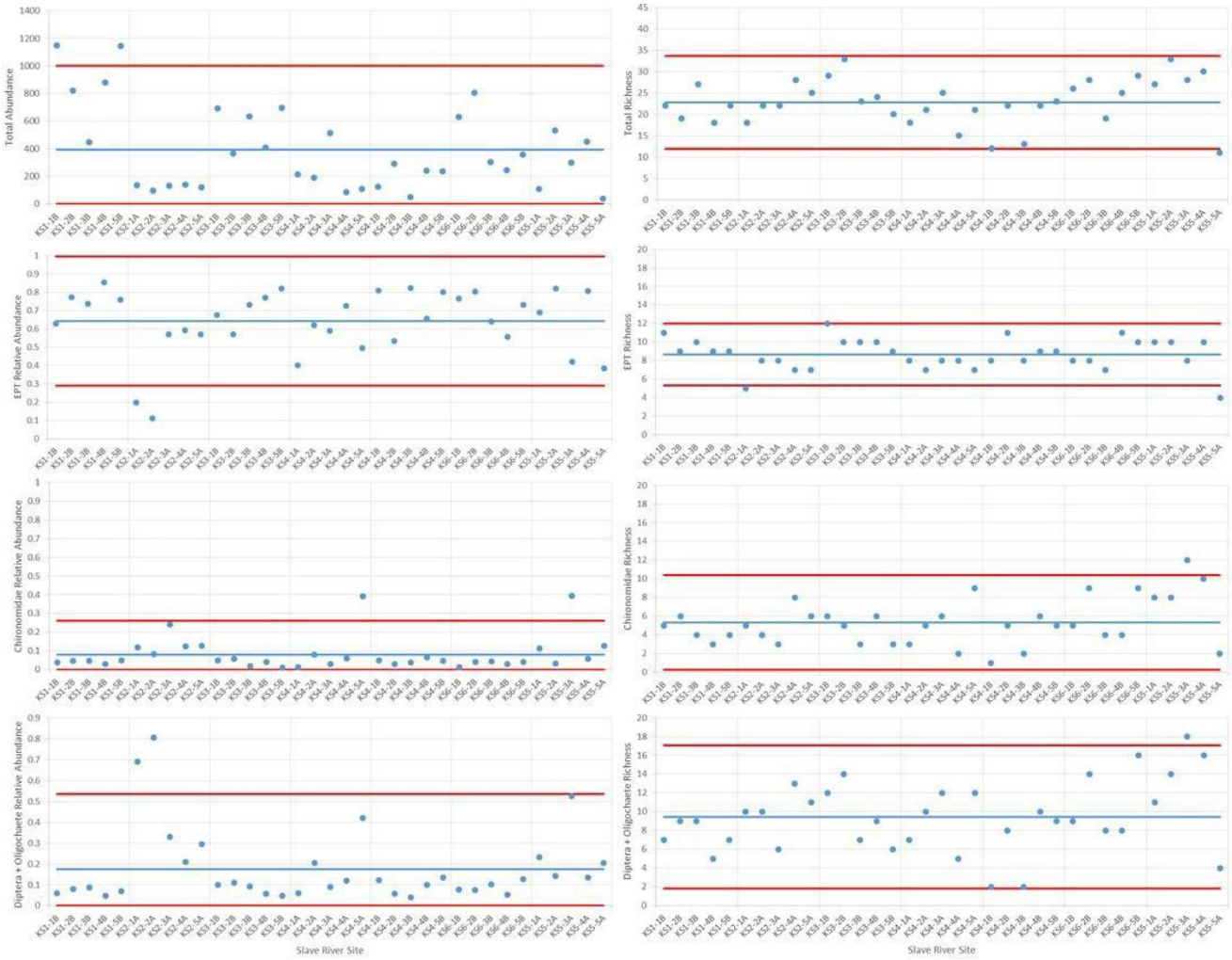


*Figure 36. Biotic metrics plotted for each site in the Slave River with the 2019 mean (blue line) and the upper and lower single-year critical effect size (CES; red lines), calculated as mean ± 2SD (calculated based on 2019 data). Each point represents a kick-site, moving from reach 1, site 1 (far left) to reach 5, site 5 (far right) on each plot. Metrics include (left column) total abundance, EPT relative abundance, Chironomidae relative abundance, Diptera + Oligochaeta relative abundance, and (right column) total taxonomic richness, EPT richness, Chironomidae richness, and Diptera + Oligochaeta richness.*

The analysis was used to quantify the normal range of variability (within-year and temporal) and critical effect size based on the BMI metrics total abundance, relative abundance of EPT, relative abundance of Chironomidae, relative abundance of Diptera + Oligchaeta, total taxonomic richness, richness of EPT, richness of Chironomidae, and richness of Diptera + Oligochaeta. As flow and BMI communities were quite different between 2017 and the last two years of sampling in the Slave River, the normal range was expected to cover a large range for most metrics.

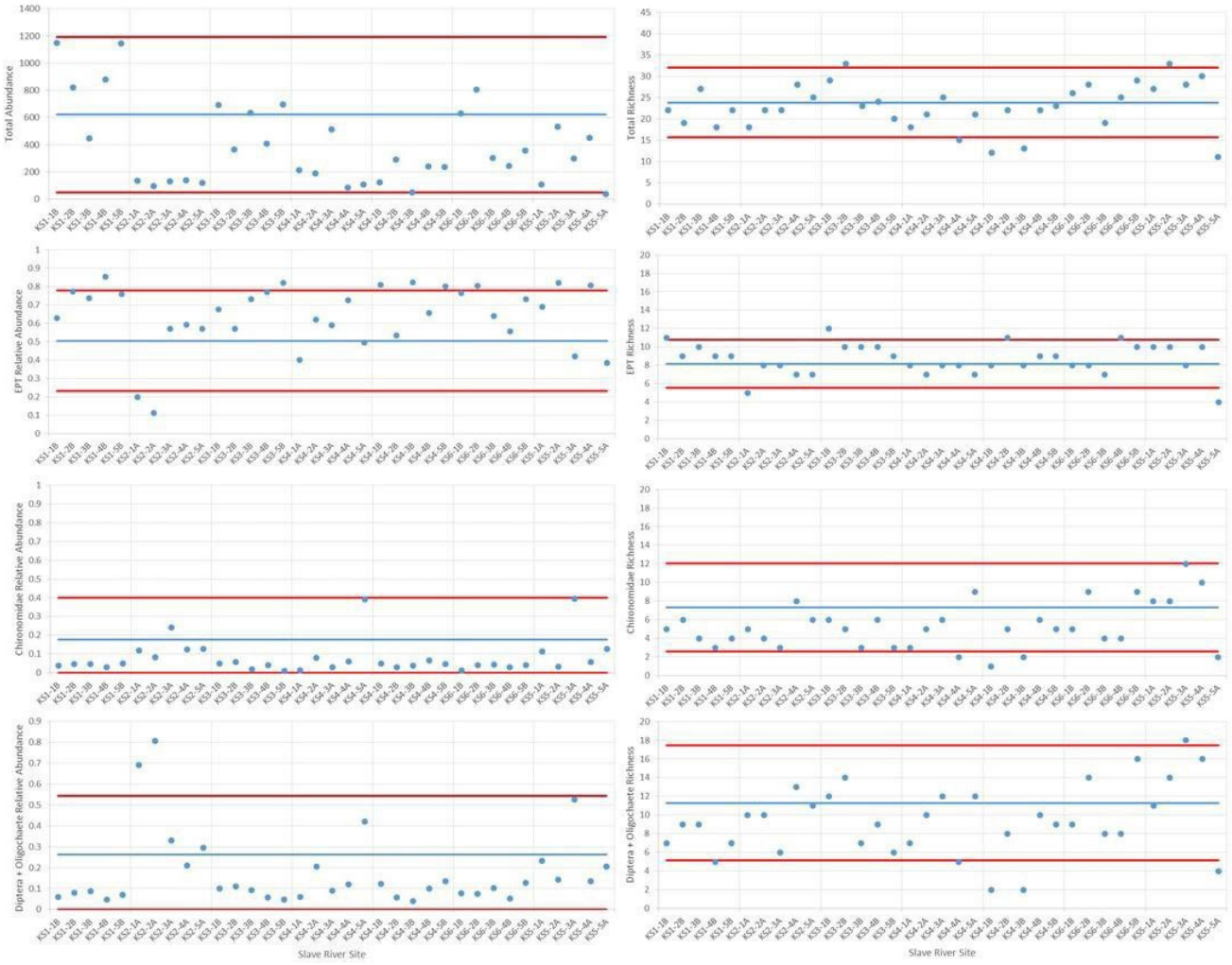


*Figure 37. Biotic metrics plotted for each site in the Slave River with a multi-year mean (mean of 2017-2019 data; blue line) and the upper and lower multi-year critical effect size (CES; red lines), calculated as mean ± 2SD (calculated based on 2017, 2018, and 2019 data). Each point represents a kick-site, moving from reach 1, site 1 (far left) to reach 6, site 5 (far right) on each plot. Metrics include (left column) total abundance, EPT relative abundance, Chironomidae relative abundance, Diptera + Oligochaeta relative abundance, and (right column) total taxonomic richness, EPT richness, Chironomidae richness, and Diptera + Oligochaeta richness.*

#### 3.2.4.1. *Within-year variability*

For the analysis of within-year variability, mean values of each metric and standard deviations across all sites were used to calculate two sets of within-year CES boundaries: the single-year CES, based on data from 2019 to identify any sites that appeared to be outliers in this year, and the multi-year CES, based on the mean and standard deviation of combined 2017-2019 data. Single-year and multi-year CES boundaries were compared with site data from 2019.

Samples collected in the Slave River in 2019 generally fell within the CES boundaries developed using only 2019 data (Figure 36). The relative abundance of EPT was below the lower CES boundary for sites

KS2-1A and KS2-2A, both of which were found to be outliers in other analyses of spatial variation in 2019 BMI data. In addition, the relative abundance of Diptera + Oligochaeta was above the upper CES for both of these sites (Figure 36). The relative abundance of Chironomidae was higher than the CES in two sites (KS4-5A and KS5-3A; Figure 36). There were fewer large deviations from normal range when richness metrics were considered. Richness of both Chironomidae and Diptera + Oligochaeta were above the upper CES in site KS5-3A (Figure 36). Richness was also found to be outside the single-year CES boundaries in KS2-1A (low EPT richness) and KS5-5A (low EPT richness and total richness).

More frequent deviations were apparent when metric data from 2019 were compared with the multi-year CES that was developed based on data from 2017-2019 (Figure 37). Some of the sites that were outside the single-year CES were also outside the boundaries of the multi-year CES. However, there were many more sites with high EPT relative abundance that was above CES, and total abundance and relative abundance of Chironomidae and Diptera + Oligochaeta were low for most sites, approaching the lower CES (Figure 37). Exceedances of CES reflected general patterns observed in the Slave River analysis for 2019, including declines in total abundance and increases in relative abundance of EPT relative to 2017. Several sites were also outside the multi-year CES boundaries for richness metrics, largely reflecting low total richness and richness of Chironomidae and Diptera + Oligochaeta in Reach 4A, Reach 4B, and Reach 5 (Figure 37).

#### *3.2.4.2. Among-year variability*

##### 3.2.4.2.1. Site-scale variability

Temporal variation at the site scale was assessed by comparing the 2017-2019 mean ± SE for each site with the normal range for the river, which was calculated as the grand mean for the river (mean of 2017, 2018, and 2019 means of all sites) ± 2SD. This analysis visualizes temporal variability within sites relative to temporal variability across all sites, and represents one way in which future data may be compared with the expected normal range in this system.

Annual means across all sites in the Slave River varied widely between 2017 and 2019, contributing to wide preliminary normal ranges for the river. For example, the preliminary CES boundaries for Diptera + Oligochaeta relative abundance covered a range of approximately 0.70 (i.e., an acceptable percent Diptera + Oligochaeta ranging from 0% to 70% of the sample; Figure 38). These wide estimates of normal range boundaries reflected the sharp decline in abundance of Chironomidae that was observed after 2017. Variation within sites was also high for several metrics (particularly abundance-based metrics), as evidenced by wide error bars, representing high temporal variability within a site (Figure 38). Though additional years of sample data would help to improve estimates of normal range for these metrics, an alternative option would be to develop two sets of normal range criteria for the river and the reaches: one based on data from 2017 and any additional sample years with similar flow levels (assuming that Chironomidae abundance returns to previous levels) and one based on samples collected in high flow years (including 2018 and 2019). The sharp contrasts in composition between years with differing flow regimes suggests that such an approach would improve the usefulness of normal range estimates by making them more narrow.

The initial estimate of the normal range of variability in site-scale analyses was more narrow for richness metrics, but did suffer from wide inter-annual variability in site means across the entire river. The exception was EPT richness, which had an extremely narrow preliminary normal range based on the

grand mean (Figure 38), but a number of sites fell outside the CES boundaries because the normal range was so narrow. Of the metrics tested for the Slave River, EPT richness appeared to have the greatest potential for developing monitoring and management triggers. However, additional years of data will be required to allow for the refinement of the CES range to better reflect inter-annual variability in this and other metrics.

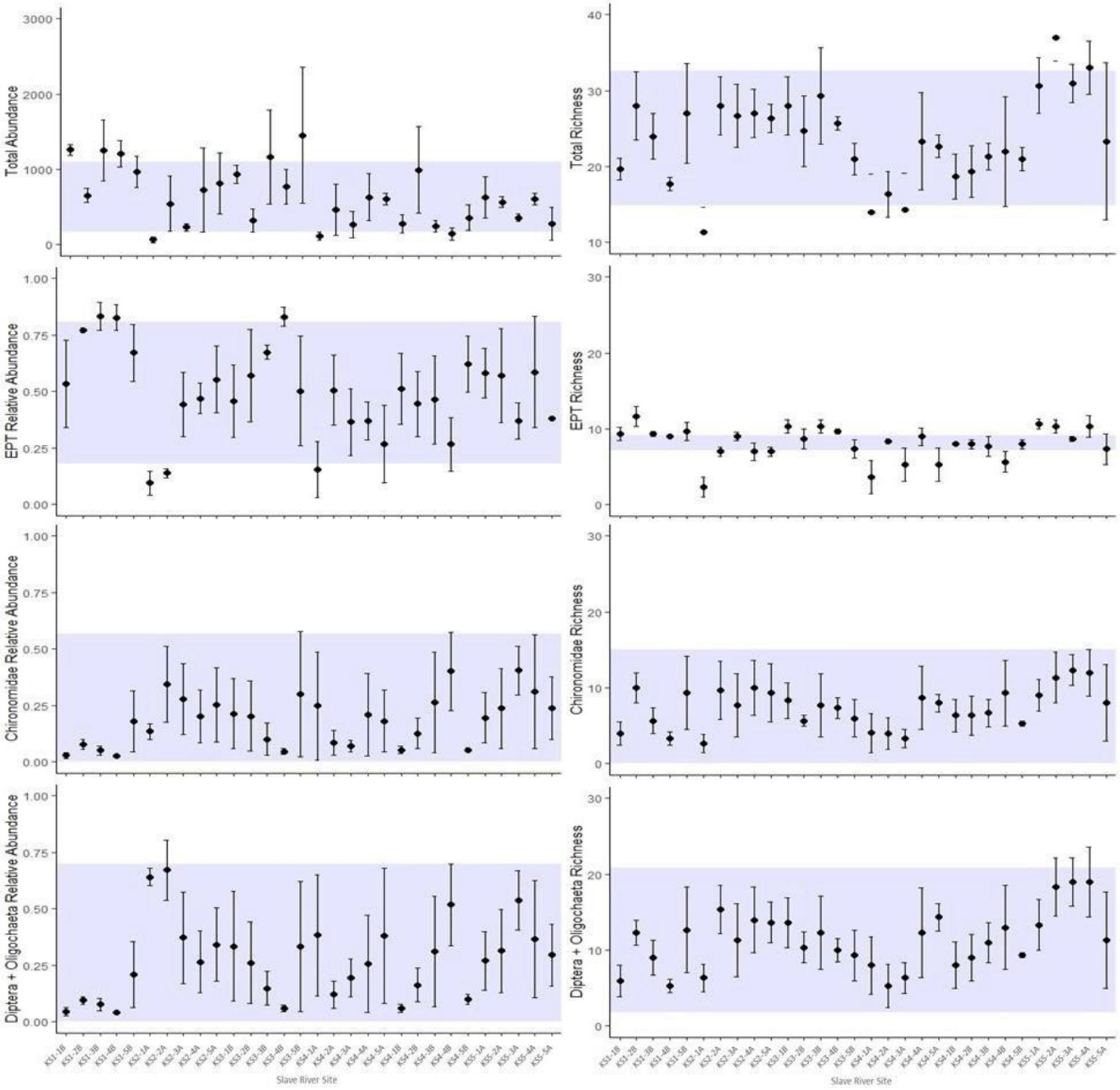


*Figure 38. Site-scale temporal variability in biotic metrics in the Slave River, showing mean ± SE for 2017-2019 for each site, with the grand mean (mean of annual means for the river) ± 2SD (normal range for the river) indicated by the shaded area. Metrics include (left, top to bottom) total abundance, EPT relative abundance, Chironomidae relative abundance, and Diptera + Oligochaeta relative abundance, and (right, top to bottom) total richness, EPT richness, Chironomidae richness, and Diptera + Oligochaeta richness.*

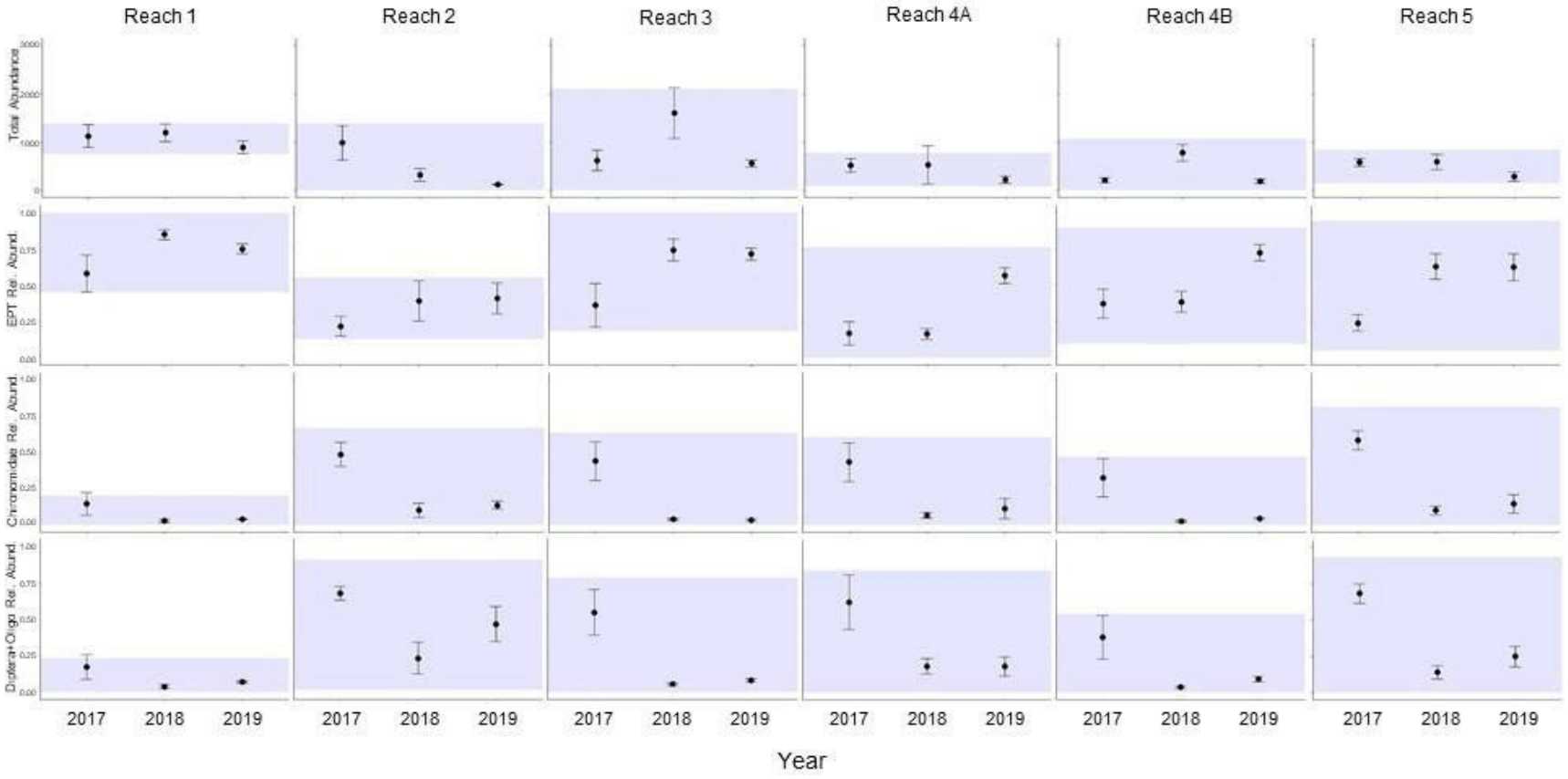


*Figure 39. Reach-scale temporal assessment of normal range and critical effect size for abundance-based metrics in the Slave River, including total abundance, relative abundance of EPT, relative abundance of Chironomidae, and relative abundance of Diptera + Oligochaeta. Points represent the mean ± SE across all sites in a reach, plotted for each year (2017, 2018, and 2019), and the shaded area represents the normal range and CES boundaries for that reach, calculated based on the grand mean (mean of annual means for the reach) ± 2 SD. Each column represents the data for a single reach.*

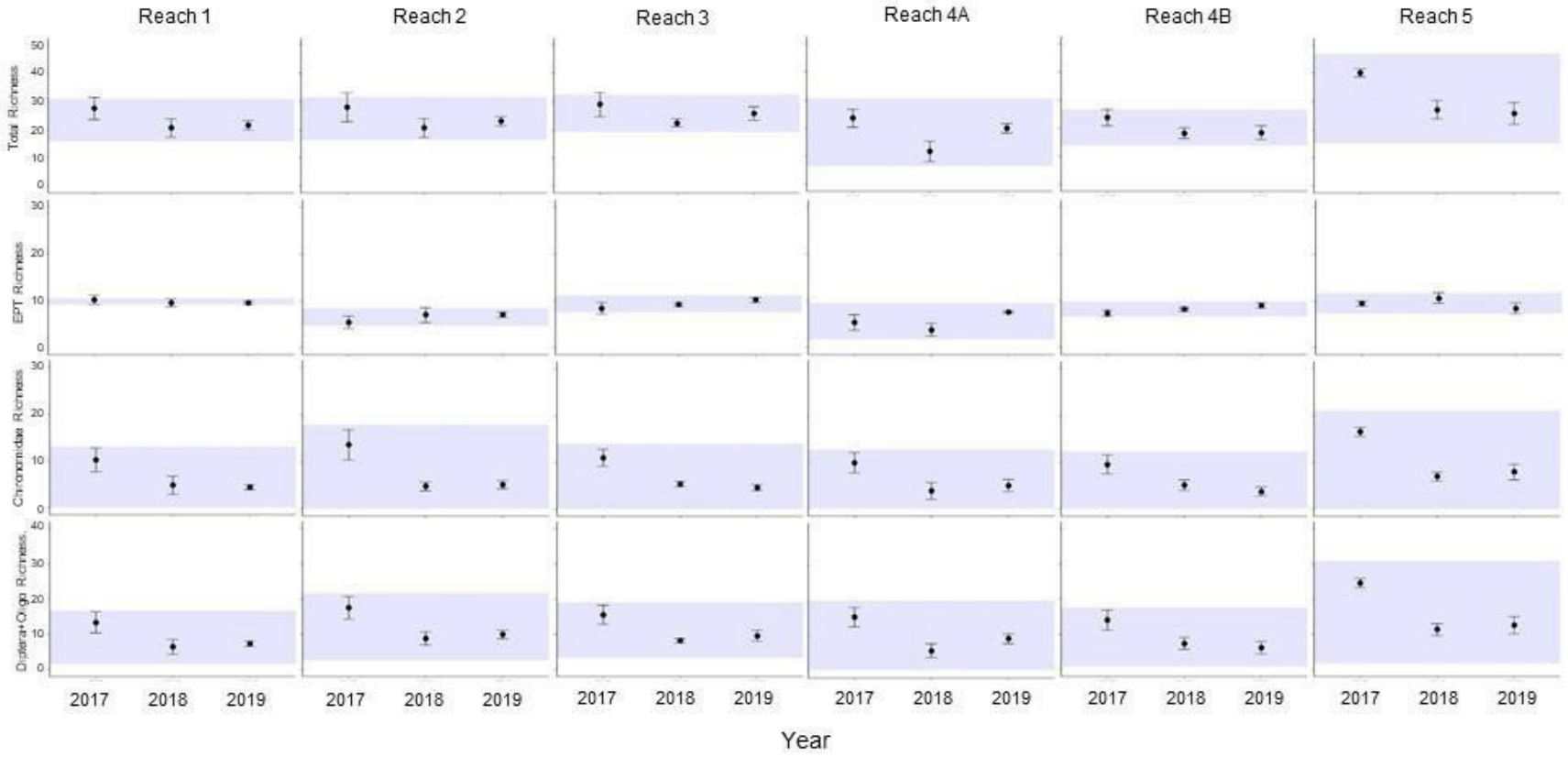


*Figure 40. Reach-scale temporal assessment of normal range and critical effect size for richness-based metrics in the Slave River, including total richness, EPT richness, Chironomidae richness, and Diptera + Oligochaeta richness. Points represent the mean ± SE across all sites in a reach, plotted for each year (2017, 2018, and 2019), and the shaded area represents the normal range and CES boundaries for that reach, calculated based on the grand mean (mean of annual means for the reach) ± 2 SD. Each column represents the data for a single reach.*

#### 3.2.4.2.2. Reach-scale variability

Temporal variability at the reach scale was quantified by estimating the reach-specific normal range and developing preliminary CES boundaries based on variability among years. The initial estimate of the normal range for each reach was calculated based on the grand mean (mean of annual means for the reach from 2017, 2018, and 2019) ± 2SD. Mean metric values ± SE for each reach in each year (averaged across sites, which are treated as replicates in this analysis) were compared with the calculated normal range. This approach develops location-specific CES that can be used in continued monitoring at each reach to identify samples that are unusual or outside the range of expected variability for within the reach. Initial evaluation of these boundaries focused on their width, as a normal range may not be useful for detecting future impairment if it encompasses too wide a range of possible values.

At the reach scale, the initial estimate of the normal range of variability was wide for most abundance-based metrics (Figure 39), reflecting the large changes in abundance and relative abundance over the three sampling years in the Slave River. The width of preliminary CES boundaries was extreme for the relative abundance of EPT and relative abundance of Diptera + Oligochaeta in many reaches. For example, CES boundaries for these two metrics in Reach 5 covered nearly the entire range of possible values (Figure 39), indicating that these metrics would have no ability to detect potential impact in future sampling years. Similarly wide and all-encompassing preliminary ranges were evident in several other reaches, indicating low diagnostic power of abundance-based metrics in the Slave River reaches. Reach 1 had the most narrow normal range of variability across abundance metrics due to its relative invariability among years. This is further support for the use of reach-specific normal ranges and CES, and data for this reach will be important in future years to ensure the normal range is refined and made more precise.

The initial estimate of the normal range of variability was more narrow for richness-based metrics, reflecting weaker temporal variability in these metrics. In particular, EPT richness had extremely low variability within reaches and among years, contributing to narrow CES boundaries (particularly in Reach 1; Figure 40). Total richness also had fairly low variability in several reaches (with the exception of Reach 4A and Reach 5; Figure 40). Although the normal range for Chironomidae richness and Diptera + Oligochaeta richness were narrower than those for abundance-based metrics, the lower CES was 0 or close to 0 in most reaches, which would not provide good diagnostic power to detect potential impairment. The lower CES for these metrics was at or near 0 because high flow years (2018 and 2019) had extremely low abundance and richness of Chironomidae in particular, and development of separate CES for high flow and low flow years may aid in improving the diagnostic capabilities of these metrics.

# 4. Recommendations and Conclusions

This report summarizes spatial and temporal patterns in BMI assemblages and supporting variables in the Hay and Slave River, and it provides the first test of site- and reach-specific normal range and CES development using temporal variability. As the normal range is refined for different metrics, the diagnostic power of this approach will become evident, but in the initial years of sampling, the normal range is highly susceptible to inter-annual variation. Arciszewski and Munkittrick (2015) noted that 12 years of data may be necessary to develop accurate and precise normal range estimates, based on their work with fish assemblages, but such development is further hampered when there is high inter-annual variability in flow. Abundance and richness of BMI were both shown to respond to site-specific

differences in flow velocity, and extreme variation in flow regimes among years (including differences in the magnitude and variation of discharge, water level, and peak flow, as well as differences in the timing of peak flow relative to sampling events) appeared to have strong effects on BMI assemblage composition.

Variability in flow appeared to be the dominant driver of biotic change in the Hay and Slave Rivers, and the findings of this report indicate that stronger consideration of flow regimes is necessary as this sampling program proceeds. For example, choice of sampling dates must be made primarily based on current hydrographs, so sampling shortly following a peak in flow can be avoided if possible. The remote nature of this work does require significant pre-planning and scheduling, and re-scheduling due to highly variable flow can be difficult, but some flexibility will be required to ensure data are not affected by antecedent hydrological conditions.

Reach-specific CES calculations in this report provide an initial estimate of the normal range for each metric, and it will be important to use additional years of data to improve the precision of these boundaries. But the development of flow-specific normal ranges should be considered, particularly for the Slave River. The change in abundance of Chironomidae with increased flow in this river was so large that abundance-based metrics lacked diagnostic power because they covered too wide a range of possible values. If the data were split into those that were collected during high flow years (2018 and 2019) and those collected during lower flow years (2017), additional sample data could contribute to the development of CES boundaries that better reflect hydrologic influences. Such an approach would require a more in-depth assessment of hydrology within the Slave River system, to define low flow, moderate flow, and high flow conditions based on historical data. This can be accomplished using Indicators of Hydrologic Alteration (IHA) metrics, which quantify measures such as the frequency and duration of extreme hydrologic events and variability in timing and magnitude of flow events through the year (Gao et al. 2009). Scenario projections of future flows could also be utilized to examine how flows are predicted to change in the Slave and Hay River basins, and assess what such changes might mean for the normal range of variability in BMI metrics. In addition, flow-based metrics of BMI composition (e.g., CEFI; Monk et al. 2008, Monk et al. 2018) could be applied to aid in the characterization of BMI response to flow in these systems and the prediction of expected changes to composition with future flows. This strategy will allow for the classification of data in future years based on flow condition, and comparison of BMI monitoring data with appropriate normal range conditions. Samples collected in 2020 can be used in combination with the 2017-2019 samples and historical flow data for the rivers to begin to explore flow-based development of assessment criteria.

# 5. References


Anderson, M.J. 2017. Permutational Multivariate Analysis of Variance (PERMANOVA). Wiley StatsRef: Statistics Reference Online: 1-15. doi: 10.1002/9781118445112.stat07841.

Anderson, M.J., Ellingsen, K.E., and McArdle, B.H. 2006. Multivariate dispersion as a measure of beta diversity. Ecol. Lett. **9**: 683-693.

Arciszewski, T.J., and Munkittrick, K.R. 2015. Development of an adaptive monitoring framework for long-term programs: An example using indicators of fish health. Integrated environmental assessment and management **11**(4): 701-718.

Arciszewski, T.J., Munkittrick, K.R., Scrimgeour, G.J., Dubé, M.G., Wrona, F.J., and Hazewinkel, R.R. 2017. Using adaptive processes and adverse outcome pathways to develop meaningful, robust, and

actionable environmental monitoring programs. Integrated environmental assessment and management **13**(5): 877-891.

Barbour, M.T., Gerritsen, J., Snyder, B.D., and Stribling, J.B. 1999. Rapid bioassessment protocols for use in streams and wadeable rivers: periphyton, benthic macroinvertebrates, and fish. Second edition. Technical Report EPA 841-B-99-002, US Environmental Protection Agency, Office of Water, Washington, DC. 337 p.

Benjamini, Y., and Hochberg, Y. 1995. Controlling the false discovery rate: a practical and powerful approach to multiple testing. J. Roy. Stat. Soc. B Met. **57**(1): 289-300.

Bonada, N., Prat, N., Resh, V.H., and Statzner, B. 2006. Developments in aquatic insect biomonitoring: a comparative analysis of recent approaches. Annu. Rev. Entomol. **51**: 495-523.

Buss, D.F., Carlisle, D.M., Chon, T.-S., Culp, J., Harding, J.S., Keizer-Vlek, H.E., Robinson, W.A., Strachan, S., Thirion, C., and Hughes, R.M. 2015. Stream biomonitoring using macroinvertebrates around the globe: a comparison of large-scale programs. Environ. Monit. Assess. **187**(1): 4132.

Canadian Council of Ministers of the Environment. 2001a. Canadian sediment quality guidelines for the protection of aquatic life. *In* Canadian Environmental Quality Guidelines, 1999. Canadian Council of Ministers of the Environment, Winnipeg, MB, Canada.

Canadian Council of Ministers of the Environment. 2001b. Canadian water quality guidelines for the protection of aquatic life. *In* Canadian Environmental Quality Guidelines, 1999. Canadian Council of Ministers of the Environment, Winnipeg.

Canadian Council of Ministers of the Environment. 2010. Canadian soil quality guidelines for the protection of environmental and human health: Polycyclic Aromatic Hydrocarbons. *In* Canadian Environmental Quality Guidelines, 1999. Canadian Council of Ministers of the Environment, Winnipeg, MB, Canada.

Culp, J.M., Lento, J., Curry, R.A., Luiker, E., and Halliwell, D. 2019. Arctic biodiversity of stream macroinvertebrates declines in response to latitudinal change in the abiotic template. Freshwater Science **38**(3): 465-479. doi: 10.1086/704887.

Culp, J.M., Lento, J., Goedkoop, W., Power, M., Rautio, M., Christoffersen, K.S., Guðbergsson, G., Lau, D., Liljaniemi, P., Sandøy, S., and Svoboda, M. 2012a. Developing a circumpolar monitoring framework for Arctic freshwater biodiversity. Biodiversity **13**(3-4): 215-227.

Culp, J.M., Glozier, N.E., Baird, D.J., Wrona, F.J., Brua, R.B., Ritcey, A.L., Peters, D.L., Casey, R., Choung, C.B., Curry, C.J., Halliwell, D., Keet, E., Kilgour, B., Kirk, J., Lento, J., Luiker, E., and Suzanne, C. 2018. Assessing ecosystem health in benthic macroinvertebrate assemblages of the Athabasca River mainstem, tributaries and Peace-Athabasca delta. Oil Sands Monitoring Program Technical Report Series No 1.7, Alberta Government. 82 p.

Culp, J.M., Goedkoop, W., Lento, J., Christoffersen, K.S., Frenzel, S., Guðbergsson, G., Liljaniemi, P., Sandøy, S., Svoboda, M., Brittain, J., Hammar, J., Jacobsen, D., Jones, B., Juillet, C., Kahlert, M., Kidd, K., Luiker, E., Olafsson, J., Power, M., Rautio, M., Ritcey, A., Striegle, R., Svenning, M., Sweetman, J., and Whitman, M. 2012b. The Arctic Freshwater Biodiversity Monitoring Plan. CAFF Monitoring Series Report Nr. 7, CAFF International Secretariat.p.

Dagg, J. 2016. Vulnerability Assessment of the Slave River and Delta. Summary report for the Community Workshop convened in Fort Smith, January 24-26, 2012, The Pembina Institute. 56 p.

Dubé, M.G. 2003. Cumulative effect assessment in Canada: a regional framework for aquatic ecosystems. Environmental Impact Assessment Review **23**(6): 723-745.

Dubé, M.G., Duinker, P., Greig, L., Carver, M., Servos, M., McMaster, M., Noble, B., Schreier, H., Jackson, L., and Munkittrick, K.R. 2013. A framework for assessing cumulative effects in watersheds: an introduction to Canadian case studies. Integrated environmental assessment and management **9**(3): 363-369.

Environment Canada. (ed.) 2011. Integrated monitoring plan for the oil sands: expanded geographic extent for water quality and quantity, aquatic biodiversity and effects, and acid sensitive lake component. EN14-49/2011E-PDF, Environment Canada, Gatineau, QC, Canada.

Environment Canada. 2012. Canadian Aquatic Biomonitoring Network Field Manual - Wadeable Streams. Dartmouth, NS, Canada, Government of Canada Publications. 57 p.

Environment Canada. 2014. Canadian Aquatic Biomonitoring Network Laboratory Methods: processing, taxonomy, and quality control of benthic macroinvertebrate samples. Dartmouth, NS, Canada, Government of Canada Publications. 36 p.

Flotemersch, J., Stribling, J., Hughes, R., Reynolds, L., Paul, M., and Wolter, C. 2011. Site length for biological assessment of boatable rivers. River Res. Applic. **27**(4): 520-535.

Gao, Y., Vogel, R.M., Kroll, C.N., Poff, N.L., and Olden, J.D. 2009. Development of representative indicators of hydrologic alteration. J. Hydrol. **374**(1-2): 136-147.

Glozier, N.E., Donald, D.B., Crosley, R.W., and Halliwell, D. 2009. Wood Buffalo National Park water quality: status and trends from 1989-2006 in three major rivers: Athabasca, Peace and Slave. Environment Canada, Environment and Climate Change Canada. 104 p.

Golder Associates. 2010. Aquatic Ecosystem Health - Report on State of Knowledge. Final Report prepared for the Government of the Northwest Territories. Report number 09-1328-0036. 93 pp.

Jackson, J.K., and Füreder, L. 2006. Long-term studies of freshwater macroinvertebrates: a review of the frequency, duration and ecological significance. Freshwater Biol. **51**(3): 591-603. doi: 10.1111/j.1365-2427.2006.01503.x.

Kilgour, B.W., Somers, K.M., Barrett, T.J., Munkittrick, K.R., and Francis, A.P. 2017. Testing against "normal" with environmental data. Integrated environmental assessment and management **13**(1): 188-197.

Lento, J. 2017. Review and development of recommendations on monitoring and assessment protocols for benthic macroinvertebrate communities in transboundary rivers. Report prepared for the Government of the Northwest Territories. Prepared for the Government of the Northwest Territories. 23 p.

Lento, J. 2018. Benthic macroinvertebrate monitoring plan for the transboundary rivers of the Northwest Territories. Report prepared for the Government of the Northwest Territories. 20 pp.

Lento, J. 2020. Benthic macroinvertebrate monitoring plan for large transboundary rivers in the Alberta-Northwest Territories region: Assessment of results from the second year of sampling (2018). Report prepared for the Alberta-Northwest Territories Bilateral Management Committee, Government of Alberta, and Government of the Northwest Territories, Government of Northwest Territories. 103 p.

Lento, J., Monk, W.A., Culp, J.M., Curry, R.A., Cote, D., and Luiker, E. 2013. Responses of low Arctic stream benthic macroinvertebrate communities to environmental drivers at nested spatial scales. Arctic, Antarctic, and Alpine Research **45**(4): 538-551.

Lento, J., Goedkoop, W., Culp, J., Christoffersen, K., Fefilova, E., Guðbergsson, G., Liljaniemi, P., Ólafsson, J.S., Sandøy, S., Zimmerman, C., Christensen, T., Chambers, P., Heino, J., Hellsten, S., Kahlert, M., Keck, F., Laske, S., Lau, D.C.P., Lavoie, I., Levenstein, B., Mariash, H., Rühland, K., Saulnier-Talbot, E., Schartau, A.K., and Svenning, M. 2019. State of the Arctic Freshwater Biodiversity Report. Conservation of Arctic Flora and Fauna (CAFF) International Secretariat. 124 p.

MacDonald Environmental Sciences Ltd. 1995. Expert's Workshop on the Development of Ecosystem Maintenance Indicators for the Transboundary River Systems within the Mackenzie River Basin: Workshop Summary Report. Government of the Northwest Territories. 56 p.

Martinez Arbizu, P. 2020. pairwiseAdonis: Pairwise multilevel comparison using adonis. (R package version 0.4).

McArdle, B.H., and Anderson, M.J. 2001. Fitting multivariate models to community data: a comment on distance-based redundancy analysis. Ecology **82**(1): 290-297. doi: https://doi.org/10.1890/0012-9658(2001)082[0290:FMMTCD]2.0.CO;2.

McCafferty, W.P. 1998. Aquatic Entomology: The Fisherman's and Ecologist's Illustrated Guide to Insects and Their Relatives. Jones & Bartlett Publishers.

Monk, W.A., Wood, P.J., Hannah, D.M., and Wilson, D.A. 2008. Macroinvertebrate community response to inter-annual and regional river flow regime dynamics. River Res. Applic. **24**(7): 988-1001.

Monk, W.A., Compson, Z.G., Armanini, D.G., Orlofske, J.M., Curry, C.J., Peters, D.L., Crocker, J.B., and Baird, D.J. 2018. Flow velocity–ecology thresholds in Canadian rivers: A comparison of trait and taxonomy-based approaches. Freshwater Biol. **63**(8): 891-905.

Munkittrick, K.R., and Arciszewski, T.J. 2017. Using normal ranges for interpreting results of monitoring and tiering to guide future work: A case study of increasing polycyclic aromatic compounds in lake sediments from the Cold Lake oil sands (Alberta, Canada) described in Korosi et al. (2016). Environ. Pollut. **231**: 1215-1222.

Munkittrick, K.R., Arens, C.J., Lowell, R.B., and Kaminski, G.P. 2009. A review of potential methods of determining critical effect size for designing environmental monitoring programs. Environmental Toxicology and Chemistry **28**(7): 1361-1371.

Ohiozebau, E., Tendler, B., Codling, G., Kelly, E., Giesy, J.P., and Jones, P.D. 2017. Potential health risks posed by polycyclic aromatic hydrocarbons in muscle tissues of fishes from the Athabasca and Slave Rivers, Canada. Environmental geochemistry and health **39**(1): 139-160.

Ohiozebau, E., Tendler, B., Hill, A., Codling, G., Kelly, E., Giesy, J.P., and Jones, P.D. 2016. Products of biotransformation of polycyclic aromatic hydrocarbons in fishes of the Athabasca/Slave River system, Canada. Environmental geochemistry and health **38**(2): 577-591.

Oksanen, J., Blanchet, F.G., Kindt, R., Legendre, P., Minchin, P.R., O'Hara, R.B., Simpson, G.L., Solymos, P., Stevens, M.H.H., and Wagner, H. 2015. Vegan: Community Ecology Package (R package version 2.3-2). Available from https://CRAN.R-project.org/package=vegan.

Paterson, M., Lawrence, M., and Sekerak, A. 1991. Benthic Invertebrates and Biomonitoring in the Slave River, N.W.T.: A Pilot Study. Report for the Slave River Environmental Quality Monitoring Program. 164 p.

Paterson, M., Lawrence, M., and Sekerak, A. 1992. Benthic Invertebrates and Biomonitoring in the Slave River, N.W.T.: 1991 Survey. Report for the Slave River Environmental Quality Monitoring Program. 59 p.

Pembina Institute. 2016. State of the Knowledge of the Slave River and Slave River Delta. Prepared for the Slave River and Delta Partnership. 124 p.

R Development Core Team 2015. R: A Language and Environment for Statistical Computing. R Foundation for Statistical Computing, Vienna, Austria. Available from http://www.R-project.org. ISBN 3-900051-07-0

Rabodonirina, S., Net, S., Ouddane, B., Merhaby, D., Dumoulin, D., Popescu, T., and Ravelonandro, P. 2015. Distribution of persistent organic pollutants (PAHs, Me-PAHs, PCBs) in dissolved, particulate and sedimentary phases in freshwater systems. Environ. Pollut. **206**: 38-48.

Resh, V.H. 2008. Which group is best? Attributes of different biological assemblages used in freshwater biomonitoring programs. Environ. Monit. Assess. **138**: 131-138.

Sanderson, J., Czarnecki, A., and Faria, D. 2012. Water and Suspended Sediment Quality of the Transboundary Reach of the Slave River, Northwest Territories. Aboriginal Affairs and Northern Development Canada. 415 p.

Somers, K.M., Kilgour, B.W., Munkittrick, K.R., and Arciszewski, T.J. 2018. An adaptive environmental effects monitoring framework for assessing the influences of liquid effluents on benthos, water

and sediments in aquatic receiving environments. Integrated environmental assessment and management.
Stantec Consulting Ltd. 2016. State of Aquatic Knowledge for the Hay River Basin. Report prepared for the Government of the Northwest Territories, Department of Environment and Natural Resources, Government of the Northwest Territories. 285 p.
Stoddard, J.L., Larsen, D.P., Hawkins, C.P., Johnson, R.K., and Norris, R.H. 2006. Setting expectations for the ecological condition of streams: the concept of reference condition. Ecol. Appl. **16**(4): 1267-1276.
ter Braak, C.J.F., and Šmilauer, P. 2002. Reference Manual and User's Guide to CANOCO for Windows (version 4.5). Center for Biometry, Wageningen.
Zar, J.H. 1999. Biostatistical Analysis. Prentice-Hall, Inc., Upper Saddle River, NJ.

# 6. Appendices

*Table 16 Names and coordinates of kick-sampling sites sampled in the Hay River and Slave River in 2019.*

| River | Reach | Site | Latitude | Longitude | Date |
|---|---|---|---|---|---|
| HAY RIVER | REACH 1 | HR-KS1-1A | 59.93403 | -116.95028 | 2019-08-13 |
| | | HR-KS1-2A | 59.93591 | -116.95175 | 2019-08-13 |
| | | HR-KS1-3A | 59.93211 | -116.95237 | 2019-08-13 |
| | | HR-KS1-4A | 59.93135 | -116.95506 | 2019-08-13 |
| | | HR-KS1-5A | 59.93124 | -116.95613 | 2019-08-13 |
| | REACH 2 | HR-KS2-1A | 59.94548 | -116.95565 | 2019-08-13 |
| | | HR-KS2-2A | 59.94617 | -116.95618 | 2019-08-13 |
| | | HR-KS2-3A | 59.94654 | -116.95647 | 2019-08-13 |
| | | HR-KS2-4A | 59.94703 | -116.95702 | 2019-08-13 |
| | | HR-KS2-5A | 59.94759 | -116.95744 | 2019-08-13 |
| | REACH 3 | HR-KS3-1A | 59.98767 | -116.93236 | 2019-08-15 |
| | | HR-KS3-2A | 59.98827 | -116.93060 | 2019-08-15 |
| | | HR-KS3-3A | 59.98845 | -116.93037 | 2019-08-15 |
| | | HR-KS3-4A | 59.99023 | -116.93049 | 2019-08-15 |
| | | HR-KS3-5A | 59.99182 | -116.93127 | 2019-08-15 |
| | REACH 4 | HR-KS4-1A | 60.00158 | -116.97036 | 2019-08-15 |
| | | HR-KS4-2A | 60.00205 | -116.97145 | 2019-08-15 |
| | | HR-KS4-3A | 60.00261 | -116.97126 | 2019-08-15 |
| | | HR-KS4-4A | 60.00308 | -116.97089 | 2019-08-15 |
| | | HR-KS4-5A | 60.00319 | -116.97009 | 2019-08-15 |
| | REACH 5 | HR-KS5-1B | 60.01064 | -116.92032 | 2019-08-14 |
| | | HR-KS5-2B | 60.01096 | -116.92088 | 2019-08-14 |
| | | HR-KS5-3B | 60.01125 | -116.92177 | 2019-08-14 |
| | | HR-KS5-4B | 60.01138 | -116.92274 | 2019-08-14 |
| | | HR-KS5-5B | 60.01163 | -116.92348 | 2019-08-14 |
| | REACH 6 | HR-KS6-1B | 60.02772 | -116.92342 | 2019-08-14 |
| | | HR-KS6-2B | 60.02779 | -116.92217 | 2019-08-14 |
| | | HR-KS6-3B | 60.02785 | -116.92155 | 2019-08-14 |
| | | HR-KS6-4B | 60.02787 | -116.92075 | 2019-08-14 |
| | | HR-KS6-5B | 60.02802 | -116.91985 | 2019-08-14 |

| River | Reach | Site | Latitude | Longitude | Date |
|---|---|---|---|---|---|
| SLAVE RIVER | REACH 1 | SR-KS1-1B | 59.40805 | -111.46321 | 2019-09-13 |
| | | SR-KS1-2B | 59.40805 | -111.46321 | 2019-09-13 |
| | | SR-KS1-3B | 59.40846 | -111.46196 | 2019-09-13 |
| | | SR-KS1-4B | 59.40879 | -111.46082 | 2019-09-13 |
| | | SR-KS1-5B | 59.40913 | -111.45985 | 2019-09-13 |
| | REACH 2 | SR-KS2-1A | 59.42689 | -111.46155 | 2019-09-13 |
| | | SR-KS2-2A | 59.42709 | -111.46199 | 2019-09-13 |
| | | SR-KS2-3A | 59.42761 | -111.46294 | 2019-09-13 |
| | | SR-KS2-4A | 59.42799 | -111.46361 | 2019-09-13 |
| | | SR-KS2-5A | 59.42858 | -111.46458 | 2019-09-13 |
| | REACH 3 | SR-KS3-1B | 59.53395 | -111.45934 | 2019-09-14 |
| | | SR-KS3-2B | 59.53451 | -111.45864 | 2019-09-14 |
| | | SR-KS3-3B | 59.53502 | -111.45774 | 2019-09-14 |
| | | SR-KS3-4B | 59.53538 | -111.45703 | 2019-09-14 |
| | | SR-KS3-5B | 59.53562 | -111.45651 | 2019-09-14 |
| | REACH 4A | SR-KS4-1A | 59.58906 | -111.41968 | 2019-09-15 |
| | | SR-KS4-2A | 59.58947 | -111.4196 | 2019-09-15 |
| | | SR-KS4-3A | 59.59122 | -111.41951 | 2019-09-15 |
| | | SR-KS4-4A | 59.59178 | -111.41949 | 2019-09-15 |
| | | SR-KS4-5A | 59.59225 | -111.41946 | 2019-09-15 |
| | REACH 4B | SR-KS4-1B | 59.58887 | -111.42283 | 2019-09-14 |
| | | SR-KS4-2B | 59.58975 | -111.42273 | 2019-09-14 |
| | | SR-KS4-3B | 59.58995 | -111.42268 | 2019-09-14 |
| | | SR-KS4-4B | 59.5909 | -111.42261 | 2019-09-14 |
| | | SR-KS4-5B | 59.59139 | -111.42264 | 2019-09-14 |
| | REACH 6 | SR-KS6-1B | 60.02772 | -116.92342 | 2019-09-12 |
| | | SR-KS6-2B | 60.02779 | -116.92217 | 2019-09-12 |
| | | SR-KS6-3B | 60.02785 | -116.92155 | 2019-09-12 |
| | | SR-KS6-4B | 60.02787 | -116.92075 | 2019-09-12 |
| | | SR-KS6-5B | 60.02802 | -116.91985 | 2019-09-12 |
| | REACH 5 | SR-KS5-1A | 59.71284 | -111.50644 | 2019-09-12 |
| | | SR-KS5-2A | 59.71304 | -111.50646 | 2019-09-12 |
| | | SR-KS5-3A | 59.71823 | -111.50577 | 2019-09-12 |
| | | SR-KS5-4A | 59.71853 | -111.50594 | 2019-09-12 |
| | | SR-KS5-5A | 59.7187 | -111.50603 | 2019-09-12 |

*Table 17 BMI names and abbreviations used in PCA ordinations.*

| Order/Group | Family | Subfamily | Code |
|---|---|---|---|
| Amphipoda | | | AMPH |
| Bivalvia | Pisidiidae | | PISID |
| Coleoptera | Elmidae | | C_Elm |
| Diptera | Ceratopogonidae | | D_Cerat |
| Diptera | Chironomidae | Chironominae | D_C_Chir |
| Diptera | Chironomidae | Diamesinae | D_C_Dia |
| Diptera | Chironomidae | Orthocladiinae | D_C_Orth |
| Diptera | Chironomidae | Prodiamesinae | D_C_Pro |
| Diptera | Chironomidae | Tanypodinae | D_C_Tany |
| Diptera | Diptera Pupa | | D_Pupa |
| Diptera | Empididae | | D_Emp |
| Diptera | Simuliidae | | D_Simu |
| Diptera | Tabanidae | | D_Tab |
| Diptera | Tipulidae | | D_Tipu |
| Ephemeroptera | Acanthametropodidae | | E_Acan |
| Ephemeroptera | Ameletidae | | E_Amel |
| Ephemeroptera | Ametropodidae | | E_Amet |
| Ephemeroptera | Baetidae | | E_Bae |
| Ephemeroptera | Caenidae | | E_Cae |
| Ephemeroptera | Ephemerellidae | | E_Ephe |
| Ephemeroptera | Ephemeridae | | E_Eph |
| Ephemeroptera | Heptageniidae | | E_Hept |
| Ephemeroptera | Isonychiidae | | E_Iso |
| Ephemeroptera | Leptophlebiidae | | E_Lept |
| Ephemeroptera | Metretopodidae | | E_Met |
| Gastropoda | | | GAST |
| Hemiptera | Corixidae | | H_Corix |
| Hirudinea | Glossiphoniidae | | GLOSS |
| Odonata | Aeshnidae | | O_Aesh |
| Odonata | Gomphidae | | O_Gomph |
| Oligochaeta | Enchytraeidae | | ENCHY |
| Oligochaeta | Lumbriculidae | | LUMB |
| Oligochaeta | Naididae | | NAID |
| Plecoptera | Capniidae | | P_Cap |
| Plecoptera | Chloroperlidae | | P_Chl |
| Plecoptera | Perlidae | | P_Perli |
| Plecoptera | Perlodidae | | P_Perlo |
| Plecoptera | Pteronarcyidae | | P_Pter |
| Trichoptera | Brachycentridae | | T_Bra |
| Trichoptera | Hydropsychidae | | T_Hpsy |
| Trichoptera | Hydroptilidae | | T_Hpti |
| Trichoptera | Lepidostomatidae | | T_Lepi |
| Trichoptera | Leptoceridae | | T_Lepto |
| Trichoptera | Limnephilidae | | T_Limn |
| Trichoptera | Philopotamidae | | T_Phil |
| Trichoptera | Polycentropodidae | | T_Poly |
| Trichoptera | Trichoptera Pupa | | T_Pupa |


*Figure 41. Pictures of sample locations, including (A) upstream view from Hay River Reach 1, (B) downstream view from Hay River Reach 1, (C) upstream view from Slave River Reach 1, and (D) downstream view from Slave River Reach 1. Photos taken in 2017.*